The Dissertation Committee for Craig Thomas Connolly Certifies that this is the approved version of the following dissertation:

Dissolved organic matter in Arctic watersheds and coastal waters

Committee:

James W. McClelland, Supervisor

Kenneth H. Dunton

Zhanfei Liu

Robert G.M. Spencer

Dissolved organic matter in Arctic watersheds and coastal waters

by

Craig Thomas Connolly

Dissertation

Presented to the Faculty of the Graduate School of

The University of Texas at Austin

in Partial Fulfillment

of the Requirements

for the Degree of

Doctor of Philosophy

The University of Texas at Austin

August 2019

Acknowledgements

This certainly has been an adventure. There are numerous people that I would like to thank for their help during this journey. I would like to especially thank my advisor, Jim McClelland, whose mentorship and support was truly invaluable. I would also like to thank the members of my committee, Ken Dunton, Zhanfei Liu, and Rob Spencer, whose advice and guidance helped shape my graduate studies into some fascinating research. In addition, I would like to thank Bayani Cardenas, Ann McNichol, Greta Burkart, Valier Galy, Diana Bull, Phil Bennett, Mary Lardie Gaylord, Li Xu, Anne Cruz, and Kalina Gospodinova for their continuous help and encouragement during my endeavors.

I would like to thank the past and present members of the McClelland lab, Patty Garlough, Claire Griffin, Matt Khosh, Stephanie Smith, Hengchen Wei, Xin Xu, and Emily Bristol, as well as all the graduate students, postdocs, technicians, faculty, and staff at the University of Texas at Austin, Marine Science Institute who overlapped with me during graduate school. It was a pleasure working with you all. We had a remarkably good time in Port Aransas. A great thanks goes to my Arctic companions, Christina Bonsell, Arley Muth, and Cliff Strain, for making fieldwork such a positive experience.

My parents and two brothers deserve special thanks for their unwavering love and support. A special thank you is also deserved to several incredible people in my life, Alex Bradford, Chris Entrup, Allan Jones, Jack Egerton, Megan and Chris Biggs, Sarah Cosgrove, Tobi Oke, and especially Ian Rambo and Valerie De Anda, who truly have been an incredible source of inspiration and friendship. Finally, the greatest thank you goes to my twin brother Kevin, who has stood by me in every step of life.

Abstract

Dissolved organic matter in Arctic watersheds and coastal waters

Craig Thomas Connolly, Ph.D.

The University of Texas at Austin, 2019

Supervisor: James W. McClelland

Arctic warming is already affecting the movement of freshwater and dissolved organic matter (DOM) from watersheds to the coastal ocean in the Arctic. Improved understanding of DOM in freshwater sources and linkages to DOM characteristics in Arctic coastal waters is needed to assess responses to and feedbacks with climate change. This work focuses on DOM characteristics that couple watershed and coastal systems in the Arctic, with specific considerations of river and groundwater inputs to lagoon ecosystems along the eastern Alaska Beaufort Sea coast. We found that spring and summer river-borne concentrations of dissolved organic carbon and nitrogen (DOC and DON) are strongly linked to variations in watershed slope and soil organic matter coverage across space and scale in the Arctic. The quantities and composition of DOM in lagoons of the eastern Alaska Beaufort Sea coast vary markedly between seasons. Specifically, lagoons experience a shift from high to low DOC and DON concentrations between the late spring sea ice break-up and winter ice-covered periods, but these concentrations are more variable during the summer open water period. Distinct seasonal transitions in ice coverage, runoff from land, and water exchange with the Beaufort Sea strongly influence the availability of lagoon DOM. During the summer, concentrations of

DOC and DON in supra-permafrost groundwater (SPGW) inputs to lagoons are much higher than those found in local rivers and lagoons. Late-summer fluxes of SPGW DOM to the northern Alaska coastline are substantial and may be the principal source of DOM to lagoons without river inputs. This SPGW DOM is sourced from readily leachable organic matter in surface soils and deeper soil horizons that likely extend into thawing permafrost. SPGW DOM contains aromatic carbon compounds that are largely resistant to microbial degradation on the order of days to months. While nearby river and lagoon water DOM has a similar composition and degradability, SPGW contains a portion of bioavailable and reactive DOM that is not present in river and lagoon waters. Inputs of SPGW DOM provide a potentially important source of energy for lagoon food webs along the Alaskan Beaufort Sea coast during the late summer.

Table of Contents

List of Tables

List of Figures

Introduction

Land-ocean coupling is a defining feature of Arctic watershed and coastal systems because a massive amount of freshwater discharge from the pan-Arctic watershed drains into a relatively small ocean basin (Aagaard and Carmack, 1989). Thus the transport and fate of water-borne nutrients from land, such as dissolved organic matter (DOM), has a marked influence on coastal biogeochemical and ecological processes in the Arctic (Benner et al., 2004). Numerous studies have been conducted over the past two decades to improve understanding of the linkages between DOM in Arctic watersheds and coastal waters. These studies reveal that distinct seasonal changes in surface hydrology drive the timing and magnitude of DOM export from northern rivers, where the vast majority of this export occurs during a short snowmelt-driven peak discharge period in the spring (McClelland et al., 2006; Holmes et al., 2012; McClelland et al., 2014). Moreover, seasonal changes in groundwater flow paths and soil structure associated with thawing of the active layer (i.e., surficial soils above frozen permafrost) strongly affect the sources and composition of fluvial DOM between the winter and summer months (Striegl et al., 2005; O'Donnell et al., 2012; Barnes et al., 2018). Increases in river discharge, thawing permafrost, and groundwater flow with Arctic warming will impact seasonal changes in watershed hydrology and soil/permafrost characteristics, and in turn, the movement of DOM from Arctic watersheds to coastal waters (Frey and McClelland, 2009). However, we lack a complete understanding of the characteristics of DOM that link watersheds and coastal waters across the pan-Arctic, in particular, on river and groundwater inputs to nearshore Arctic estuaries. This information is urgently needed to anticipate responses to and assess feedbacks with warming on land-ocean systems in the Arctic.

Concerted efforts have been made recently to establish baseline understanding of DOM export from north-flowing rivers and to characterize linkages with biogeochemical cycling in coastal margins of the Arctic Ocean (Dittmar and Kattner, 2003; Amon, 2004; Holmes et al., 2013) and yet, there is still a dearth of information on DOM export from approximately one-third of the pan-Arctic watershed (Holmes et al., 2013). Scaling is one common approach to extrapolate DOM fluxes to these data-poor regions, but there is observable variability in DOM yields among northern rivers, suggesting that spatial differences in watershed basin characteristics impart strong effects on riverine DOM export (Raymond et al., 2007; Holmes et al., 2013; McClelland et al., 2014). Specifically, several studies have found that variations in watershed slope (i.e., a measure of catchment steepness) correlate to concentrations of DOM, which includes dissolved organic carbon and nitrogen (DOC and DON), in rivers of Alaska during the summer (D'Amore et al., 2016; Harms et al., 2016; Khosh et al., 2017). Watershed slope may represent a simple but powerful indicator of concentrations of DOC and DON within rivers across the pan-Arctic domain. Generalizing these relationships for the pan-Arctic watershed could help improve understanding of spatial variability in DOM export. These relationships could also be useful as tools for estimating riverine DOM fluxes where field data are lacking, thus improving our ability to estimate pan-Arctic watershed export as a whole.

Seasonal cycles in runoff from land and sea-ice dynamics are inherent to temporal changes in physical, chemical, and biological interactions of Arctic coastal environments (McClelland et al., 2012). These seasonal cycles are more extreme within nearshore Arctic estuaries, such as lagoon systems along the Alaskan Beaufort Sea coast (Dunton et al., 2006). It is well recognized that temporal shifts in lagoon physicochemical conditions are strongly linked to distinct seasonal transitions in ice-coverage, runoff from land, and water exchange with the Beaufort Sea between the winter and summer periods (Harris et

al., 2017). Lagoons are more unique than other coastal systems because they receive direct inputs from land in the absence of fringing wetlands and are protected by barrier islands that limit water exchange with the open ocean. Lagoon ecosystems are also highly productive and serve as hotspots for the biogeochemical cycling of organic matter (Connelly et al., 2015; Harris et al., 2018). However, there is little information on variations in seasonally-distinct resources in lagoons systems, such as the quantities and composition of DOM, which forms the basis for their productivity. Seasonally-explicit field studies that identify temporal patterns in lagoon DOM characteristics are needed to improve understanding of the coupling between watershed nutrient export and DOM availability for biological production in nearshore estuaries of the Arctic.

While river transport is an important source of DOM for biological production in Arctic coastal waters, supra-permafrost groundwater (SPGW) flow through seasonally thawed active layer soils (i.e., surficial soils above permafrost) may be another significant source of DOM to these waters that has been largely overlooked. SPGW peaks during the late summer when the amount of local rainfall and active layer thaw are at a maximum (Walvoord et al., 2012). Thawing of the active layer also exposes organic-rich soils, which can introduce a major source of soil leachate DOM to Arctic streams and rivers through lateral SPGW transport (Guo and Macdonald, 2006; Wickland et al., 2007; Neilson et al., 2018). However, there are virtually no studies on direct SPGW DOM inputs to Arctic coastal waters. Substantial SPGW inflow to lagoons of the eastern Alaska Beaufort Sea coast has been observed during the late summer. SPGW thus may be a significant source of DOM to lagoon ecosystems of northern Alaska, in particular, along stretches of coastline without rivers and during the late summer when river flow is typically low. SPGW may also provide a more biologically labile (biolabile) source of DOM than river inputs because SPGW circumvents major losses and transformations

associated with photo-degradation that surface waters experience during the summer (Cory et al., 2014) and likely experiences little biological degradation owing to cold, waterlogged, anoxic soil conditions during transport (Frey and McClelland, 2009). A comprehensive characterization of direct SPGW DOM inputs to Arctic coastal waters, including its quantities, composition, and bioavailability, is needed in order to gain a full understanding of the relationships between watershed inputs, biological production, and biogeochemical cycling in Arctic coastal regions. The immediate and on-going impacts of climate change add urgency to this research need since Arctic warming is causing permafrost (i.e., ground below perennially freezing temperatures) to rapidly thaw, which increases active layer thickness, liberates previously frozen and trapped stores of soil organic matter, and alters groundwater flow paths (Walvoord et al., 2012; Schuur et al., 2013; Vonk et al., 2015). The synergetic effects of these myriad impacts will undoubtedly alter the movement of groundwater DOM to Arctic coastal waters (Frey and McClelland, 2009; St. Jacques and Sauchyn, 2009; O'Donnell et al., 2012).

The primary goal of this dissertation is to expand upon current knowledge of DOM characteristics that link Arctic watersheds and coastal waters, with a more specific consideration of river and groundwater inputs to lagoon ecosystems of the eastern Alaska Beaufort Sea coast. Chapter 1 focuses on generalizing relationships between watershed slope and concentrations of DOC, DON, and nitrate (NO_3^-) from pan-Arctic rivers that differ markedly in location and catchment size. To demonstrate the application of these tools, concentrations calculated from watershed slope-derived relationships were paired with discharge data to estimate annual fluxes of DOM from five Eurasian rivers in data-poor regions. Chapter 2 focuses on improving fundamental understanding of seasonal patterns in DOM within coastal lagoons of northeastern Alaska. Here, the quantities and composition of DOM were investigated by measuring lagoon concentrations of DOC,

ratios of DOC to DON (C:N), and chromophoric DOM (CDOM) optical properties, $SUVA_{254}$ and $S_{275\text{-}295}$, during spring ice break-up (late June), the summer open water period (August), and during full ice cover over the winter (April). Temporal changes associated with distinct transitions in ice-coverage, runoff, and connectivity with the Beaufort Sea were examined by comparing patterns in DOM with shifts in salinity. Chapter 3 focuses on the leaching potential of DOM from nearshore Arctic soils and the quantities of SPGW DOM inputs to coastal waters of the Alaskan Beaufort Sea during late summer. Here we examined (1) the relationship between soil organic matter in the active layer and shallow permafrost and the production/leaching potential of DOM from these soils; (2) the soil-DOM sources in SPGW DOM inputs using radiocarbon (^{14}C) dating; and (3) SPGW DOM fluxes that were derived from measurements of DOC and DON concentrations paired with groundwater discharge estimates from a steady-state excess radon (^{222}Rn) mass balance model. Finally, Chapter 4 focuses on the quality of SPGW DOM and its potential to fuel biology activity in lagoons. Biodegradable DOC experiments, ultra-high resolution DOM molecular composition analysis (FT-ICR MS), and serial thermal oxidation (RPO) coupled to measurements of activation energy (*E*), stable carbon, and radiocarbon isotopic composition ($\delta^{13}C$ and $\Delta^{14}C$) were employed to determine the bioavailability, chemical composition, and reactivity of DOM in SPGW inputs to lagoons along the eastern Alaska Beaufort Sea coast.

Chapter 1: Watershed slope as a predictor of fluvial dissolved organic matter and nitrate concentrations across geographical space and catchment size in the Arctic

ABSTRACT

Understanding linkages between river chemistry and biological production in Arctic coastal waters requires improved estimates of riverine nutrient export. Here we present the results of a synthesis effort focusing on relationships between watershed slope and seasonal concentrations of river-borne dissolved organic carbon (DOC), dissolved organic nitrogen (DON), and nitrate (NO_3^-) around the pan-Arctic. Strong negative relationships exist between watershed slope and concentrations of DOC and DON in Arctic rivers. Spring and summer concentration-slope relationships for DOC and DON are qualitatively similar, although spring concentrations are higher. Relationships for NO_3^- are more variable, but a positive relationship does exist between summer NO_3^- concentrations and watershed slopes. These results suggest that watershed slope can serve as a master variable for estimating spring and summer DOC and DON concentrations, and to a lesser degree NO_3^-, from drainage areas where field data are lacking, thus improving our ability to develop pan-Arctic estimates of watershed nutrient export.[1]

[1]Citation of published version of Chapter 1: Connolly, C.T., Khosh, M.S., Burkart, G.A., Douglas, T.A., Holmes, R.M., Jacobson, A.D., Tank, S.E., McClelland, J.W. (2018). Watershed slope as a predictor of fluvial dissolved organic matter and nitrate concentrations across geographical space and catchment size in the Arctic. *Environmental Research Letters*, 13(10), 104015. C.T. Connolly led the research design with guidance from co-authors of the published article. C.T. Connolly synthesized the previously collected data, conducted the analysis, generated all figures and tables, and wrote the chapter and its published version. Co-authors contributed to the writing through minor edits and suggestions for revision.

INTRODUCTION

Land-ocean coupling is strong in the Arctic, where north-flowing rivers account for over 10 % of the global runoff and connect a land area of ~20.5×10^6 km^2 to an ocean basin that contains only ~1 % of the global ocean volume (Aagaard and Carmack, 1989; Shiklomanov, 1998). Together these rivers transport globally significant quantities of dissolved organic matter (DOM), which is reported herein as dissolved organic carbon and nitrogen (DOC and DON), to the Arctic Ocean resulting in markedly high concentrations of land-derived organic matter relative to other ocean basins (Opsahl et al., 1999; Dittmar and Kattner, 2003; Benner et al., 2004; McClelland et al. 2012).

Major efforts have been made to characterize fluvial biogeochemistry at a variety of scales and locations within the pan-Arctic watershed during the past 20 years (e.g., Gordeev et al., 1996; Lobbes et al., 2000; Dornblaser and Striegl, 2007; Frey et al., 2007; Bowden et al., 2008; McClelland et al., 2014; McClelland et al., 2015; Lehn et al., 2017). Data from these studies have improved understanding of land-water connectivity in permafrost-influenced watersheds and established a basis for predicting potential climate change impacts on watershed nutrient export. The majority of annual riverine fluxes of water, organic matter, and inorganic nutrients to the Arctic Ocean occur during a short snowmelt period in the spring (Finlay et al., 2006; McClelland et al., 2006; Townsend-Small et al., 2011; Holmes et al., 2012; McClelland et al., 2016). A large fraction of this river-borne DOM is biolabile (20–40 %; Holmes et al., 2008; Mann et al., 2012) and may provide a substantial carbon subsidy to coastal food webs in the Arctic (Dunton et al., 2012; Casper et al., 2014; Harris et al., 2018). Fluvial transport of dissolved inorganic nitrogen (DIN) also merits attention as it has been identified as an important nitrogen source supporting primary production in Arctic estuaries (Amon and Meon, 2004; Tank et al., 2012; Le Fouest et al., 2013).

Despite recent efforts to characterize Arctic river biogeochemistry and land to ocean fluxes, a lack of concentration measurements in remote locations still hinders our ability to estimate fluxes from approximately one third of the pan-Arctic watershed (Holmes et al., 2013). This limits our ability to understand contemporary linkages between river inputs and biogeochemical cycling in the Arctic Ocean as well as our ability to forecast how changes in river inputs may influence biogeochemical cycling (including carbon storage/release and food web dynamics) in the future.

Defining watershed characteristics that correlate with river chemistry may prove useful for estimating fluvial nutrient concentrations in these remote, largely inaccessible, data-poor regions. Previous studies have demonstrated that topography, hydrology, and wetland coverage play a major role in regulating the release of DOC, DON, and nitrate (NO_3^-) in monitored catchments of temperate forests and can be used as indicators to estimate concentrations in other forested regions (Hinton et al., 1998; Schiff et al., 2002; Inamdar and Mitchell, 2006, 2007; Creed et al., 2008; Creed and Beall, 2009; Winn et al., 2009). Likewise, variability in DOM and inorganic nutrients across landscape gradients in Alaska have been attributed to differences in catchment topography and hydrology, wetland and permafrost coverage, characteristics of soils and vegetation, and seasonal thaw (McNamara et al., 2008; McClelland et al., 2014; D'Amore et al., 2016; Harms et al., 2016; Khosh et al., 2017; Lehn et al., 2017). Watershed slope has been highlighted as a particularly promising indicator of variations in fluvial DOM and NO_3^- among catchments (e.g., Schiff et al., 2002; Inamdar and Mitchell, 2006; Winn et al., 2009; Harms et al., 2016; Khosh et al., 2017).

Here, we present the results of a synthesis effort focusing on DOC, DON, and NO_3^- concentration measurements from 70 drainage areas within the pan-Arctic watershed spanning seven orders of magnitude (ranging from < 1 km^2 to 2.67×10^6 km^2).

These drainages are primarily located on the North Slope of Alaska but also include the Yukon and Mackenzie in North America and the Ob', Yenisey, Lena, and Kolyma in Eurasia. We quantify seasonal relationships between watershed slope and fluvial concentrations of DOC, DON, and NO_3^- and examine similarities and differences in these relationships across basins. Our analysis considers relationships between watershed slope and concentrations of DOC, DON, and NO_3^- over a much wider range of catchment sizes and geographic locations than previously considered in Arctic regions, thus facilitating broader conclusions about the robustness and generality of these relationships. Additionally, we examine whether an underlying relationship between watershed slope and soil organic matter content helps to explain spatial variability in fluvial DOC, DON, and NO_3^-. Lastly, we consider the utility of these relationships for estimating river concentrations and fluxes from remote areas of the pan-Arctic where field data on water chemistry are lacking. To demonstrate the application of these tools, concentrations calculated from slope-derived regression relationships were paired with discharge data to estimate annual fluxes from the Pechora, Mezen, Severnaya Dvina, Olenek, and Yana rivers on the Eurasian side of the Arctic.

MATERIALS AND METHODS

Concentration Data Collection and Analysis

River chemistry data from sites visited between 2003 and 2014 are included in this study (Figure 1.1). Concentration data for the six largest Arctic rivers (2003-2014) are from the Arctic Great Rivers Observatory (Arctic-GRO) project. Water samples were collected from the Yukon at Pilot Station, Mackenzie at Tsiigehtchic, Yenisey at Dudinka, Ob' at Salekhard, Lena at Zhigansk, and Kolyma at Cherskiy (n = 270). River

chemistry data from the North Slope of Alaska were collected from downstream locations on the Colville, Kuparuk, and Sagavanirktok in 2006 and 2007 (n = 123) (McClelland et al., 2014); six catchments in the headwaters of the Kuparuk and Sagavanirktok (upper Kuparuk, Imnavait, Atigun, Roche, Oksrukuyik and Trevor) in 2009 and 2010 (n = 480) (Khosh et al., 2017; Lehn et al., 2017); and eight rivers east of the Sagavanirktok (Kavik, Canning, Hulahula, Okipilak, Jago, Aichilik, Kongakut, and Turner) in 2011-2014 (n = 48). In total, data from 921 samples were included in this synthesis effort.

Procedures for sample collection and analysis for the eastern North Slope rivers are described in Appendix A. Refer to Holmes et al. (2012), McClelland et al. (2014), and Khosh et al. (2017) for details on the other river systems. Concentration data for each sampling location were binned into seasons that correspond to distinct hydrologic phases: winter low flow from 1 October to 15 May, spring high flow between 16 May and 30 June, and summer intermediate flow from 1 July to 30 September. Although there is variability in the timing of seasonal river discharge across the pan-Arctic (McClelland et al. 2012), these bins successfully capture the major seasonal transitions in flow that have been documented in all of the regions included in this study (Holmes et al., 2012; McClelland et al., 2012; McClelland et al., 2014; Khosh et al., 2017). However, winter flow only applies to the larger rivers included in this study since none of the rivers draining the North Slope of Alaska exhibit appreciable flow during the winter period. Each sampling location was assigned a single concentration value for DOC, DON, and NO_3^- for each season where data were available (seasonal coverage varied among sites). In some catchments east of the Sagavanirktok River, seasonal concentration values were from single sampling events. Where several days within a season and/or multiple years of data were collected at the same site, mean values were calculated for each season. In these cases, seasonal and yearly coverage ranged from 2 to 33 discrete samples collected

per season throughout a 1 to 10 year time period. All three constituents were measured with exception of NO_3^- and DON for 8 of the 52 summer sites and 2 of the 35 spring sites east of the Sagavanirktok. Although it would have been desirable to account for changes in concentration related to river discharge variability within seasons (Eimers et al., 2008; McClelland et al., 2014), discharge data were not available for most of the study sites.

Slope-Concentration Regression Models

Methods used to define watershed boundaries, slopes, and soil organic matter content for the contributing areas upstream of each sampling location are described in the supplementary information accompanying Appendix A. Season-specific regression relationships between watershed slope values and constituent concentrations were examined using two different datasets: 1) an "all data" case where data from all sites were used and 2) a "balanced" case where only data from sites with equal spring and summer sampling coverage were included. The number of data points in each case can be found in Table A.1. This approach allowed us to characterize relationships using maximum data coverage while also accounting for potential differences between regression relationships that could result from unbalanced seasonal sample coverage. Relationships between watershed slope and concentrations of DOC and DON were best explained using a natural log-linear fit of the data. The relationships between NO_3^- concentration and watershed slope were best defined using a standard linear fit. An analysis of co-variance (ANCOVA) was employed using R software to test for significant differences in slopes and intercepts between spring and summer regression lines for relationships using all available data and the balanced dataset. Regression coefficients can be found in Table A.1. We could not determine relationships between winter river concentrations and watershed slope using the small subset of available data (n = 6),

although it is possible patterns would emerge with better data coverage. To observe scale-dependent effects, data were additionally grouped for assessment within the following watershed size intervals: 0–100 km^2, >100–2,000 km^2, >2,000–5,000 km^2, >5,000–60,000 km^2, and >60,000–2,700,000 km^2.

Estimation of DOM Fluxes for Select Eurasian Arctic Rivers

Daily discharge measurements for the Pechora, Mezen, Severnaya Dvina, Olenek, and Yana rivers were gathered from the ArcticRIMS stream discharge database (http://www.wsag.unh.edu/arctic/RIMS-Old/group/real_time/) and from personal communications with A. Shiklomanov (University of New Hampshire). Average annual discharge was calculated during the 2001-2008 timeframe for the Pechora, 2003-2013 for the Mezen, 2002-2013 for the Severnaya Dvina, 2002-2008 for the Olenek, and 2002-2013 (except 2008) for the Yana. In a few cases where daily values were missing, mean values from the same month were used for interpolation.

Spring and summer DOC and DON concentrations for the Pechora, Mezen, Severnaya Dvina, Olenek, and Yana rivers were estimated using the "balanced" regression relationships in Table A.1. Winter concentrations for these rivers were estimated by averaging winter data from the six largest Arctic rivers (5.4 ± 2.3 SD mg DOC L^{-1} and 0.16 ± 0.05 SD mg DON L^{-1}). Seasonal discharge was estimated by the sum of daily discharge values corresponding to the season-specific concentration bins and then multiplied by these concentrations to estimate seasonal fluxes. Annual fluxes were estimated from the sum of winter, spring, and summer fluxes and averaged across years.

RESULTS AND DISCUSSION

Our analysis revealed that concentrations of DOC and DON are tightly coupled to mean watershed slope across a wide range of catchment sizes and geographical locations in the Arctic. Strong negative non-linear relationships exist between watershed slope and concentrations of DOC and DON, where lower catchment slopes correspond with higher concentrations and steeper catchment slopes correspond with lower concentrations (Figure 1.2). These relationships are qualitatively similar between the spring and summer periods; however, concentrations are higher during the spring. This seasonal difference is particularly evident in the balanced dataset for DOC, where the ANCOVA test identifies that regression line slope values are the same, but a significant difference in y-intercept values exists between the spring and summer periods (Table A.1). This demonstrates that there is a consistent offset between spring and summer concentration data across the range of catchment slopes. The observed seasonal shift is consistent with previous findings for Arctic regions, where frozen ground constrains snowmelt to surface and shallow soil flow paths that facilitate leaching of organic-rich soils and overlying vegetative material from the previous growing season (Guo and Macdonald, 2006; Spencer et al., 2008; Khosh et al. 2017; Lehn et al., 2017). Overall, watershed slope explains a remarkable 75 % and 70 % of the variability in spring concentrations of DOC (mg C L^{-1}) and DON (mg N L^{-1}) and 62 % and 65 % of the variability in summer concentrations of DOC and DON across catchments that span seven orders of magnitude and a broad geographic scope (Figure 1.2). Moreover, the 95 % confidence intervals bounding these relationships (Table A.1; dashed lines in Figure 1.2) demonstrate that the regression models are well constrained across the wide range of conditions represented. These results are consistent with those reported by D'Amore et al. (2016), revealing that

catchment slope was the best predictor of spring and fall stream DOC concentrations of the Alaskan perhumid coastal temperate rainforest.

While seasonality accounts for much of the temporal variability in concentrations of DOC and DON observed in Arctic rivers, and a large proportion of annual DOM export occurs during the spring (Holmes et al., 2012), this analysis demonstrates that seasonal variations within individual rivers are relatively small compared to variations in DOC and DON concentrations across catchments with different morphometry. For example, concentrations of DOC at specific watershed slope values differ by one to two-fold between spring and summer (balanced dataset), while DOC concentrations differ by an order of magnitude across the full range of slopes represented in this study (Figure 1.2). As a more specific example, consider two adjacent rivers with very different watershed slope values: the Kuparuk has a slope of 2.5 % whereas the Sagavanirktok has a slope of 29 %. Differences between spring and summer DOC concentrations for the Kuparuk (8.5 and 5.1 mg DOC L^{-1} respectively) and Sagavanirktok (3.3 and 1.3 mg DOC L^{-1} respectively) are much smaller than season-specific differences in DOC concentrations between these two rivers.

Changes in DOC and DON concentrations among catchments generally reflect differences in proportional contributions of peatland and/or coastal plain versus mountainous terrain and may be more specifically related to contrasts in soil organic matter content and water flow through soils among drainage basins (Judd and Kling, 2002; Neff and Hooper, 2002; Frey and Smith, 2005; McGuire et al., 2005). These gradients in terrain can be seen visually in Figure 1.1 (bottom panel), where watershed coverage by coastal plain tundra and vegetation (green areas) decreases relative to coverage by mountainous terrain (pink areas) moving from west to east across the North Slope of Alaska. Our analysis of variations in soil organic carbon content (SOCC) among

the study watersheds shows that SOCC is significantly related to watershed slope (Figure 1.3), with a markedly similar negative non-linear relationship compared to DOM relationships. Overall, watershed slope explains 57 % of the variability in SOCC among the drainage basins analyzed in this study. The extent to which high SOCC is related to watershed DOM concentrations, however, depends on the pervasiveness of soil saturation and water flow from land to streams (Creed et al., 2003, 2008). Longer water residence times have the potential to facilitate more leaching of DOM from soil organic matter stocks in low relief peatland terrain, which is shunted to stream and river networks during periods of high hydrologic connectivity (Ågren et al., 2008; Creed and Beall, 2009; Winn et al., 2009). The linkage between watershed slope and fluvial DOC and DON concentrations around the pan-Arctic likely reflects a strong correlation with functional wetland coverage that integrates variability in SOCC as well as hydrologic connectivity to stream and river networks (D'Amore et al., 2016; Harms et al., 2016). This is supported by a substantial body of literature demonstrating that low relief regions or wetlands play a key role in regulating DOM export and are a major source of DOM to rivers (e.g., Dillon and Molot, 1997; Gorham et al., 1998; Hinton et al., 1998; Gergel et al., 1999; Xenopoulos et al., 2003; Pellerin et al., 2004; Inamdar and Mitchell, 2006, 2007). We do not see clear evidence of scale-dependent effects on slope-concentration relationships for DOM that would allow us to determine how (if at all) watershed size correlates to fluvial DOC and DON concentrations (Figure 1.2). However, as additional catchment slope and fluvial DOC and DON concentration data are collected in the future, some aspects of scale dependence may emerge.

Patterns for NO_3^- are more variable, but a significant positive relationship exists between summer NO_3^- concentration (mg N L^{-1}) and watershed slope (Figure 1.2). The lack of a relationship between watershed slope and NO_3^- concentration during the spring

suggests that sources and losses of NO_3^- do not differ among catchments when water flow paths are constrained to near-surface soil layers and cold temperatures moderate biological uptake rates. A positive relationship between NO_3^- and watershed slope emerges in the summer, when thawing soils allow water penetration to deeper soil layers. In general, this is consistent with steeper catchments having 1) a greater proportion of mineral soils relative to organic soils, and 2) short water residence times in soils. This is supported by previous studies demonstrating that lower NO_3^- concentrations are expected where low slopes promote water-saturated anoxic conditions that facilitate denitrification and low flow rates that facilitate NO_3^- uptake by primary producers (Jones et al., 2005; Inamdar and Mitchell, 2006; Creed and Beall, 2009; Harms and Jones, 2012; Louiseize et al., 2014; Harms et al., 2016). On the other hand, fluvial NO_3^- concentrations are typically higher in catchments with steeper slopes because rapid water transit during rain events promotes the export of stored NO_3^- in mineral soils that make up a greater portion of the seasonally thawed active layer (Schiff et al., 2002; Inamdar and Mitchell, 2006; Harms et al., 2016; Khosh et al., 2017). Thus, as for DOM, differences in water residence times, hydrologic connectivity to surface waters, and the proportion of mineral to organic soils (expressed as SOCC) are factors that help explain the positive relationship between summer NO_3^- concentrations and watershed slope. However, the relatively weak relationship between concentration and watershed slope for NO_3^- as compared to DOM suggests that additional factors contribute to the variability in fluvial NO_3^- concentrations across catchments. In contrast to DOM, there is some evidence for scale dependence of watershed slope-concentration relationships for NO_3^-: the overall increase in summer NO_3^- concentrations as a function of watershed slope appears to be, in part, driven by data from catchments < 5,000 km^2 (Figure 1.2). This may reflect increasing (cumulative) process/removal effects as NO_3^- is transported downstream within large catchments.

Concentration and flux estimates for the Pechora, Mezen, Severnaya Dvina, Olenek, and Yana rivers in Eurasia demonstrate how the generalized relationships between DOM and watershed slope can be applied to other drainage basins within the pan-Arctic domain. Estimates of DOC and DON concentrations for these rivers ranged from 5.3 to 14.2 mg C L^{-1} and 0.19 to 0.39 mg N L^{-1}, respectively (Table 1.1). In combination with river discharge data, these concentrations translate into flux estimates of 183 to 998 Gg per year for DOC and 5 to 29 Gg per year for DON (Table 1.1). In most cases, our slope-based concentration estimates are similar to concentration values previously reported in the literature (Table 1.1). One notable exception is the Yana, where our estimates of DOC and DON concentrations are substantially higher. This may be due to a difference in seasonal representation: samples for the Yana were collected during August for the Lobbes et al. (2000) study, when lower values would be expected. Recent DOC estimates from a seasonally-explicit field study of the Severnaya Dvina River (Johnston et al., 2018) may provide the best opportunity for comparison since temporal transitions in discharge were considered and samples were collected multiple times within a season over several years (2013–2016). Our estimates of DOC concentrations for the Severnaya Dvina are similar to field measurements from Johnston et al. (2018) for the spring (14.6 ± 0.8 mg C L^{-1}), but are lower than their measurements for the summer (13.7 ± 1.1 mg C L^{-1}). This suggests that our slope-based model may be over-estimating spring to summer decreases in DOC concentrations in the Severnaya Dvina region. Comparing our flux estimates to other studies (e.g., review by Dittmar and Kattner, 2003) is challenging because inter-annual variations in water-borne constituent fluxes primarily reflect differences in water discharge between years (McClelland et al., 2012). The study by Johnston et al. (2018) does, however, provide one recent opportunity for comparing flux estimates. Our annual DOC flux and discharge estimates for the

Severnaya Dvina (896 ± 54 Gg and 99 ± 5.8 km^3 yr^{-1} between 2002–2013) are similar to the 1190 ± 72 Gg and 86 ± 3.7 km^3 yr^{-1} estimates between 2014–2016 from Johnston et al. (2018). For the other rivers in Table 1.1, our flux values can be considered updates to the older estimates because they are based on more recent discharge data and explicitly address seasonal differences in concentrations.

CONCLUSIONS

We synthesize data from a wide variety of rivers within the pan-Arctic watershed that differ in location and size to quantify relationships between watershed slope and fluvial concentrations of DOC, DON, and NO_3^-. We find that variations in spring and summer concentrations of DOC and DON are strongly related to variations in watershed slope across a broad range of geographic locations and catchment sizes in the Arctic. Summer concentrations of NO_3^- also correlate with watershed slope, but greater variability in this relationship points to other dominant factors contributing to differences in fluvial NO_3^- among catchments. It appears that watershed slope serves as a master variable for estimating concentrations of DOC and DON in rivers across the pan-Arctic domain and that slope-related variability in soil organic matter content helps to explain this linkage. Owing to the remote locations and challenges associated with working in the Arctic, there is a general lack of river chemistry data that can be used as a basis for modeling and assessing contemporary watershed nutrient export. The relationships defined herein provide a tool for deriving first-cut estimates of DOC and DON concentrations in Arctic watersheds where undertaking direct field measurements is logistically prohibitive. Furthermore, when paired with gauged, modeled, or remotely sensed river water discharge data, these relationships enable improved DOM flux estimation for catchments without chemistry data.

Although our data did not show clear geographic differences in slope-concentration relationships for DOM, it is likely that regional distinctions related to other basin characteristics such as wetland abundance, hydrologic connectivity, permafrost coverage, and dominant vegetation types, which interestingly may also be directly controlled by watershed slope, would emerge with better data coverage. As additional concentration data are collected across the pan-Arctic, the development of region-specific relationships would be desirable. Given that the Arctic system is rapidly changing, these relationships cannot be reliably applied to future scenarios. They do, however, provide a basis for near-term estimation of DOC and DON concentrations as well as an opportunity for longer-term assessment of integrated changes in watershed biogeochemistry. In particular, tracking changes in slope-concentration relationships over time may be useful as an indicator of permafrost thaw, associated shifts in hydrology, and the transport of stored nutrients and organic matter from land to sea. Where water flow through mineral soils of low relief terrain or steeper catchments is enhanced, DOM export could decrease while fluxes of dissolved nutrients increase. Where organic-rich soils extend deep into permafrost, on the other hand, thawing coupled with changes in subsurface flow may actually mobilize large stores of soil organic matter and increase the delivery of DOM to stream and river networks. These landscape-scale changes may be visible from an upward or downward shift in relationships between fluvial DOC, DON, and NO_3^- concentrations and watershed slope.

Table 1.1 Average annual water discharge (km^3/y), estimated annual fluxes (10^9 g), and spring and summer concentrations (mg L^{-1}) of dissolved organic carbon (DOC) and nitrogen (DON) for the Mezen, Olenek, Pechora, Severnaya Dvina, and Yana rivers. Concentrations were calculated using the balanced regression models defined in Table A.1. Concentration estimates from Lobbes et al. (2000)[a], Gordeev et al. (1996)[b], and Johnston et al. (2018)[c] are included for comparison. Values are ± 1 standard error. Standard errors for concentration values reflect estimates of error in the modeled concentration data, while standard errors for flux values reflect inter-annual variability in discharge.

	DOC (mg C L^{-1})			DON (mg N L^{-1})			DOC (10^9 g)	DON (10^9 g)	Q (km^3 y^{-1})
River	Spring	Summer	Other studies	Spring	Summer	Other studies	Annual fluxes between 2000-2013		
Mezen	13.6 ± 1.7	10.0 ± 1.2	12[a]	0.37 ± 0.04	0.34 ± 0.04	0.22[a]	183 ± 15	5.3 ± 0.42	20 ± 1.1
Olenek	10.5 ± 2.2	7.6 ± 1.5	10[a]	0.30 ± 0.05	0.26 ± 0.05	0.25[a]	401 ± 23	12 ± 0.70	44 ± 2.6
Pechora	11.8 ± 2.0	8.6 ± 1.4	13[b]	0.33 ± 0.05	0.30 ± 0.04	.	998 ± 62	29 ± 1.8	108 ± 6.4
S Dvina	14.2 ± 1.6	10.4 ± 1.1	14-15[c]	0.39 ± 0.04	0.35 ± 0.03	.	896 ± 54	26 ± 1.6	99 ± 5.8
Yana	7.4 ± 2.7	5.3 ± 1.9	2.8[a]	0.22 ± 0.07	0.19 ± 0.06	0.09[a]	221 ± 12	7.3 ± 0.37	37 ± 1.8

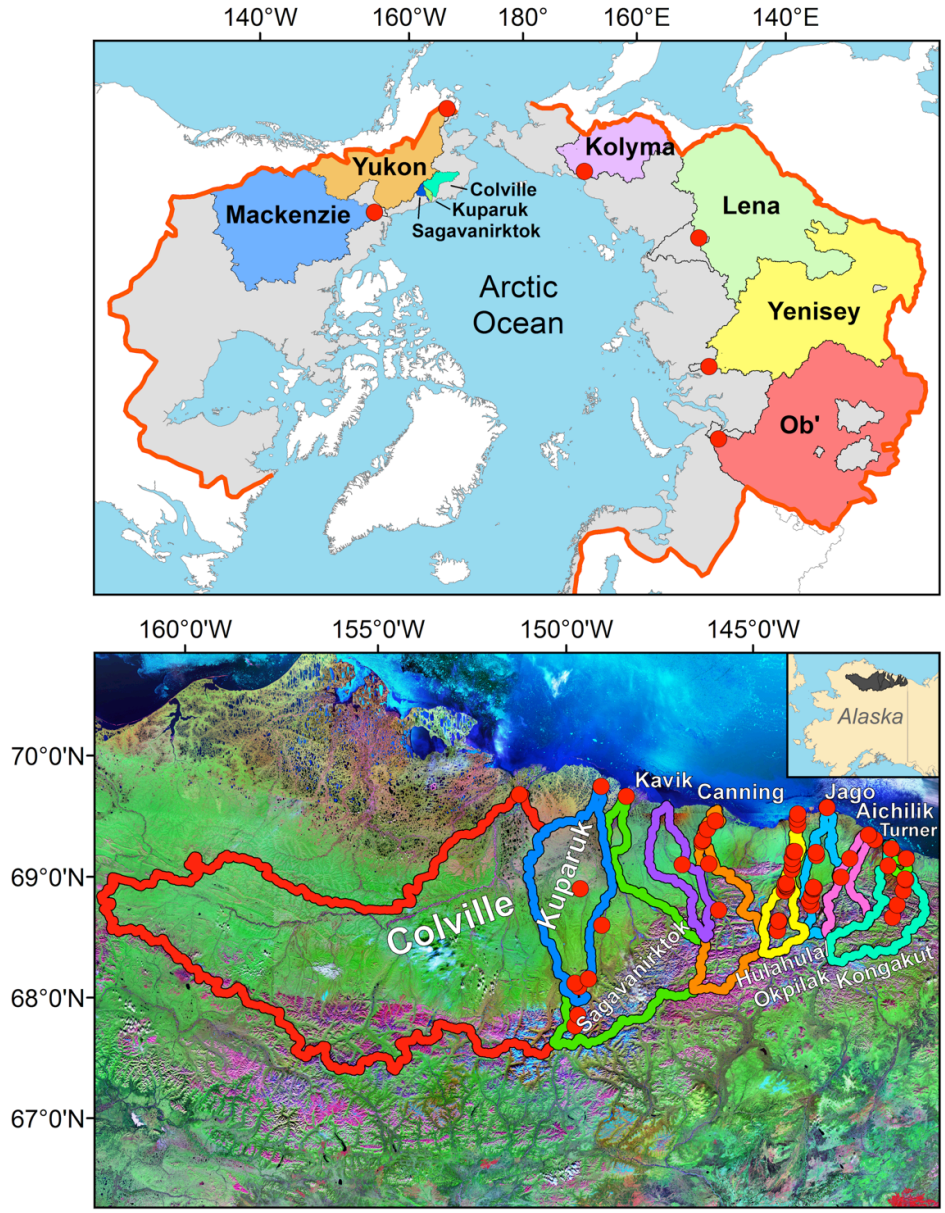

Figure 1.1. Sampling locations (red dots) within drainage basins of the 20.5×10^6 km^2 pan-Arctic watershed (top; bold red line) and the North Slope of Alaska (bottom). Watershed boundaries on the North Slope of Alaska are superimposed on a false color composite image that displays bare soil and rock as pink/magenta and vegetation as bright green.

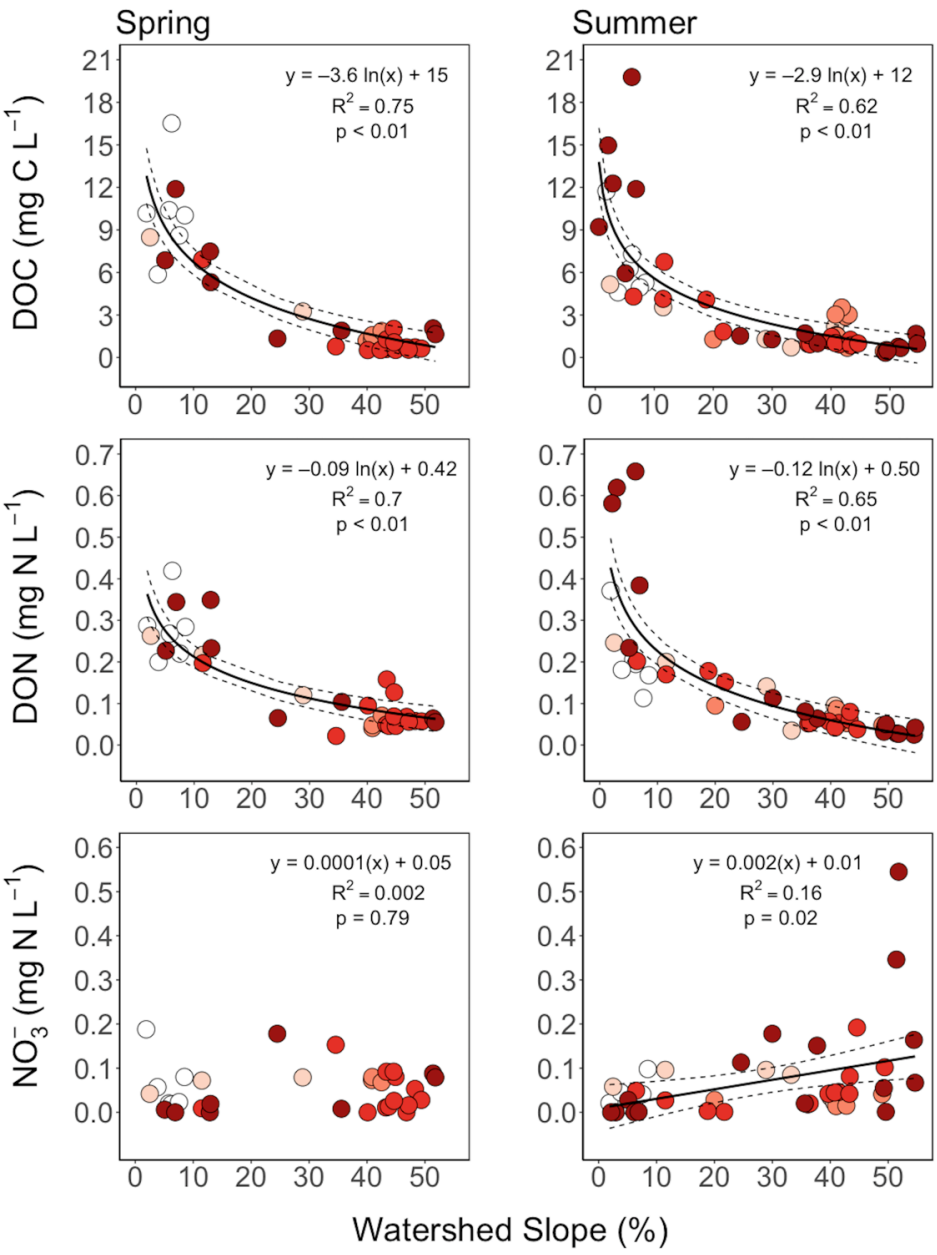

Figure 1.2. Spring (left) and summer (right) relationships between watershed slope and concentrations of fluvial dissolved organic carbon (DOC; top), dissolved organic nitrogen (DON; middle), and nitrate (NO_3^-; bottom) of river water collected from catchments of various sizes using all available data: 0–100 km^2 (●), >100–2,000 km^2 (●), >2,000–5,000 km^2 (●), >5,000–60,000 km^2 (●), and >60,000–2,700,000 km^2 (○). Dashed lines mark the upper and lower limits of the 95 % confidence interval bands.

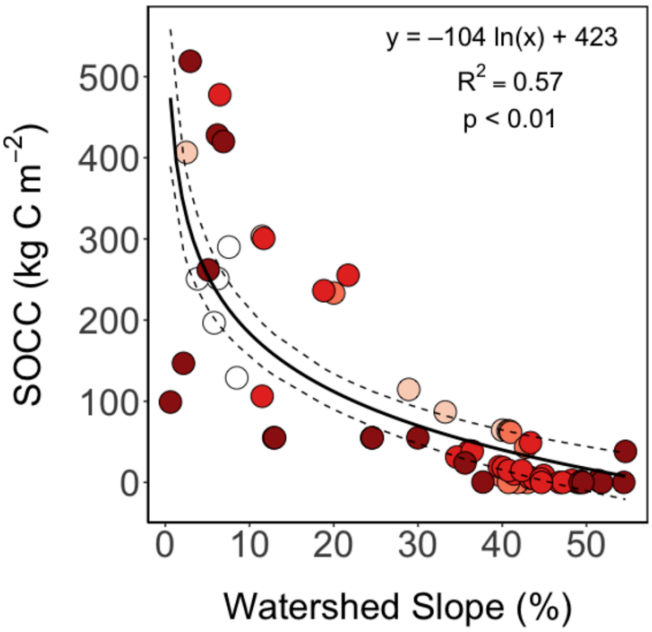

Figure 1.3. Relationship between watershed slope and soil organic carbon content (SOCC) of all watersheds and sub-catchments included in this study except the Ob'. Dashed lines mark the upper and lower limits of the 95 % confidence interval bands. Symbol colors are as defined in Figure 1.2.

Chapter 2: Seasonality of dissolved organic matter in lagoon ecosystems along the eastern Alaska Beaufort Sea coast

ABSTRACT

Seasonality is a defining feature of the physicochemical environment in Arctic coastal regions, but fundamental understanding of temporal patterns in dissolved organic matter (DOM) among lagoons ecosystems in the Arctic are lacking to date. Here we investigated seasonal patterns in the quantity and composition of DOM in lagoons along the eastern Alaska Beaufort Sea coast during ice break-up (late June), the open water period (August), and full ice cover (April). We measured bulk concentrations of dissolved organic carbon (DOC), ratios of DOC to DON (C:N), and chromophoric DOM (CDOM) optical properties, $SUVA_{254}$ and $S_{275\text{-}295}$, and found that the quantities and composition of DOM in Arctic lagoons vary markedly among seasons. We saw a general shift from high to low DOC, C:N, and $SUVA_{254}$ values between June and April. These parameters were more variable during August, spanning the range observed during the other two seasons. $S_{275\text{-}295}$ values were lower and well-constrained during June and higher but more variable in August and April. Patterns in DOM reflect distinct seasonal transitions in ice coverage, runoff from land, and connectivity with the Beaufort Sea that are coupled to changes in the sources and composition of DOM in Arctic lagoons. More specifically, lagoon DOM in the spring is strongly influenced by river-borne material that inundates the Beaufort Sea coastline. The composition of DOM during the summer reflects variability in runoff and water exchange with the open ocean between the spring and late summer periods. In some cases, DOC concentrations build-up beneath the ice over the winter, indicating that inputs of regenerated organic matter are important contributors to the winter DOM pool. Together this work provides new information on

linkages between terrestrial inputs, nutrient cycling, and ocean mixing in Arctic coastal waters that is critical for assessing climate change impacts.

INTRODUCTION

Arctic coastal waters are characterized by marked seasonality and strong land-ocean interactions that define their unique physiochemical and biological character (Macdonald, 2000; Carmack and Wassmann, 2006; McClelland et al., 2012). Nearshore systems in particular experience major temporal shifts in day length, temperature, ice-coverage, runoff from land, and connectivity with the open ocean between the winter and summer periods (Dunton et al., 2006). Distinct seasonal transitions of these variables in turn influence salinity regimes, land-derived inputs, and the availability of aquatic organic matter and nutrients (Connelly et al., 2015; Harris et al., 2017). Challenges associated with conducting fieldwork in remote Arctic regions, however, have limited the number of seasonally-explicit field studies on organic matter cycling in northern coastal systems. To date, knowledge of seasonal variations in dissolved organic matter (DOM) within Arctic lagoons is missing. This information is needed to improve understanding of linkages between biogeochemical cycling and biological production in Arctic coastal waters as well as to assess the immediate effects of on-going climate change.

Coastal waters of the Alaska Beaufort Sea are completely or partially covered by ice and snow for about 9 months each year (roughly November to May), and only ice free for about 3 months per year (roughly July to September). During this time, nearshore waters are salty (full strength seawater to hypersaline), primary production is minimal, and inputs of freshwater and nutrients from land are virtually absent (Harrison et al., 1982; McClelland et al., 2014; Connelly et al., 2015; Harris et al., 2017). As day length increases and air temperatures rise in the late spring (May to early June), snowmelt facilitates an increase in discharge from numerous streams and rivers draining the North Slope of Alaska (McClelland et al., 2012; Khosh et al., 2017). Rivers draining into the Alaska Beaufort Sea deliver well over half of their annual supply of freshwater, nutrients,

and organic matter during a short two-week period in the spring (McClelland et al., 2014). This tremendous pulse of warmer river water inundates the coastal environment and adds an albedo effect, which together mixes and/or displaces marine water further offshore and accelerates sea ice break-up (Dean et al., 1994; Macdonald, 2000). As a result, nearshore waters become estuarine in character by the summer (July to October). With the disappearance of sea-ice comes an increase in light attenuation, leading to a rise in primary production in the late spring. Primary productivity is typically low in nearshore coastal systems during mid to late summer as enhanced biological activity depletes inorganic nutrients that built-up over the winter (Dunton et al., 2012; Dunton and Crump, 2014). During the summer open water period, coastal waters freely exchange water with the Beaufort Sea. Rivers return to baseflow conditions, while increases in direct groundwater flow and coastal erosion provide a new source of land-derived material to nearshore systems (Brown et al., 2003; Connolly et al., 2019a). These systems are largely heterotrophic throughout the summer owing to low *in situ* primary productivity and high rates of decomposition of terrestrial organic matter (Borges and Abril, 2011; Connelly et al., 2015). Local food webs thriving in Arctic nearshore estuaries rely heavily on this terrestrial material as a source of fuel and energy (Garneau et al., 2006; Dunton et al., 2006, 2012; Mohan et al., 2016; Harris et al., 2018).

While variations in physical environmental conditions (e.g., salinity and temperature) are important drivers of biological production in Arctic coastal systems, the transfer of energy through trophic levels is largely controlled by allochthonous and autochthonous inputs of organic matter (Peterson et al., 1994). Most of the bioavailable organic matter in aquatic systems is in the dissolved form (i.e., DOM), which includes dissolved organic carbon and nitrogen (DOC and DON). The two major DOM sources to nearshore waters during the spring and summer periods are [i] land-derived inputs from

freshwater inflows (i.e., streams, rivers, and groundwater) and eroding coastal soils (McClelland et al., 2014; Gibbs and Richmond, 2015; Connolly et al., 2019a) and [ii] locally-sourced inputs, for example, from marine phytoplankton, microphytobenthos, small zooplankton, and heterotrophic protists (Harris et al., 2018). A third DOM source is from the decomposition of particulate organic matter (POM) and detritus in the water column and held within benthic sediments (Connelly et al., 2015). This *in situ* regenerated DOM may be particularly important over the winter when inputs from land and primary production are almost entirely absent.

Estuaries around the world experience distinct gradients in the amount and types of DOM as freshwater sources from land mix with marine sources from the open ocean. Estuarine DOM simultaneously undergoes substantial transformation during transit to the open ocean owing to photochemical and biological degradation (Raymond and Bauer, 2000, 2001; Aarnos et al., 2012; Fichot and Benner, 2012). While these collective processes are generally recognized as drivers of the cycling, bioavailability, and fate of estuarine DOM (Fichot and Benner, 2014), this understanding is not well developed in Arctic lagoon ecosystems that experience stronger land-ocean interactions and more extreme temporal cycles than other coastal margins. Lagoons along the eastern Alaska Beaufort Sea coast receive direct inputs from land and the benthic environment because lagoons are free of fringing wetlands and are very shallow (typically < 4 m). Water exchange with the open ocean is highly dynamic because mixing is limited to relatively small openings between barrier islands, thereby promoting inter-seasonal shifts in water column stratification and lagoon water residence times (Harris et al., 2017). Moreover, these effects are superimposed by variability in lagoon geomorphology, sea ice coverage, sea level, runoff from land, and currents and waves (Dunton et al., 2006).

In this study, we examined seasonal patterns in the quantity and composition of DOM in coastal lagoons of the eastern Alaska Beaufort Sea. We measured salinity, bulk concentrations of DOC, DOC to DON ratios (C:N), and chromophoric DOM (CDOM) optical properties, $SUVA_{254}$ and $S_{275\text{-}295}$, during spring ice break-up (late June), the summer open water period (August), and full ice cover over the winter (April). Lagoon systems make up well over half of the Alaska Beaufort Sea coastline and represent unique coastal features that experience extreme seasonal cycles, which are now subject to rapid shifts driven by climate change. This work is part of a larger effort aimed at understanding how variations in terrestrial inputs, local production, and exchange between lagoons and the Alaska Beaufort Sea interact to control food web dynamics through the cycling of carbon and nitrogen over seasonal timeframes.

Climate change adds some urgency to this research need since nearshore systems in the Arctic are especially vulnerable to changes occurring at their land and ocean domains (Lantuit et al., 2011). Warming in the Arctic is accelerating at a rate that is twice the global average and coastal systems are already experiencing impacts associated with changes in the hydrologic cycle (Rawlins et al., 2010), thawing permafrost (Frey and McClelland, 2009; Schuur et al., 2013, 2015), river discharge (Peterson et al., 2006; McClelland et al., 2006; Rawlins et al., 2019), coastal erosion (Jones et al., 2009), sea ice dynamics and wave activity (Forbes, 2011), and the frequency and severity of storms (Hinzman et al., 2005). Synergetic change associated with these impacts will undoubtedly alter DOM properties in Arctic coastal waters, with broad implications of shifts in the timing and magnitude of biological production and biogeochemical cycling. Seasonally-explicit studies on DOM dynamics within Arctic coastal waters are therefore needed for assessing responses to and feedbacks with climate change.

MATERIALS AND METHODS

Study Sites

Several sites inside and outside of barrier islands along the eastern Alaska Beaufort Sea coast between the Hulahula River delta (144.190 °W) and Demarcation Bay (141.267 °W) were sampled for measurements of DOC concentrations and its C:N ratios, and CDOM optical properties in August 2011, and April, June, and August 2012 and 2013 (Figure 2.1). Four lagoons, Kaktovik (KA), Jago (JA), Angun (AN) and Nuvagapak (NU), and one site outside the barrier islands near Barter Island (BPDL) were sampled in all three seasons. Two additional lagoons, Tapkaurak (TA) and Demarcation Bay (DE), and three sites outside the barrier islands, near the Hulahula River (HU), Bernard Spit (BE) and Demarcation Point (DP), were also sampled in August. In August 2013, however, only KA, JA, AN, BPDL and BE were sampled due to severe weather. During June and April, generally two stations per site were sampled, while in August, samples were collected from two to three stations per site. One notable exception was the BPDL site, where only one station was sampled during each season.

Environmental Conditions

Salinities in our lagoon systems range from completely fresh to hypersaline (0 to > 45) with temperatures ranging from –2 to 14 °C depending on the time of year (Harris et al., 2017). In April, lagoons are predominately made up of marine water from the Beaufort Sea. Ice forms between 1.5 and 2 m thick over the winter, which leads to brine rejection and the development of hypersaline conditions where water exchange with the open ocean is limited (i.e., if lagoons have few or small openings between barrier islands). In June, numerous valley streams and small rivers drain into our lagoons sites at the onset of the spring freshet, which marks the beginning of hydrologic year. The freshet

pulse pushes salty water out of the lagoons and speeds up sea ice break-up and melting, causing lagoons to become nearly fresh in late June. However, in some cases lagoons maintain well-stratified and hypersaline bottom waters (typically ≥ 3 m) if runoff is not strong enough to vertically mix the entire water column (Harris et al., 2017). In August, wind and tidal-driven transport circulates marine water back into lagoons, typically leading to mixed estuarine environments depending on lagoon geomorphology and the degree of summer runoff (Harris et al., 2017).

Sample Collection

One to three water depths were sampled at each station depending on overall water column depth and stratification conditions. Samples in April and June were collected from ≤ 2 m and ≥ 3 m below the top of the ice or water surface with a peristaltic pump set-up (Geotech GeoPump with Masterflex C-flex tubing). A depth of 2 m below the top of the ice surface corresponds to ~0.5 m from the ice-water interface. August samples were collected from near the surface (between 0.25 m and 0.75 m) by submerging carboys into the water. Samples from deeper in the water column (between 1 to 4 m) were collected at specified depths using a peristaltic pump. Water for DOC, total dissolved nitrogen (TDN), and dissolved inorganic nitrogen (DIN) measurements were 0.45 μm field-filtered using disposable Geotech membrane cartridges. Salinity was measured with a YSI sonde at all sites and depths where water samples were collected. Acid-washed and Milli-Q rinsed polycarbonate bottles were used to store DOC/TDN samples, while acid-washed and Milli-Q rinsed HDPE bottles were used to store DIN samples. Both types of samples were stored frozen until analysis.

Chemical Analysis

DOC/TDN was measured at the University of Texas, Marine Science Institute (UTMSI) on a Shimadzu TOC-V CSH analyzer with a TNM-1 total nitrogen detector. DON was estimated from TDN minus DIN, which includes nitrate plus nitrite (NO_3^- + NO_2^-) and ammonium (NH_4^+). Concentrations of DIN were determined at UTMSI using standard colorimetric measurements scaled down for analysis with a 96-well microplate spectrophotometer (Mooney and McClelland, 2012; Khosh et al., 2017). Values measured below the detection limit for NO_3^- plus NO_2^- and NH_4^+ were reported as zero. Chromophoric dissolved organic matter (CDOM) absorbance spectrums were measured with a portable Ocean Optics UV-Vis spectrophotometer immediately after field collection and filtration in Alaska. CDOM parameters, $SUVA_{254}$ and $S_{275\text{-}295}$, were calculated according to Helms et al. (2008) and Spencer et al. (2008). It is important to note that fewer measurements of CDOM were made relative to DOM, but the spread of CDOM data does include the full range of study sites, waters depths, and salinities where DOM samples were collected.

Statistical Analysis

DOC, C:N, $SUVA_{254,}$ and $S_{275\text{-}295}$ data were averaged by season, June (spring), August (summer), and April (winter) for samples collected inside lagoons as well as outside lagoons for comparison. To tease apart relationships that occur within specific salinity ranges (i.e., are reflective of different source waters and mixtures irrespective of season), lagoon DOM variables were averaged according to the following salinity bins: 0–5 as freshwater, 6–30 as estuarine, 31–33 as marine, and 34–44 as hypersaline waters. Lagoon DOM variables were also plotted against their respective salinity values and grouped visually by month to observe temporal variations with salinity for individual

seasons. Pair-wise t-tests were performed in R software to compare average DOM data across seasons for sites sampled inside and outside lagoons. Pair-wise comparisons were also made on DOM data between inside and outside groups for the same season. A Tukey HSD test was performed to compare average DOM data between salinity groups. Log-transformed DOC, C:N, and $SUVA_{254}$ values, but non-transformed salinity and $S_{275\text{-}295}$ data were used for these statistical comparisons. A principal components analysis (PCA) was performed with lagoon DOC concentrations, C:N, $SUVA_{254}$ and $S_{275\text{-}295}$ data and grouped visually by salinity. The PCA was performed in R software ("*prcomp"* package) using non-transformed variable data that were scaled and centered as opposed to normalized. Values tended to be negative on the biplot, so PCA scores were transposed to positive values for better readability/visual graphic representation.

RESULTS

Salinity

Here and in the proceeding sections, we describe our results starting in June to follow changes along the progression from the spring freshet through the summer open water period and culminating at the end of the winter ice covered period. As expected, lagoon salinity values varied markedly across seasonal timeframes (Table 2.1). Average salinities within and outside lagoons were lower in June than August, which were both lower than in April (Table 2.1). Average salinities between inside and outside lagoons were similar in April and June, but salinity was higher outside of lagoons in August (Table 2.1). It is important to note that we found a non-normal distribution in lagoon salinity data in June (ranging from < 1 to 44, with a median of 3.5) and August (ranging from ~2 to 44, with a median 38.6).

Quantities of Dissolved Organic Matter

Average concentrations of lagoon DOC collected during June were higher than August and April (Table 2.1). August and April lagoon DOC concentrations were similar to each other; however, August concentrations were slightly higher (Table 2.1). We found a similar seasonal trend in DOC concentration from outside of lagoons. Average DOC concentrations outside of lagoons were higher in June than in August and April. DOC concentrations outside of lagoons in August and April were similar to each other, but August concentrations were slightly higher (Table 2.1). Average DOC concentrations between inside and outside lagoon sites were similar in June, but were higher inside lagoons in August and April (Table 2.1).

DOC concentrations in near fresh lagoon waters (208 ± 12.5 μM C) were on average higher than estuarine (129 ± 6.4 μM C), marine (94 ± 3.9 μM C), and hypersaline lagoon waters (137 ± 5.3 μM C) (Figure 2.2a). DOC concentrations were on average higher in hypersaline lagoon waters compared to estuarine and marine lagoon waters (Figure 2.2a). DOC concentrations in estuarine lagoon waters were similar to marine lagoon waters, although the weak statistical similarity (*p-value* = 0.06) indicates that estuarine DOC concentrations were slightly higher (Figure 2.2a).

Patterns in DOC concentration with salinity reveal that near fresh lagoon waters experienced a wide range of DOC concentrations in June (teal circles in Figure 2.3). In some cases, hypersaline lagoon waters were found in June with lower concentrations of DOC relative to near fresh lagoon waters (Figure 2.3). August lagoon DOC concentrations were less variable and lower than June, over a wider range of salinities from fresh to near full-strength seawater (black circles in Figure 2.3). August DOC concentrations were higher in low-salinity estuarine lagoon waters (~12–25), while DOC concentrations were lower in high-salinity estuarine lagoon waters (~25–29) (Figure 2.3).

April DOC concentrations within marine and hypersaline lagoon waters were typically lower than those found in near fresh lagoon waters in June, but were more similar to lagoon DOC concentrations in August (red circles in Figure 2.3). April DOC concentrations were consistently low in marine lagoon waters and were higher in hypersaline lagoon waters (Figure 2.3). April DOC concentrations were markedly similar to those found in June within hypersaline lagoon waters (Figure 2.3).

Composition of Dissolved Organic Matter

Average lagoon C:N ratios and $SUVA_{254}$ values were higher in June than August and April (Table 2.1). Average lagoon C:N and $SUVA_{254}$ were similar in August and April; however, August values were higher (Table 2.1). Likewise, C:N and $SUVA_{254}$ values from outside of lagoon sites were higher in June than August and April, which were again similar to each other (Table 2.1). C:N ratios between inside and outside lagoon sites were similar in June, August, and April (Table 2.1). $SUVA_{254}$ values between inside and outside lagoon sites were similar in June and April, but were higher inside lagoons in August (Table 2.1). Average lagoon $S_{275\text{-}295}$ values were similar in June and August, but were higher in April (Table 2.1). $S_{275\text{-}295}$ values from outside of lagoon sites in June were similar to August and April, but June $S_{275\text{-}295}$ values were slightly lower than those found in April, while August $S_{275\text{-}295}$ values were higher than April $S_{275\text{-}295}$ values (Table 2.1). Average $S_{275\text{-}295}$ values between inside and outside lagoons were similar in June and August, but were higher inside lagoons in April (Table 2.1).

C:N and $SUVA_{254}$ values in fresh lagoon waters (28.7 ± 2.0 molar ratio; 3.7 ± 0.1 L mg C^{-1} m^{-1}) were on average higher than estuarine (18.5 ± 0.9 molar ratio; 2.9 ± 0.1 L mg C^{-1} m^{-1}), marine (16.6 ± 1.8 molar ratio; 2.5 ± 0.4 L mg C^{-1} m^{-1}), and hypersaline lagoon waters (15.1 ± 1.6 molar ratio; 2.3 ± 0.1 L mg C^{-1} m^{-1}) (Figure 2.2b,c). Average

C:N ratios in estuarine lagoon waters were slightly higher than hypersaline lagoons waters, but average C:N between estuarine and marine as well as between marine and hypersaline lagoon waters were similar (Figure 2.2b). We found similar trends in our $SUVA_{254}$ values; however, in comparison to patterns in C:N, $SUVA_{254}$ in estuarine lagoon waters tended to be higher than marine and hypersaline lagoon waters (Figure 2.2b,c). Average $S_{275\text{-}295}$ values in fresh lagoon waters ($13.8 \pm 0.2 \times 10^{-3}$ nm^{-1}) were on average lower than hypersaline lagoon waters ($16.5 \pm 0.8 \times 10^{-3}$ nm^{-1}), but were similar to estuarine ($14.8 \pm 0.6 \times 10^{-3}$ nm^{-1}) and marine ($13.7 \pm 1.7 \times 10^{-3}$ nm^{-1}) lagoon waters (Figure 2.2d). $S_{275\text{-}295}$ values in marine lagoon waters were slightly lower than estuarine, which were both slightly lower than hypersaline lagoon waters (Figure 2.2d).

Patterns in C:N ratios with salinity show that near fresh lagoon waters experienced a wide range of C:N in June (Figure 2.4a). In some cases, hypersaline lagoon waters were found in June with lower C:N relative to near fresh lagoon waters (Figure 2.4a). August lagoon C:N ratios were typically lower and less variable than June across the summer range of salinities (Figure 2.4a). Unlike patterns in DOC concentration, there appears to be no observable relationship between August C:N ratios and salinity (Figure 2.4a). Similar to patterns in DOC concentration, April C:N ratios within marine and hypersaline lagoon waters were typically lower than those found in near fresh lagoon waters in June, but were similar to lagoon C:N values in August (Figure 2.4a). However, unlike patterns in DOC concentration, April C:N values were consistently low across marine and hypersaline lagoon water salinities (Figure 2.4a). April C:N ratios were similar to those found in June in hypersaline lagoon waters (Figure 2.4a).

$SUVA_{254}$ values in near fresh lagoon waters were tightly bound between 3.0 and 5.3 L mg C^{-1} m^{-1} (Figure 2.4b). August lagoon $SUVA_{254}$ values tended to be similar to June in low-salinity lagoon water, but were lower at salinities approaching full-strength

seawater (Figure 2.4b). April $SUVA_{254}$ values were lower than those found in June, and to a less degree in August, across the winter range of high salinities (Figure 2.4b). Similar to patterns in C:N ratios, there appears to be no observable difference in April $SUVA_{254}$ values between marine and hypersaline lagoon salinities (Figure 2.4b). April and June $SUVA_{254}$ values in hypersaline lagoon waters were similar (Figure 2.4b).

$S_{275\text{-}295}$ values in near fresh lagoons were tightly bound around 12.5 and 15.1×10^{-3} nm^{-1} (Figure 2.4c) during June. August $S_{275\text{-}295}$ values were both lower and higher than those found in June and do not show any clear relationship with salinity (Figure 2.4c). Likewise, April $S_{275\text{-}295}$ values tended to be higher than June values, and to a lesser degree in August, and do not show any clear relationship with salinity (Figure 2.4c).

PCA of Dissolved Organic Matter Variables

The first two components of our PCA collectively explain a remarkable 82.5 % of the variance in our lagoon DOC, C:N, $SUVA_{254}$, and $S_{275\text{-}295}$ data. Principal component one (PC1) explains 43.6 % of the data and correlates positively with high values of lagoon DOC, C:N, and $SUVA_{254}$, but correlates slightly negatively with lagoon $S_{275\text{-}295}$ values (Table 2.2; Figure 2.5). Principal component two (PC2) explains 38.8 % of the data and correlates positively with high values of lagoon $S_{275\text{-}295,}$ and to a lesser degree lagoon DOC and C:N values (Table 2.2; Figure 2.5). Interestingly, PC2 correlates negatively with high values of $SUVA_{254}$. Low-salinity samples collected in June have the highest positive relationships on PC1. Some August samples with mid-range salinities also appear to have positive but weaker relationships on PC1. August and April samples in the mid-to-high range of salinities tend to have negative relationships on PC1. High-salinity samples from April have negative relationships on PC1 in particular. Mid-to-high salinity samples from August and April both have high positive and high negative

relationships on PC2, while low-salinity samples from June appear to have weaker or no relationships on PC2. There is little overlap between low-salinity samples from June and higher salinity samples from August and April with respect to PC1 and PC2. In contrast, low-to-high salinities from August and April overlap considerably, especially on PC2.

DISCUSSION

In this study, we demonstrate that nearshore lagoon ecosystems experience marked seasonal changes in the quantities and sources of DOM between the spring and winter months. Here we discuss temporal shifts in environmental conditions that influence the quantities, sources, and composition of lagoon DOM during the seasonal/hydrologic progression from (1) sea ice break-up following the spring freshet to (2) the ice-free summer open water period and then to (3) the winter ice-covered period.

Lagoon DOM in June is predominately made up of river-borne organic matter that overwhelms lagoon environments following peak discharge in the late spring. Rivers draining the North Slope of Alaska typically have high DOC concentrations and C:N ratios during the spring freshet owing to large contributions of leachates derived from snowmelt-driven flow through decomposing litter and shallow organic-rich soils above frozen ground (Spencer et al., 2008; McClelland et al., 2014; Connolly et al., 2018). We found markedly similar high DOC concentrations and C:N ratios within low-salinity lagoon waters following peak discharge in June (Table 2.1). While inputs from spring primary production (i.e., phytoplankton blooms and the growth of benthic/sea ice algae) may also contribute to the observed high DOC concentrations in June, $SUVA_{254}$ and $S_{275-295}$ values from these samples (Table 2.1) reveal a strong terrestrial-freshwater signal that resembles that of larger northern rivers during the freshet period (Spencer et al., 2008, 2009; Mann et al., 2012). These results suggest that lagoon DOM in June is strongly

influenced by recently produced vegetation leachates from rivers draining the North Slope of Alaska during the freshet. Inputs from primary production, on the other hand, appear to make up a relatively small component of the spring lagoon DOM pool. This may in part be because autochthonous DOM is more bioavailable and tends to degrade relatively quickly compared freshet-derived riverine DOM, which degrades on the order of weeks to months (Holmes et al., 2008; Mann et al., 2012). The quantities and composition of DOM between inside and outside lagoon sites are similar in June (Table 2.1), which indicates that river-borne DOM from the freshet overwhelms coastal waters during the late spring. The large terrestrial-freshwater contributions likely mask an autochthonous CDOM signal. These results align well with other studies from around the Arctic, which found that peak discharge in the spring accounts for the high observed DOC concentrations in coastal margins, when large north-flowing rivers deliver the vast majority of their annual export of freshwater and DOM (Amon, 2004; McClelland et al., 2012; Holmes et al., 2012). This demonstrates that our findings are consistent with studies conducted elsewhere in the Arctic despite major differences in scale.

Interestingly, we found a large spread in DOC concentrations and C:N ratios within low-salinity lagoon waters during June despite strong evidence that lagoon DOM is derived from terrestrial material (Figures 2.3 and 2.4). One possible explanation is that lagoons experience varying degrees of dilution as DOM from river water mixes with meltwater from sea ice during the break-up period (Harris et al., 2017). To investigate this further, we compared lagoon DOC concentrations and C:N ratios with stable oxygen isotope ($\delta^{18}O$) data from a subset of low-salinity (salinity < 5) lagoon water samples collected in June (Figure B.1a,b; data from Harris et al., 2017). Here we found that $\delta^{18}O$ does not correlate with lagoon DOC concentrations or C:N ratios as expected if dilution from meltwater was the primary driver of the observed spread in June DOC and C:N

data. Likewise, this finding indicates that differences in the number or size of rivers draining into lagoons cannot solely explain the observed trends either. Spatial differences in riverine concentrations of DOC and DON draining into these lagoons is perhaps a more reasonable explanation of the wide range in DOC concentrations and C:N ratios within low-salinity lagoon waters. A recent study found that concentrations of DOC and DON in rivers draining into or near our lagoon sites vary markedly during both the spring and summer (Connolly et al., 2018). The large range of fluvial concentrations of DOC and DON were attributed to spatial differences in the amount of soil organic matter in watersheds draining this region, which relates to their relative coverage by organic-rich coastal plain terrain versus organic-poor mountainous terrain (Connolly et al., 2018).

The observed decrease in lagoon DOC concentrations, C:N ratios, and $SUVA_{254}$ values between June and August can in part be explained by the exchange of water from the freshet with marine water from the Beaufort Sea during the open water period (Table 2.1). DOC concentrations, C:N ratios, and $SUVA_{254}$ values in estuarine lagoon waters generally fall in-between those found in fresh and marine lagoon waters (Figure 2.2), which indicates that conservative mixing between lagoon freshwater and marine DOM end-members plays a key role in lowering lagoon DOC concentrations by August. This is supported by an observable conservative mixing behavior in the DOM data with salinity between June and August (Figures 2.3 and 2.4). Given that DOC concentrations are highly variable in lagoon freshwaters in June, but marine DOC concentrations and $SUVA_{254}$ values are reasonably well-constrained (i.e., those found in April), the observed non-conservative spread in August DOM data with salinity could simply arise from the conservative mixing of marine water with lagoon freshwaters with varying starting DOC concentrations (Figures 2.3 and 2.4). We also found that waters outside of lagoons remain estuarine during August (Table 2.1), which provides evidence that freshwater and DOM

from the freshet residing outside of lagoons mixes slowly with the open ocean between the late spring and summer months. In other words, DOM from the freshet may actually mix back and forth between inside and outside of lagoons during this time period. The magnitude of freshwater exchange likely decreases later in the summer, however, when marine water from the Beaufort Sea has more thoroughly mixed with coastal waters adjacent to lagoons. The residence time of freshet-derived DOM in lagoons following spring sea ice break-up is likely affected by lagoon geomorphology, such as water depth and the number/size of openings between barrier islands (Harris et al., 2017).

In contrast, differences in the DOM variables between inside and outside lagoon sites provide evidence that additional factors affect the observed quantities of lagoon DOC in August. DOC concentrations and fluxes from northern Alaska streams and rivers are typically much lower in August due to a combination of low surface hydrologic flow and enhanced biological and photo-degradation in soil/surface water networks (Striegl et al., 2005; McClelland et al., 2014; Cory et al., 2014). Rivers draining the North Slope of Alaska also have lower C:N ratios during the summer, due to higher proportional DOM contributions from processed leachates in deeper active layer soils (Spencer et al., 2008; McClelland et al., 2014; Connolly et al., 2018). Thus changes in the composition and supply of DOM carried by rivers in the weeks/months following the freshet can help explain the decrease in lagoon DOC concentrations and C:N ratios between June and August. As discussed earlier, spatial variability in fluvial concentrations of DOC and DON draining into our lagoon sites is also an important consideration. Since river discharge decreases substantially following the freshet, differences in the size and number of rivers draining into lagoons may have a strong effect on lagoon DOM pools over the summer. Inputs from coastal erosion and supra-permafrost groundwater (i.e., groundwater flow through the active layer above permafrost) represent another major, but

largely unstudied source of DOM to lagoons that may be influencing the quantities and composition of summer lagoon DOM as well (Ping et al., 2011; Connolly et al., 2019a).

While we found similar $S_{275\text{-}295}$ values between June and August (Table 2.1), there appears to be more variability in $S_{275\text{-}295}$ values in estuarine lagoon waters than expected for a conservative mixture of fresh and marine water end-members (Figure 2.2). This demonstrates that DOM source/sink processes may also be affecting the observed quantities of lagoon DOC in the summer. It is well recognized that warmer temperatures that promote biological activity and intense photo-degradation over the summer reduces concentrations and alters the composition of DOM in Arctic surface waters (Spencer et al., 2009; Fichot and Benner, 2014; Cory et al., 2014). More specifically, Connelly et al. (2015) demonstrated that the composition of lagoon POM in August reflects consumer-mediated transformations, which probably alters summer DOM as well. The wide range in our August $S_{275\text{-}295}$ data indicates that photo-degradation, as well as mixing between highly photo-degraded DOM in marine water with unaltered terrestrial DOM, could be affecting lagoon DOM concentrations during the summer (Helms et al., 2008).

In comparison to June and August, April results show that marine water that is inherently low in DOC concentrations, C:N ratios, and $SUVA_{254}$ values replaces lagoon water from the previous spring/summer over the course of the winter (Table 2.1). The marked similarity between June and April DOM data in hypersaline lagoon waters indicates that in some cases, marine water from the winter remains in lagoons if late spring runoff is not strong enough to vertically mix the entire water column. We found marked differences in lagoon DOM variables between inside and outside lagoons sites, indicating that additional factors increase DOC concentrations and lower $S_{275\text{-}295}$ values within lagoons relative to adjacent coastal waters (Table 2.1). This is also supported by similar patterns in the DOM data between the marine and hypersaline lagoon water end-

members (Figure 2.2). The increases in DOC concentrations that we observed with salinity during the winter could be explained by two mechanisms: the introduction of new sources of DOM or pre-existing re-concentrated DOM. As ice forms over the winter, the process of water exclusion can re-concentrate DOM in the underlying lagoon water column (Macdonald and Yu, 2006). This process would be most evident in lagoons that already have high concentrations as winter approaches and/or experience little water exchange with the open ocean (thus promoting hypersalinity). While the build-up of river water could increase lagoon concentrations of DOC and DON prior to the winter (Cauwet and Sidorov, 1996; Kuzyk et al., 2008), we found different trends in DOC concentrations and C:N ratios between marine and hypersaline lagoon waters (Figures 2.2b,c, 2.3, and 2.4a). This suggests that new internal sources of DOM are being added to lagoons over the winter. Inputs of regenerated DOM to lagoons from *in situ* degradation of POM could be one possible source. Connelly et al. (2015) found that these lagoons contain moderate amounts of POM in April, derived from spring/summer fluvial organic matter as well as from decomposing detritus, such as diatoms, dinoflagellates, and benthic invertebrates that thrive year-round (Schell et al., 1984; Dunton et al., 2006; Churchwell et al., 2015). Low dissolved oxygen levels were also found in April, suggesting that heterotrophic communities (metazoan and microbial) remain active beneath the ice despite freezing water temperatures and nutrient limitation (Darnis and Fortier, 2012; Nguyen et al., 2012; Connelly et al., 2015). The addition of regenerated DOM that contains higher proportions of DON relative to DOC likely result in higher DOC concentrations, but lower C:N ratios over the winter, with the strongest evidence appearing in isolated hypersaline lagoons.

The observed trends in lagoon C:N over the winter could also arise from inputs of regenerated DOM as water circulates through decomposing POM in lagoon benthic sediments and detritus (Giblin et al., 1997; Joyce and Anderson, 2008). Several studies

have found that inorganic nitrogen builds-up beneath the ice within Arctic coastal systems due to the remineralization of organic matter and limited water movement (Cauwet and Sidorov, 1996; Hardison et al., 2017). High concentrations of ammonium have been observed in our lagoon sites in particular (Dunton and Crump, 2014). Thus the remineralization of organic material held in lagoon sediments is likely supplying DOM to the water column over the winter as well. Since organic matter in lagoon sediments probably shares similar POM sources as those found in the water column, then we would expect similar ratios of C:N from benthic inputs of DOM. The presence of regenerated DOM over the winter is supported by our trends in April $S_{275\text{-}295}$, where we found higher $S_{275\text{-}295}$ values inside lagoons compared to outside lagoon sites (Table 2.1). Likewise, we found higher $S_{275\text{-}295}$ values in hypersaline waters in comparison to marine waters (Figure 2.2d). These collective results indicate benthic-coupling within lagoons is strong over the winter, and may introduce processed DOM that contains higher proportions of low-molecular weight compounds.

Our PCA reveals that both mixing and processing effects account for the high percentage of variability in our lagoon DOM data explained by PC1 and PC2. The positive correlation between PC1 and high values of DOC, C:N, and $SUVA_{254}$ is a strong indicator that PC1 represents the separation of allochthonous versus autochthonous-derived DOM (Table 2.2; Figure 2.5). It is clear that low-salinity samples collected in June tend to have a strong positive relationship with allochthonous-derived DOM, supporting our conclusion that June lagoon DOM pools are being affected by runoff from the spring freshet and to a much lesser degree, by inputs from *in situ* primary production. Likewise, the wide range of points representing June samples on PC1 indicates that variations in riverine inputs to lagoons helps explain the spread in June DOC data. We see that some mid-salinity lagoon samples collected in August have a weak but positive

relationship with allochthonous-derived DOM, indicating that terrestrial inputs make up an important component of summer lagoon DOM pools as expected. On the other hand, the weaker relationship of August data on PC1 could arise from DOM derived from *in situ* primary production. Many mid-to-high salinity lagoon samples collected in August, and almost all samples collected in April, have a negative relationship with allochthonous DOM (or a positive relationship with autochthonous DOM). The transition on PC1, from low-salinity June lagoon waters containing allochthonous DOM to mid/high salinity August and April lagoon waters containing autochthonous DOM, demonstrates that mixing between these end-members explains the variability in DOM data represented by PC1. Given PC1 explains nearly half of the variability in our DOM data (Table 2.2), then mixing between freshwater and marine sources is clearly an important driver of seasonal variations in the quantities and composition of DOM.

We see a strong positive correlation between PC2 and high values of $S_{275\text{-}295}$, a weak positive correlation with high values of DOC and C:N, and a strong negative correlation with high values of $SUVA_{254}$ (Table 2.2; Figure 2.5). These collective results suggest that variability explained by PC2 reflects mixing as well as processing effects on lagoon DOM pools. Both mixing and DOM transformation processes would be expected to change the molecular size and aromaticity of lagoon DOM. For instance, highly photo-degraded and autochthonous-derived DOM typically corresponds to decreases in DOM molecular size and aromaticity, whereas allochthonous DOM typically contains high molecular weight, aromatic dominated compounds (Nelson et al., 2004; Retamal et al., 2007; Helms et al., 2008; Spencer et al., 2009; Romera-Castillo et al., 2010). It is clear that low-salinity June samples tend to have a weak or no relationship on PC2, which is expected given lagoon spring DOM pools are primarily made up of land-derived inputs that have not been thoroughly mixed with marine water or degraded yet. The wide range

of DOM data on PC2 among August and April lagoon samples do not show any clear patterns with salinity, demonstrating that some degree of variability represented by PC2 cannot be explained solely by simple conservative mixing of freshwater and marine end-members. Photo- or consumer-mediated degradation of DOM and/or the introduction of regenerated forms of DOM in August and April (when river inputs are typically lower) could result in the observed range of DOM molecular sizes and aromatic compounds over the summer and winter periods. Given PC2 explains ~37 % of the variability in our DOM data (Table 2.2), then processing is another important factor driving seasonal variations in the quantities and composition of DOM.

SUMMARY AND IMPLICATIONS FOR A CHANGING ARCTIC

Nearshore estuaries in northern Alaska are well recognized as highly productive ecosystems throughout the year and yet, we know relatively little about seasonal variations in the amounts and sources of DOM that form the basis of this productivity. Here we investigated the seasonality of the quantities and composition of DOM within lagoon systems along the eastern Alaska Beaufort Sea coast in June (spring), August (summer), and April (winter). We found that the concentrations and sources of DOC vary strongly between the spring and winter periods. Shifts in lagoon DOM pools are tightly coupled to changes occurring at their land and ocean margins, including distinct seasonal transitions in runoff, ice coverage, and connectivity with the open ocean. Lagoon DOM in the spring is dominated by snowmelt-driven runoff from the North Slope of Alaska. Interestingly, low-salinity lagoon waters still exhibit a high degree of variability in DOC concentrations and C:N ratios in the late spring, which may be due to spatial differences in riverine DOM fluxes across lagoon domains. The wide range of lagoon DOM quantities in the summer is driven primarily by variability in the mixture of land-derived

freshwater and marine sources, but processing effects (such as biological and photo-degradation) may also be important and require further consideration. Lagoon DOM is typically lower during the winter since lagoons contain predominantly marine water, but there is strong evidence that regenerated forms of DOM from *in situ* production are important during this time. Overall this study provides critical baseline understanding of seasonal changes in DOM as a resource supporting biological production, which is inherently linked to local food web dynamics and the cycling of carbon and nitrogen in coastal lagoon ecosystems in northern Alaska. This information is essential to assess responses to and feedbacks with the immediate threats of Arctic warming.

Arctic estuaries are especially vulnerable to climate change impacts given their unique position between changes that are already occurring at their land and ocean margins. Many of these impacts are associated with shifts in the timing and magnitude of river discharge and sea-ice coverage as well as the release of organic matter as permafrost thaws. Air temperatures are rising in the Arctic, leading to an increase in annual river discharge from Alaska's North Slope (Peterson et al., 2006). The timing of peak freshet discharge is occurring earlier in the spring (McClelland et al., 2006). Sea-ice extent during the summer is decreasing across the Arctic, causing the duration of the open water period to increase (Parkinson et al., 1999; Zhang et al., 2000; Yang et al., 2002; Hinzman et al., 2005; Stroeve et al., 2008). Lastly, major shifts in surface and subsurface hydrology as permafrost thaws are anticipated to alter the movement of nutrients and organic matter from land to Arctic coastal waters (Frey and McClelland, 2009).

These collective climate-linked impacts will undoubtedly impart numerous, seasonally-distinct, effects on nearshore lagoon ecosystems in northern Alaska. Since many lagoon systems are coupled to small watersheds that drain organic-rich coastal plain terrain, we anticipate that increases in the export of land-derived DOM from rivers,

groundwater, and coastal erosion will provide a greater source of energy supporting lagoon food webs during the spring and summer (McClelland et al., 2014; Harris et al., 2018; Connolly et al., 2019a). However, the degradation of this DOM will undoubtedly increase CO_2 release from lagoon systems, possibly constituting a positive feedback to climate change. If the timing of sea ice break-up shifts to earlier in the year, lower incident light levels may decrease the magnitude of the spring phytoplankton bloom, but promote longer periods of uptake and cause inorganic nutrients to become less available for summertime biological activity. If the freshet occurs much earlier than sea ice break-up in the future, nutrient-rich waters that accumulated over the winter may be flushed from lagoons and replaced with nutrient-poor river water. This could cause a widespread decrease in peak primary production within nearshore lagoons as sea ice retreats. These effects may be counteracted by enhanced mineralization of land-derived DOM into inorganic nutrients, but potential increases in sediment loads would likely decrease light attenuation and limit primary production. Lastly, projected increases in storm frequency and intensity during a longer open water period will facilitate greater exchange of marine water into and out of lagoons over the summer (Hinzman et al., 2015), which may increase the availability DOM and nutrients for biological production in waters of the inner Beaufort Sea shelf, but decrease the availability of DOM and nutrients in lagoon ecosystems. The synergy of these climate-driven impacts on lagoon ecosystems is unclear. Additional studies are needed with a strong sense of urgency to understand their immediate compounding effects and future feedbacks.

Table 2.1. Seasonal changes in salinity and DOM values from inside and outside the lagoon sites. Values are ± 1 standard error. Numbers in parentheses reflect sample size (*n*). Seasonal values that share a different lower-case letter are significantly different within inside and outside lagoon groups. Values that are bolded are significantly different between inside and outside lagoon groups for the same season. A threshold of $\alpha = 0.05$ was used for pair-wise comparisons.

Season	Salinity	DOC (μmol C L^{-1})	DOC:DON (molar ratio)	$SUVA_{254}$ (L mg C^{-1} m^{-1})	$S_{275\text{-}295}$ ($\times 10^{-3}$ nm^{-1})
Inside Lagoons					
June	14.8 ± 2.8 (*39*) [a]	195 ± 11 (*38*) [a]	25.8 ± 2.0 (*32*) [a]	3.56 ± 0.12 (*33*) [a]	13.7 ± 0.22 (*33*) [a]
August	**21.7 ± 0.6 (*90*)** [b]	**130 ± 6.1 (*68*)** [b]	18.1 ± 0.8 (*67*) [b]	**2.86 ± 0.13 (*50*)** [b]	14.7 ± 0.58 (*50*) [a]
April	37.1 ± 0.8 (*30*) [c]	**117 ± 4.9 (28)** [b]	16.3 ± 1.5 (*26*) [c]	2.25 ± 0.15 (*26*) [c]	**16.6 ± 0.89** (*26*) [b]
Outside Lagoons					
June	7.6 ± 3.6 (*5*) [a]	222 ± 20 (*5*) [a]	36.1 ± 4.7 (*5*) [a]	3.56 ± 0.12 (*4*) [a]	14.0 ± 0.39 (*4*) [a]
August	**25.4 ± 0.8 (*32*)** [b]	**90.3 ± 3.6 (*22*)** [b]	16.6 ± 1.6 (*22*) [b]	**2.34 ± 0.20 (*11*)** [b]	15.8 ± 1.9 (*11*) [ab]
April	31.1 ± 0.2 (*4*) [b]	**80.3 ± 2.2 (4)** [b]	15.1 ± 1.9 (*3*) [b]	1.95 ± 0.23 (*4*) [b]	**10.6 ± 0.47** (*4*) [ac]

Table 2.2. Principal Components Analysis scores of the first two principal components (PC1 and PC2) using lagoon DOC concentration, C:N, $SUVA_{254}$, and $S_{275-295}$ data. The % variances explained by PC1 and PC2 are indicated.

Variables	PC1	PC2
DOC (μM)	0.643	0.208
C:N (molar ratio)	0.631	0.274
$SUVA_{254}$ (L mg C^{-1} m^{-1})	0.427	−0.581
$S_{275-295}$ ($\times 10^{-1}$ nm^{-1})	−0.078	0.738
% of variance	43.6	38.8

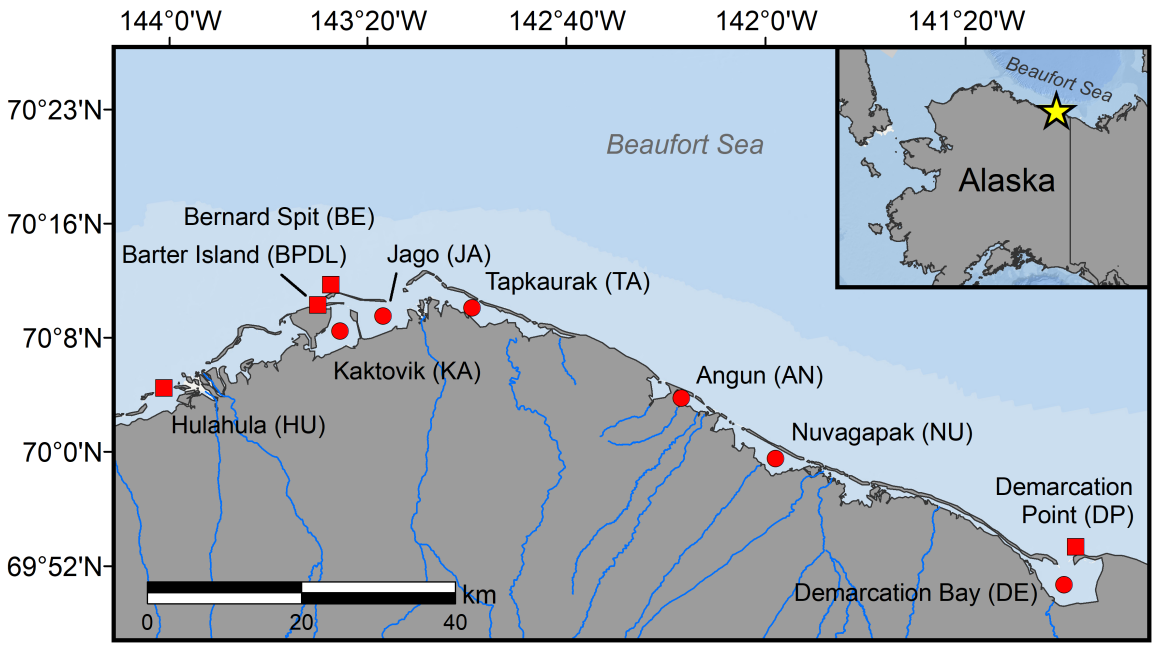

Figure 2.1. Map of the inside (circles) and outside (squares) lagoon study sites along the eastern Alaska Beaufort coast visited during April, June, and August between 2011 and 2013.

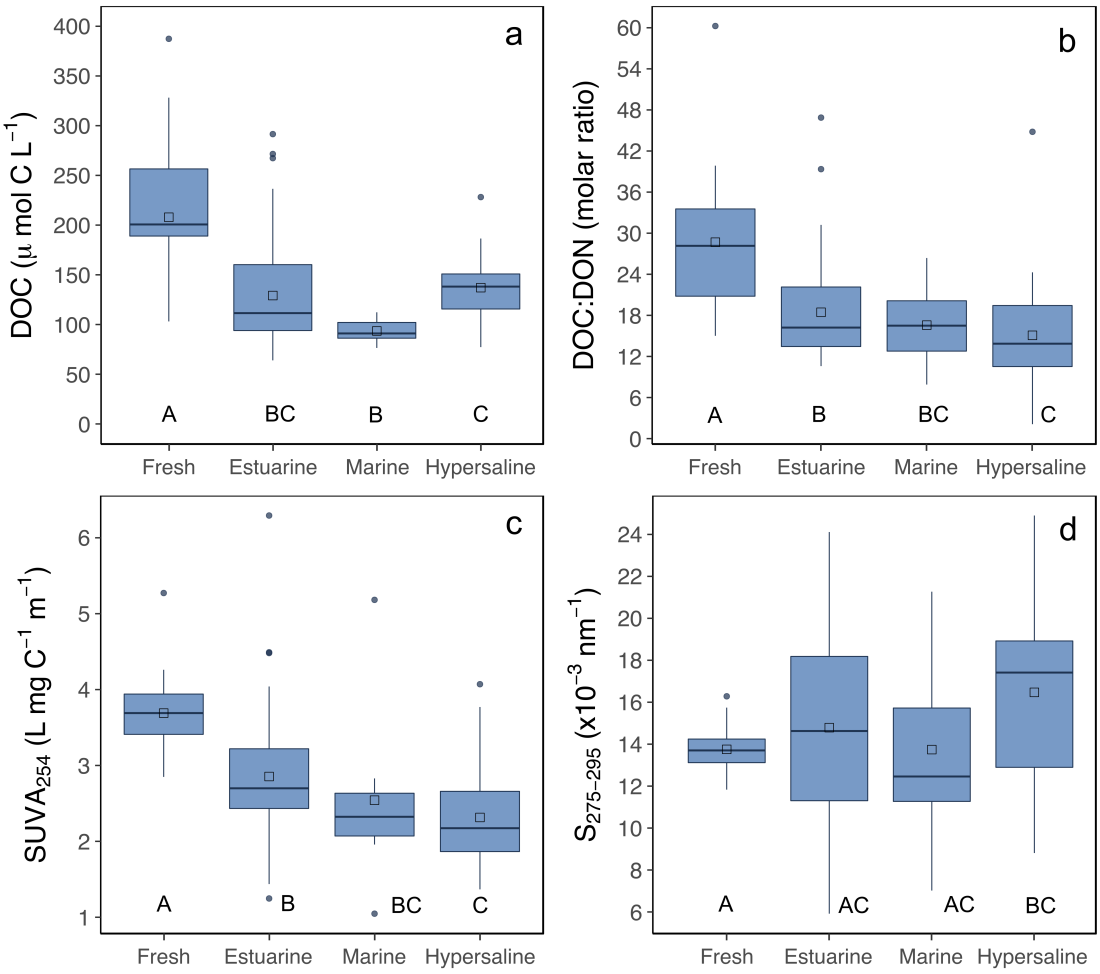

Figure 2.2. Boxplots of (a) DOC concentration, (b) C:N molar ratios (c), $SUVA_{254}$, and (d) $S_{275\text{-}295}$ values of lagoon samples collected in this study grouped by the following salinity bins: fresh (0–5), estuarine (6–30), marine (31–33), and hypersaline (34–44). Groups that share a letter are not significantly different ($\alpha = 0.05$). Whiskers extending from the hinge to the highest or lowest value are within 1.5 × the inter-quartile range of the hinge. Data points beyond the end of the whiskers are outliers as specified by Tukey. Hollow squares represent mean values.

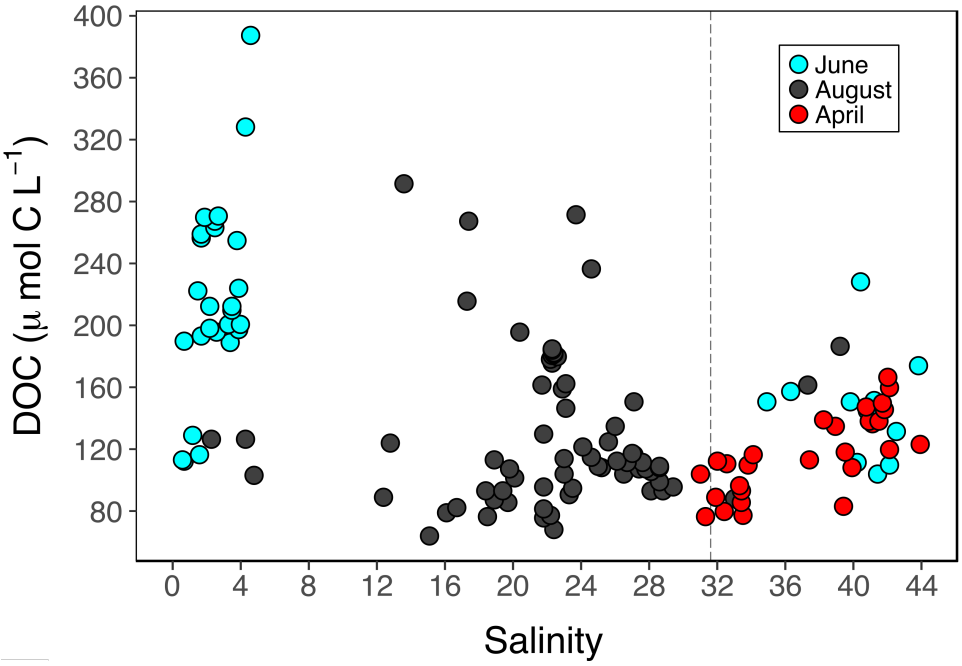

Figure 2.3. Concentrations of lagoon DOC and their respective salinity values from water samples collected during June (teal), August (black), and April (red) for all sites visited between 2011 and 2013. The dashed gray line indicates the salinity of the polar mixed layer, which represents the open ocean salinity end-member (31.6 ppt; Alkire and Trefry, 2006).

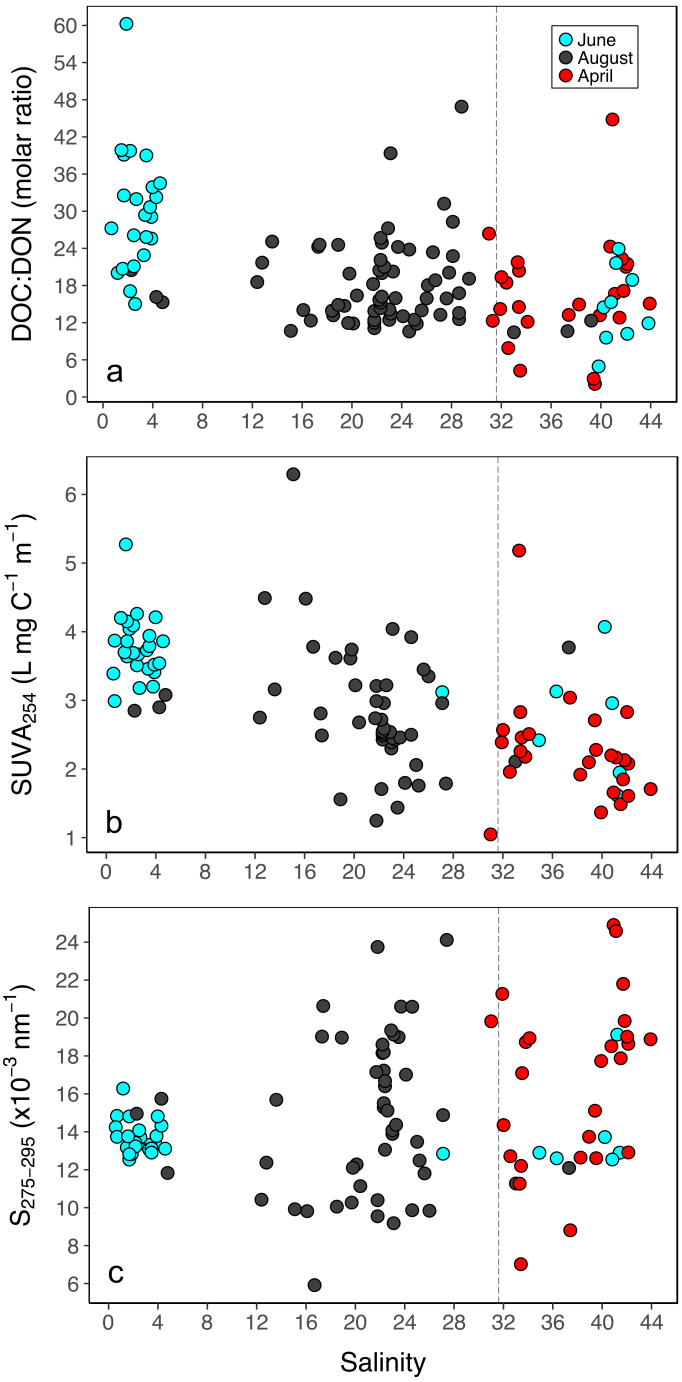

Figure 2.4. Lagoon (a) C:N, (b) $SUVA_{254}$, and (c) $S_{275\text{-}295}$ values plotted against their measured salinity values from water samples collected during June (teal), August (black), and April (red) for all sites visited between 2011–2013. The dashed line indicates polar mixed layer salinity.

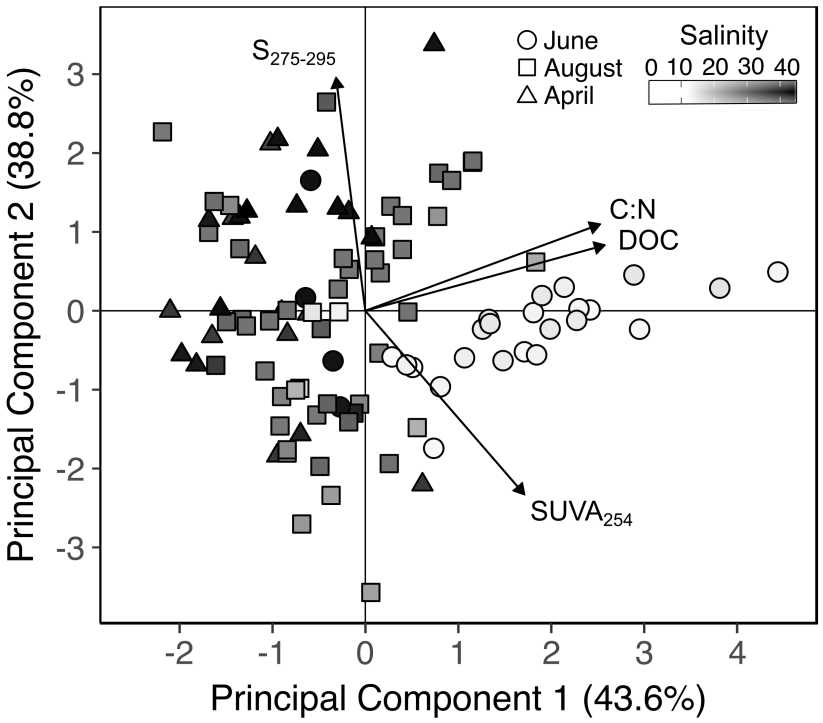

Figure 2.5. Principal Components Analysis of lagoon water DOM variables: DOC concentration, C:N ratios, and CDOM compositional parameters, $SUVA_{254}$ and $S_{275\text{-}295}$. Data points grouped by month are represented by different shapes (June = circles; August = squares; April = triangles) and shaded relative to their salinity values along a gradient from low (white) to high (black).

Chapter 3: Groundwater as a major source of dissolved organic matter to Arctic coastal waters

ABSTRACT

Groundwater is projected to become an increasing source of freshwater and nutrients to the Arctic Ocean as permafrost thaws, yet few studies have attempted to quantify groundwater inputs to Arctic coastal waters under contemporary conditions. New measurements along the Alaska Beaufort Sea coast show that dissolved organic carbon and nitrogen (DOC and DON) concentrations in supra-permafrost groundwater (SPGW) near the land-sea interface are up to two orders of magnitude higher than in rivers. This groundwater dissolved organic matter (DOM) is sourced from readily leachable organic matter held in surface soils as well as deeper centuries- to millennia-old soils that extend into thawing permafrost. SPGW delivers upwards of 2,128 m^3 of freshwater, 70.6 kg of DOC, and 4.3 kg of DON to the coastal ocean per km of shoreline per day during late summer. This study provides novel estimates of SPGW DOM fluxes to Arctic coastal waters. These fluxes are substantial under contemporary conditions, and are expected to increase as massive stocks of trapped organic matter in permafrost are liberated in a warming Arctic.

INTRODUCTION

Groundwater is the largest active reservoir in the global hydrologic cycle and its movement from land to sea represents a major source of freshwater and nutrients for coastal ecological and biogeochemical processes (Moore, 2010). However, there is little information on direct groundwater nutrient export from watersheds to the coastal ocean in the Arctic (Lecher, 2017). This is partly because of a perception that permafrost constrains water to surface flow paths on land in northern high-latitude coastal regions. Supra-permafrost groundwater (SPGW) does, however, flow through seasonally thawed active layer soils (surficial soils above permafrost) during the summer and early fall periods (Romanovsky and Osterkamp, 2000; Walvoord and Striegl, 2007). Thus SPGW may potentially deliver appreciable quantities of terrestrially-derived nutrients to Arctic coastal waters. SPGW is firmly separated from sub-permafrost groundwater, which flows beneath several hundred meters of permafrost on the Arctic coastal plain (Jorgenson et al., 2008; Kane et al., 2013) and is therefore not a major component of groundwater at the coastal land-sea interface. In other words, SPGW is the principal form of land-derived groundwater entering nearshore coastal waters in the Arctic.

In the Arctic, SPGW flow and material transport from soils are tightly coupled because soil-water interactions are largely confined to the shallow (typically < 1 m), but laterally extensive and highly permeable active layer (Kling et al, 1991; Kling, 1995; Neilson et al., 2018). Primary productivity exceeds soil decomposition rates in northern high-latitude permafrost landscapes, leading to soils that contain high amounts of organic matter and with a high capacity to release dissolved organic matter (DOM) to aquatic systems (Judd and Kling, 2002). DOM production and export is highest during the spring (May to June) when the thawed portion of the active layer is shallow and water flow is confined to near surface organic-rich soils and overlying litter layers (Guo and

Macdonald, 2006; Spencer et al., 2008; Khosh et al., 2017; Lehn et al., 2017). Peak runoff during the spring facilitates the export of large amounts of DOM via surface waters, which accounts for the majority (up to 75 %) of annual riverine fluxes of DOM to the Arctic Ocean (Finlay et al., 2006; McClelland et al., 2006; Townsend-Small et al., 2011; Holmes et al., 2012; McClelland et al., 2014). Terrestrial DOM production and export is lower during the summer (July to October) when active layer thaw exposes deeper soil horizons and groundwater recharged from local rainfall and melting ground ice saturates higher proportions of mineral soils (McNamara et al., 1997; MacLean et al., 1999; Petrone et al., 2006). For these reasons, concerted efforts have been made over the past decade to improve understanding of SPGW connectivity to inland waters across the pan-Arctic domain. These studies reveal that groundwater processes within the active layer govern the summer transfer of organic and inorganic nutrients from land to streams and therefore provide a control for riverine export of DOM to the coastal ocean (Striegl et al., 2005; Walvoord and Striegl, 2007; O'Donnell et al., 2012; Neilson et al., 2018).

In contrast, very few studies have focused on the role that groundwater plays in the direct transfer of organic matter and inorganic nutrients from land to the coastal ocean in the Arctic (Lecher, 2017). Estimates of groundwater inputs to the coastal ocean are needed to support a more complete understanding of what fuels biological production and biogeochemical cycling in Arctic coastal waters. Climate change adds some urgency to this need since warming is increasing groundwater discharge across circumpolar regions (Smith et al., 2007; St. Jacques and Sauchyn, 2009; Walvoord et al., 2012), enhancing organic matter decomposition in the active layer, and liberating globally significant stores of organic matter held in northern high-latitude soils and permafrost (Tarnocai et al., 2009; Frey and McClelland, 2009; Schuur et al., 2013; Hugelius et al., 2014; Schädel et al., 2016). This is concerning from a climate feedback perspective because the

reintroduction of permafrost-derived organic matter to the contemporary global carbon cycle constitutes a positive feedback to warming (Schuur et al., 2015; Spencer et al., 2015; Drake et al., 2015; Ward and Cory, 2015; Vonk et al., 2015). A baseline understanding of how groundwater mobilizes organic matter held in coastal soils and permafrost in the Arctic is missing. This needs to be filled in order to predict responses to and feedbacks with climate change.

This study examines the leaching potential of DOM, which is reported herein as dissolved organic carbon and nitrogen (DOC and DON), from nearshore Arctic soils and quantifies inputs of SPGW DOM to coastal waters of the eastern Alaska Beaufort Sea. We first determined the relationship between soil organic carbon (SOC) and nitrogen (SON) contents residing in different active layer and permafrost soil horizons along the coast and the production and leaching potential of DOM from this soil organic matter (SOM). We then determined the relationship between leachable DOM sources and direct SPGW DOM inputs using radiocarbon (^{14}C) data from SPGW DOM and leachable soil-DOM samples. Lastly, we estimated DOM fluxes using average concentrations of SPGW DOC and DON paired with groundwater discharge estimates that were derived from a steady-state excess radon (^{222}Rn) mass balance model (Dimova and Burnett, 2011; Dimova et al., 2013, 2015; Appendix C). Data from groundwater and nearby river water were used to compare SPGW and riverine inputs to the Alaska Beaufort Sea coast. To the best of our knowledge this is the first study to quantify fluxes and sources of DOM in direct SPGW inputs to Arctic coastal waters.

Field measurements and sample collection were conducted in mid-to-late August 2014, 2015, and 2017. We sampled four soil horizons (0–5 cm, 15–20 cm, 30–40 cm, and 5–10 cm below the permafrost frozen boundary) at three sites on the landward sides of Kaktovik and Jago Lagoons on the eastern Alaska Beaufort Sea coast (red circles in

Figure 3.1). Thaw depths (the depth of the ice table) at the soil collection sites were 40 cm, 53 cm, and 54 cm, meaning permafrost was sampled at respective depths of approximately 45–50 cm, 58–63 cm, and 59–64 cm. Soil-DOM leaching experiments were conducted by mixing bulk soils with a 0.001 N $NaHCO_3$ Milli-Q solution (Wickland et al., 2007) for 24 hours at 4 ºC and then filtering leachate through a 0.7-µm glass fiber filter (pre-combusted at 450 °C > 5 hrs). ^{222}Rn activity was measured concurrently in lagoon water, SPGW, and lagoon benthic sediments as components of the mass-balance model. SPGW was sampled using piezometers installed to permafrost on the beach of Kaktovik and Jago Lagoons (yellow stars in Figure 3.1). River water data was collected previously from the Hulahula, Okpilak, and Jago Rivers for comparison (blue circles in Figure 3.1).

MATERIALS AND METHODS

Water Sampling

SPGW DOM samples were collected along the landward sides of Kaktovik Lagoon on 16–17 August 2014 (*n = 10*) and 8–12 August 2015 (*n = 10*), and then along Jago Lagoon on 17 August 2017 (*n = 15*). In total, 35 groundwater DOM samples were collected during the study period. SPGW was extracted using piezometer wells that were installed to the depth of frozen ground (~1 m) running parallel to the shoreline. Samples from these piezometers capture groundwater that has moved through the active layer to the lagoons without becoming channelized surface-water flow. Some samples were also collected along a transect running from the beach to ~50 m inland as well as from groundwater springs that emerge on the beach as small surface water streams in order to capture SPGW in transit to the coast. Groundwater was collected using a peristaltic-pump

system attached with acid washed and Milli-Q rinsed Master-Flex tubing. Groundwater was pumped until clear water was flowing and then filtered through a 0.45 μm GeoTech membrane capsule directly into acid washed and Milli-Q rinsed high-density polyethylene (HDPE) or polycarbonate bottles. Samples were transported in a cooler to the U.S. Fish & Wildlife Arctic National Wildlife Refuge (ANWR) facilities in Kaktovik, Alaska where they were stored frozen until analysis. River water DOM samples were collected previously in August 2011 and 2012 with a similar sampling procedure. SPGW and lagoon water ^{222}Rn samples were collected with widely used procedures (Dimova and Burnett, 2011; Dimova et al., 2013, 2015). Four discrete groundwater ^{222}Rn samples were collected along a transect from the beach to the tundra surface at the Kaktovik Lagoon site on 12 August 2015. These included three SPGW samples from piezometers and one from a small groundwater-fed stream. Lagoon water ^{222}Rn samples were collected from the interior and perimeter areas of Kaktovik Lagoon using a submersible pump deployed near the lagoon bottom on 21 and 22 August 2017. The water was directly pumped into a degassing chamber connected to three radon-in-air gas analyzers (Durridge RAD7 connected to the RAD-AQUA module) which analyzed the samples in sequence every 10 minutes over a 30 minute cycle, i.e., each RAD7 measured ^{222}Rn every 30 minutes. This work was conducted over two consecutive days in order to sample the entire lagoon.

Soil and Lagoon Sediment Sampling

Three soil cores that include the seasonally thawed active layer and shallow permafrost were collected within high-centered polygons (the primary surface type) on the landward sides of Kaktovik Lagoon on 9 August 2015 and Jago Lagoon on 8–9 August 2016 for bulk SOM measurements. At all three sampling sites, we observed a general transition of soil type with depth from organic-rich peat and litter at the surface

(~0–10 cm), to more mineral-like soil (~10–20 cm), to a mixture of peat and muck (~20 cm to frozen ground), and to largely muck below frozen ground. Soil samples were collected by hand at four depths: surface–5 cm, 15–20 cm, 30–40 cm, and at 5–10 cm below the ice table. These soil increments were chosen in order to gain a wide range of soil types and depths within the active layer and shallow permafrost where changes in organic matter quantity and age are anticipated. Bulk soils were placed into whirl-packs, stored frozen at the ANWR facility, and taken back to the University of Texas at Austin, Marine Science Institute (UTMSI) for soil-water leaching experiments and chemical analysis. Seven benthic sediment samples were collected from the interior and perimeter areas of Kaktovik Lagoon on 23 August 2017 for ^{222}Rn activity measurements. Bulk sediments were placed in plastic Ziploc bags, dried, and stored at the University of Texas at Austin until ^{222}Rn analysis.

Soil-water Leaching Experiments

Soil samples (> 300 g frozen) were allowed to thaw in a refrigerator (4 °C) until the soils appeared moist, but not dripping with water (at most 24 hours). Thawed soils of the same type were then placed on combusted aluminum foil (550 °C for 1 hour) and gently homogenized. Care was taken to maintain common soil features and to ensure the sample remained close to its natural condition. This also included removing large roots and anomalous material not representative of the soil horizon. Three subsamples were collected to obtain an average wet weight: dry weight ratio. Subsamples were dried in an oven at 60 °C for 24 hours. Thawed soils were kept in the refrigerator for a total of 48 hours before leaching. Sample wet weight: dry weight ratios were used to calculate the equivalent of 35 g of dry soil. Field-moist soils were then placed in a combusted glass beaker with 500 mL of a 0.001 N $NaHCO_3$ Nanopure solution (> 18.0 Ω-cm), which was

used to buffer changes in pH and mimic the natural ionic strength of water in natural systems (Wickland et al., 2007). The wet soil: solution ratio of the leaching experiments ranged from ~1:10 to 1:4. The yields of DOC per g soil were similar between these soil: solution ratios in a study that took a more rapid leaching approach (Dou et al., 2008). We expect no bias in our results related to differences in soil: solution ratios since our leaching experiments were conducted for a longer period of time. The beakers were covered with combusted aluminum foil and stored in a refrigerator at 4 °C. Beakers were shaken intermittently during a 24 hour incubation period to simulate groundwater flow through the soil profile. Following, the soil-water was filtered through a combusted glass filtration system holding a combusted 0.7 μm glass fiber filter. The filtrate was then dispensed into acid washed and Milli-Q rinsed polycarbonate bottles and stored frozen until DOC and DON concentration and $DO^{14}C$ analysis. Bulk soils were stored in a drying oven (60 °C) for several weeks before they were finely ground using a mortar and pestle. Ground soil samples went through a vapor fumigation acid/base treatment step to remove inorganic carbon. This step involved storing soil samples in a vacuum-sealed desiccator in a drying oven (60 °C) with a beaker of concentrated HCl for 24 hours. Soil samples were then removed and placed in another vacuum-sealed desiccator with a dish of NaOH pellets, and again stored in a drying oven at 60 °C for another 24 hours. This latter step was conducted to neutralize excess HCl that was not absorbed by the sample.

Chemical and Tracer Data Collection and Analysis

Concentrations of DOC and total dissolved nitrogen (TDN) were determined using high-temperature oxidation performed on a Shimadzu TOC analyzer fitted with a total nitrogen module for chemiluminescence detection of nitrogen. Inorganic nitrogen (NO_3^- and NH_4^+) was analyzed on a Seal-QuAAtro inorganic nutrient analyzer.

Concentrations of DON were calculated from TDN minus NO_3^- plus NH_4^+. NO_3^- measurements made on the Seal-QuAAtro are the equivalent to NO_3^- plus NO_2^-. All 35 groundwater samples were measured for DOC, whereas the 20 samples collected in 2014 and 2015 were measured for DON. Riverine DOC and DON concentrations near Kaktovik Lagoon were estimated using the average of samples collected in August 2011 from the Hulahula (*n = 1*), Jago (*n = 1*), and Okpilak (*n = 2*) rivers in Connolly et al. (2018). For the Okpilak River, two samples were averaged prior. Collective riverine DOC and DON concentrations for the entire North Slope of Alaska were estimated using the average of data from the Turner (*n* = 1), Okpilak (*n* =4), Hulahula (*n* = 1), Jago (*n* = 1), Canning (*n* = 1), Kuparuk (*n* =5), Sagavanirktok (*n* =5), and Colville (*n* = 3) rivers between July and the end of September 2006–2012 from data in Connolly et al. (2018).

We analyzed $DO^{14}C$ on SPGW samples collected at three individual locations in August 2015. A single river water composite sample was formed from equal amounts of water collected in August 2011 from the Hulahula, Okpilak, and Jago rivers for $DO^{14}C$ analysis. DOC concentrations are similar enough between river sites that we do not suspect any individual river disproportionately affected the collective $DO^{14}C$ age. DOC samples were prepared for ^{14}C analysis using the UV-oxidation method (Beaupré et al., 2007) at the Woods Hole Oceanographic Institution, National Ocean Sciences Accelerator Mass Spectrometry facility (WHOI/NOSAMS). Sample water was diluted with pre-treated UV-oxidized nanopure water (to bring the total volume up to 1 L) and placed in a quartz reactor. The combined sample water plus treated nanopure water solution was acidified with 35 g of ultra-high purity (UHP), UV-treated full strength phosphoric acid and then purged with UHP nitrogen gas to remove any inorganic carbon. Pure UHP O_2 was subsequently sparged through the system to provide an oxidant for the UV-oxidation of DOC. The sample was then oxidized with UV and the resulting CO_2

was transferred to a vacuum line and cryogenically purified. Purified CO_2 gas samples were converted to graphite targets by reducing CO_2 with an iron catalyst under 1 atm H_2 at 550°C. Bulk soil samples were also high-temperature combusted using an Elementar el Vario Cube C/N analyzer. Bulk soil % C and % N were quantified during this step. The resulting CO_2 was transferred to a vacuum line and cryogenically purified. The purified CO_2 gas samples (soil C) were converted to graphite targets using a closed-tube Zn reduction CO_2 graphitization method (Xu et al., 2007). Targets were subsequently analyzed for stable and radiocarbon isotopes ($\delta^{13}C$ ‰ and ^{14}C as fraction modern carbon). All $\Delta^{14}C$ data (in ‰) were corrected for isotopic fraction using measured $\delta^{13}C$ values that were quantified during the ^{14}C-AMS procedure. We measured $\delta^{13}C$ in these samples separately on a VG Prism Stable Mass Spectrometer at NOSAMS. $\Delta^{14}C$ and radiocarbon age were determined from percent modern carbon using the year of sample analysis according to Stuiver and Polach, (1997).

Underway boat-based ^{222}Rn measurements were made around Kaktovik Lagoon using a circuit of three RAD7 Radon-in-air monitors (Durridge Co., Inc.) connected to a RAD AQUA device following procedures outlined in Dimova and Burnett (2011) and Dimova et al. (2013). The survey started after the system reached full gas/radioactive equilibrium. Measurements at ~1 m depth from the lagoon bottom were made in survey mode while driving a small inflatable boat around the lagoon. To optimize spatial resolution, the three RAD7 units analyzed samples staggered with 15-min intervals with water pumping at flow rates > 6 L min^{-1}. ^{222}Rn concentrations shown at each location in Figure C.1 represent an average of a continuous measurement made along some distance traveled before each RAD7 instrument calculated the average. ^{222}Rn concentrations in SPGW samples were collected using the Wat-250 ml protocol (RAD AQUA). ^{222}Rn

production measurements were conducted with dry lagoon sediments (ranging from 328 to 546 g) using a RAD bulk emissions chamber and methods outlined in the user manual.

Estimation of Groundwater Fluxes using ^{222}Rn

Total groundwater discharge was calculated using a steady-state excess ^{222}Rn mass balance model as described in Dimova and Burnett (2011) and Dimova et al. (2013). It is important to note that there are several primary assumptions of the model: (1) lagoon ^{222}Rn used for the calculation reflects the lagoon average concentrations over days to weeks; (2) the only significant ^{222}Rn source is from the tundra active layer and lagoon benthic sediments, and does not include water that enters the lagoon via river inputs; and (3) the only losses of ^{222}Rn are due to decay and atmospheric evasion. In addition, we assume marine inputs do not affect the ^{222}Rn inventory in Kaktovik Lagoon since there is very little water exchange with the Beaufort Sea and lagoon water residence time is long during the summer (weeks to months) in comparison to the decay rate of ^{222}Rn (3.8 d). The mass-balance model incorporates various end members that include data measured directly by this study as well as data acquired elsewhere. Minor assumptions regarding this data are outlined in Appendix C. SPGW ^{222}Rn concentration was estimated from the average of three collected samples (223 ± 20 Bq/m^3), while lagoon ^{222}Rn was estimated from the average of data collected across two surveys (32.4 ± 3.85 Bq/m^3). ^{222}Rn production was measured from dry lagoon sediments and then converted to estimates of ^{222}Rn in pore water (2,932 ± 650 Bq/m^3). Calculations regarding this conversion can be found in Appendix C. Standard errors in these values reflect variability in concentrations between samples as opposed to analytical uncertainty. A description of the uncertainty in our groundwater discharge estimate can be found in Appendix C. We did not measure ^{226}Ra in this study, but rather used estimates from Elson Lagoon in Dimova et al. (2015).

Therefore we also assume that the ^{226}Ra concentration between these lagoons is the same. Total groundwater ^{222}Rn input was estimated using an iterative approach that accounts for the ^{222}Rn flux from lagoon sediments, atmospheric losses (using wind speed and water temperature data), and the introduction of ^{222}Rn through the decay of ^{226}Ra in the lagoon.

RESULTS AND DISCUSSION

We found that active layer and shallow permafrost soils along the eastern Alaska Beaufort Sea coast contain high amounts of SOM and produce large quantities of readily leachable DOM. The highest SOM content (% C) was observed within surface soils (which includes the litter layer) between 0–5 cm (Table 3.1). The amount of SOM decreased at 15–20 cm, but increased again in deeper soils between 30–40 cm and in thawed permafrost samples (Table 3.1). We found a similar pattern in the release of DOM from these soil layers, where surface soils and thawed permafrost tend to have the highest production (mg DOC g $soil^{-1}$) and carbon-normalized leaching potential (mg DOC g soil C^{-1}) of DOM (Table 3.1). These results demonstrate that only a small amount of coastal soil is needed to rapidly produce high concentrations of DOC and DON. Interestingly, there are some notable offsets between our SOM content and leachable DOM values. The leaching potential of DON in surface soils is lower than DOC. Likewise, the production and leaching potential of DOC and DON in deeper active layer soils (30–40 cm) are relatively low given their high SOC and SON contents. However, the production and leaching potential of DOC and DON in thawed permafrost samples is relatively high given their more intermediate SOC and SON contents.

These observations are consistent with the notion that soils in northern high-latitude permafrost landscapes contain large amounts of leachable organic matter that can be exported to aquatic systems (Judd and Kling, 2002). Previous studies have

demonstrated DOM export is highest from litter layers and organic-rich soils near the surface (< 5 cm) because SOM from these horizons experienced little decomposition and fewer leaching events (Guo and Macdonald, 2006; Wickland et al., 2007; Shaver et al., 2014). On the other hand, lower DOM export is expected in deeper, more mineral-rich, soil horizons (> 20 cm) because these soils have faced more leaching events, enhanced microbial mineralization over time, and are more stable because of mineral particle adsorption of DOM (Gersper et al., 1980; McNamara et al., 1997; Mack et al., 2004; Petrone et al., 2006; Guo et al., 2007; Barnes et al., 2018). While our results from the upper most soil horizons (organic rich) and the next deepest layer (lower organic matter content) are consistent with these other studies, increases in organic matter content farther down the soil profile suggest that cryoturbation (i.e., mixing of the active layer and previously thawed permafrost), leaching, and/or decomposition processes concentrate organic matter near the permafrost boundary. Our results from frozen permafrost samples are consistent with a number of other studies demonstrating that permafrost contains considerable amounts of readily leachable organic matter and releases high concentrations of DOC and DON upon thaw (Douglas et al., 2011; Vonk et al., 2013a, 2013b; Abbott et al., 2014; Abbott et al., 2015; Mann et al., 2015; Fritz et al., 2015; Tanski et al., 2016). This is in part because permafrost can contain processed leachates and soils that have been well-preserved and frozen for millennia before thawing (Abbott et al., 2014). Patterns in SOC and leachable soil DOC from coastal soils of Elson Lagoon near Utqiagvik (formerly known as Barrow) on the western side of the Alaska Beaufort Sea may provide the best opportunity for comparison (Dou et al., 2008). Our trends are markedly similar to those found in Dou et al. (2008), which show that DOC yield is highest in the organic-rich surface layer (0–5 cm), lowest in more mineral-like horizons (5–20 cm), but increase in deeper active layer soils (20–50 cm) and shallow permafrost

(50–75 cm). While it is challenging to compare the magnitude of leachable DOM produced between our two studies because of differences in experimental design, Dou et al. (2008) also found that active layer and shallow permafrost soils rapidly produce high concentrations of DOC and DON. Overall convergence of our findings provides evidence that coastal soils produce large amounts of readily leachable DOM that can be exported to lagoons in northern Alaska during late summer.

Our analysis of ^{14}C-DOC data reveals that SPGW DOC entering lagoons along the eastern Alaska Beaufort Sea coast is sourced from a combination of surface soils that contain freshly produced organic carbon and deeper soil horizons that may extend into thawing permafrost (Table 3.2). ^{14}C-SOC age increased from modern (i.e., the time period between present day and 1950) near the land surface to ~5,400 years before present (yBP; i.e., before 1950) below the permafrost boundary (Table 3.2). Likewise, leachable soil ^{14}C-DOC age increased from modern to ~3,700 yBP with depth in the permafrost samples. Interestingly, there is a consistent offset between the ^{14}C ages of bulk SOC and leached DOC below the surface (> 5 cm), indicating that the fraction of readily leachable SOC is younger than the fraction of stable SOC in these deeper soil horizons. This supports the idea that a portion of older SOM is protected from leaching, for instance, by strong organo-mineral associations (Petrone et al., 2006). We found that groundwater has a ^{14}C-DOC age of ~1,300 yBP (Table 3.2). In comparison to our ^{14}C-SOC and soil leachate ^{14}C-DOC data, it is clear that SPGW DOM must be derived from a combination of organic-rich surface soils and deeper soil horizons. To further consider the potential sources of leachate DOM in SPGW, we used our experimental leaching results and Δ^{14}C data to estimate the percent contributions of each soil-DOM source and the expected ^{14}C-DOC age. Here we assume that SPGW receives DOM inputs from each soil horizon that is proportional to their amount of leachable soil-DOM (i.e., mg DOC g

soil^{-1} data in Table 3.1). We then weighed these proportions by each soil horizon thickness (described in the Materials and Methods section). If we consider SPGW DOM is sourced only from within the active layer, we estimate that surface organic soils contribute the highest proportion of leachable DOM to SPGW (56 ± 11 %; ca. from 0–5 cm), followed by deeper active layer soils above permafrost (38 ± 12 %; ca. from 30–40 cm), and mineral-like soils directly below the surface horizon (6 ± 2 %; ca. from 15–20 cm). The expected Δ^{14}C-DOC value and age of these collective inputs is –129 ± 30 ‰ and 1,040 yBP, respectively, which is younger (but within error) of the observed ^{14}C-DOC age of SPGW (Table 3.2). If we consider permafrost contributes a small amount of DOM, then these proportions change slightly (Figure 3.2), where 9 % of SPGW DOM is now derived from shallow permafrost (ca. using a 5 cm thickness). The expected Δ^{14}C-DOC value and age with permafrost included is –153 ± 21 ‰ and 1,270 yBP, respectively, which is closer to the observed ^{14}C-DOC age of SPGW. However, given the ^{14}C-SOC ages of the 30–40 cm and permafrost sections are markedly similar, these collective deeper soils represent a transition zone of "peri-permafrost" that likely experience a range of thaw conditions (from annual to less frequent) near the permafrost-active layer boundary. Although we oversimplify the factors affecting inputs of DOM from different soil types (e.g., horizon thickness), this exercise reinforces the idea that a significant fraction of SPGW DOM is derived from deeper soil layers.

It is important to note that groundwater flowing through the active layer of high-centered polygons travels relatively slowly (~1 to 10 cm day^{-1}; Wales et al., 2019), with shorter expected residence travel times during and following rain events and as SPGW experiences steeper hydraulic gradients near the coastal bluff. Thus SPGW likely travels from its source to lagoons on the order of months to years, which indicates that our groundwater ^{14}C-DOC age of thousands of years reflects the ^{14}C age of the soil source of

the leached DOC rather than the time since the leached soil DOC formed. That said, $\delta^{13}C$ values were lower, while C:N ratios were higher in soil leachate DOM samples compared to SPGW DOM (Table 3.2). This provides evidence that microbial processing may cause a small change in ^{14}C-DOC age between newly leached soil DOM and SPGW DOM entering Arctic coastal waters

Measurements of DOC and DON demonstrate that SPGW supplies highly concentrated inputs of DOM to Arctic coastal waters during late summer (Figure 3.2). Average SPGW DOC and DON concentrations including all collected data (n = 35) are 33.2 ± 1.8 mg DOC L^{-1} and 2.0 ± 0.1 mg DON L^{-1}. Our SPGW DOC concentration is over an order of magnitude greater than a recent estimate of the global average DOC concentration in groundwater aquifers from 15 countries and 4 continents at lower latitudes (2.7 mg DOC L^{-1}) (McDonough et al., 2018).

Results from a ^{222}Rn mass-balance model demonstrate that total groundwater discharge to Arctic lagoons is significant during the late summer. Naturally occurring ^{222}Rn ($t_{1/2}$ = 3.8 d) is recognized as a valuable geochemical tracer of water flow through rocks and soil/sediments and thus serves a useful tool for quantifying submarine groundwater discharge (Moore, 2010). A caveat of this approach is that submarine groundwater discharge estimates do not differentiate terrestrial and marine inputs, i.e., porewater circulating through and discharged from lagoon benthic sediments. We found that ^{222}Rn concentrations in Kaktovik Lagoon were 32.4 ± 3.9 Bq/m^3 (Figure C.1); from three samples, the average SPGW ^{222}Rn concentration is 223 ± 20 Bq/m^3. Total groundwater inputs (from land and benthic circulation) to Kaktovik Lagoon is an estimated 8.6×10^5 m^3 day^{-1} or 42.6 m^3 day^{-1} m^{-1} (~20 km of shoreline representing the lagoon perimeter). These values are similar in magnitude to previously reported values of

18 ± 10 Bq/m^3 ^{222}Rn concentration and discharge of 12 ± 4 m^3 day^{-1} m^{-1} (assuming ~10 km shoreline perimeter) in Elson Lagoon (Dimova et al., 2015; Lecher, 2017).

While the role of groundwater in the coastal ocean has gained marked attention over the past two decades, it has proven challenging to determine how much of this groundwater is terrestrial versus marine derived (Moore, 2010). Terrestrial-derived groundwater is typically a minor component of total groundwater contributions in the coastal ocean (1–10 %), but much higher percentages (e.g., 20–35 %) have been observed in coastal systems with strong topographic gradients at the land-sea interface and/or low wave and tidal-driven marine groundwater recirculation (Gallagher et al., 1996; Li et al., 1999; Hussain et al., 1999; Kim et al., 2003; Burnett et al., 2003; Taniguchi and Iwakawa, 2004; Taniguchi et al., 2006; Kaleris, 2006; Boehm et al., 2006; Moore and de Oliveira, 2008; Kwon et al., 2014; Dimova et al., 2015). We anticipate that the percentage of terrestrial SPGW discharge in our lagoon system is in the lower range of previous estimates (< 10 %) because Kaktovik Lagoon is surrounded by flat tundra terrain in a region of continuous permafrost. However, terrestrial SPGW discharge is likely greater than 1 % because tidal amplitudes and wave activity are very small. Therefore, assuming that 1 to 5 % of the groundwater discharge that we measured with ^{222}Rn in Kaktovik Lagoon is terrestrially-derived, we estimate that SPGW delivers roughly 8.6×10^3 to 4.3×10^4 m^3 of freshwater day^{-1}, 284 kg to 1420 kg of DOC day^{-1}, and 17 to 86 kg of DON day^{-1} to Kaktovik Lagoon in late summer. This equates to 426 to 2.1×10^3 m^3 freshwater, 14.1 to 70.6 kg DOC, and 0.9 to 4.3 kg DON per km of shoreline per day in late summer. Minimum and maximum values associated with these flux estimates range from 59 % lower to 76 % higher than average estimates (Appendix C). While quantifying organic matter inputs associated with marine groundwater is beyond the scope of this study, lagoon benthic substrate is largely made up of terrestrial

material from runoff and coastal erosion, especially in lagoons that contain alluvium that extends to the beaches (Dunton et al., 2012) Thus, marine-circulated groundwater inputs to coastal lagoons likely include a large amount of terrestrially-sourced DOM as well.

Comparison of ^{14}C-DOC ages between SPGW (1,300 yBP) and local rivers (1,270 yBP) potentially suggests that riverine DOC along the eastern North Slope of Alaska is strongly influenced by SPGW sources during late summer. This finding is consistent with previous studies focusing on larger Arctic rivers, where seasonal changes in hydrology correlate to shifts in riverine ^{14}C-DOC age from: (1) modern during the spring when frozen ground constrains high snowmelt-driven flow to litter and shallow surface soils; to (2) older during the summer (maximum age 489 yBP) and winter (maximum age 972 yBP) when low river flow is made up of higher proportions of groundwater that incorporates aged OC from deeper soil horizons or long-term storage in groundwater aquifers (Neff et al., 2006; Raymond et al., 2007; Aiken et al., 2014). Interestingly, our riverine ^{14}C-DOC age is older than those reported for water leaving the major pan-Arctic rivers during the summer, but is more similar to ages found in the winter (Raymond et al., 2007). On the other hand, ^{14}C-DOC ages reaching as much as 4,846 yBP have been observed in upstream locations of the Yukon River watershed in Alaska during the summer (Aiken et al., 2014). Together these results demonstrate that DOM leaving small rivers of the eastern North Slope of Alaska is more strongly influenced by SPGW inputs than DOM leaving large pan-Arctic rivers during the late summer. This difference is in part explained by a strong inverse relationship between hydrologic flow and ^{14}C-DOC age that appears consistent among Arctic rivers during the summer and winter time periods. During late summer, subsurface flow along the coastal plain of the North Slope is slower and has more contact time with deeper organic-rich and readily leachable soil layers at the permafrost boundary, which produce high

concentrations of DOC and DON that are carried to small streams and rivers via lateral groundwater transport (Neilson et al., 2018). Here we also found that concentrations of SPGW DOC and DON are one to two orders of magnitude higher than measurements from these nearby rivers (1.35 ± 0.25 mg C L^{-1}; 0.10 ± 0.03 mg N L^{-1}) during the late summer (data from Connolly et al., 2018). While direct SPGW inputs and local rivers share similar DOM sources, concentrations in rivers are much lower potentially due to a combination of intense photo-oxidation and microbial degradation that surface waters experience during the summer (Cory et al., 2014).

Results from the eastern Alaska Beaufort Sea coast provide strong evidence that SPGW can be a substantial source of freshwater, DOC, and DON to Arctic coastal waters. If we assume that SPGW fluxes are similar along the remainder of the Alaska Beaufort Sea coast, we estimate that direct SPGW fluxes range from 8.3×10^5 to 4.2×10^6 m^3 freshwater day^{-1}, 27.6 to 138×10^3 kg DOC day^{-1}, and 1.7 to 8.4×10^3 kg of DON day^{-1} along the entire Alaska Beaufort Sea coastline (1,957 km; Ping et al., 2011). For comparison, average August discharge from all rivers draining the North Slope of Alaska is an estimated 8.0×10^7 m^3 day^{-1} (data from 1990–2010 in Rawlins et al., 2019). While collective SPGW discharge may account for only a small percentage of total riverine discharge from the North Slope in August (1–5 %), if we consider summer DOC and DON concentrations of these rivers are 2.45 mg C L^{-1} and 0.14 mg N L^{-1} (averaged data from Connolly et al., 2018), then SPGW DOC and DON fluxes due to their high relative concentrations are a potentially much higher ~14 to 71 % of total riverine fluxes in August. Furthermore, it is important to keep in mind that the relative contributions of direct SPGW versus river inputs must vary substantially along the coastline. While SPGW inputs are probably minor in areas where major rivers, such as the Colville, flow

into the Alaska Beaufort Sea, SPGW may be the dominant source of freshwater, DOC, and DON along extensive stretches of coastline without sizable rivers.

Groundwater-borne nutrients are recognized as a fundamental component of ecological and biogeochemical processes in the coastal ocean worldwide, and yet information on SPGW DOM inputs to Arctic coastal waters is scarce. This information is sorely needed to improve understanding of linkages between organic matter inputs from land and biological production in Arctic coastal environments. Here we conclude that contemporary SPGW fluxes potentially supply substantial quantities of DOC and DON to coastal waters of the Alaska Beaufort Sea and thus represent an underappreciated source of energy for Arctic coastal ecosystems. The relative importance of SPGW DOM inputs is greatest during the late summer when river flow depreciates and groundwater discharge increases with maximum thawing of the active layer. The DOM found in SPGW during late summer is sourced from organic matter spanning the entire thawed soil profile, but primarily from highly leachable SOM near the surface and from deeper peri-permafrost horizons. Given that direct SPGW inputs are not exposed to sunlight before entering the coastal ocean, they may contain a higher proportion of less degraded DOM than that found in river water (particularly during late summer). Furthermore, as warming continues in the Arctic, accelerated permafrost thaw and associated groundwater discharge have the potential to mobilize increasing amounts of soil organic matter.

Table 3.1. Soil organic matter content residing in coastal soils and associated soil DOC and DON concentrations from soil-water leaching experiments. The permafrost category represents soils at approximately 5–10 cm below the ice table. Values are ± 1 standard error, $n = 3$ for all samples.

Sample	Soil OM Content		Leachable Soil DOM			
	% C (100 × mg C mg soil^{-1})	% N (100 × mg N mg soil^{-1})	mg DOC g soil^{-1}	mg DON g soil^{-1}	mg DOC g soil C^{-1}	mg DON g soil N^{-1}
0–5 cm	21.3 ± 4.1	1.3 ± 0.24	0.48 ± 0.12	0.015 ± 0.009	2.36 ± 0.52	1.10 ± 0.48
15–20 cm	5.1 ± 1.0	0.25 ± 0.09	0.05 ± 0.01	0.001 ± 0.001	1.06 ± 0.25	1.24 ± 1.13
30–40 cm	16.8 ± 8.5	0.95 ± 0.45	0.13 ± 0.05	0.006 ± 0.003	1.02 ± 0.35	1.34 ± 1.03
permafrost	9.2 ± 3.7	0.58 ± 0.29	0.17 ± 0.54	0.009 ± 0.004	2.68 ± 1.10	2.57 ± 1.77

Table 3.2. Radiocarbon and stable carbon isotopic compositions and C:N ratios in SOC, leachable soil-DOC, and SPGW DOC. Values are ± 1 standard error, $n = 3$ for all samples.

Sample	Fraction of Modern	$\Delta^{14}C$ (‰)	^{14}C age (yr BP)	$\delta^{13}C$ (‰)	C:N (molar ratio)
SOC					
0–5 cm	1.046 ± 0.035	38 ± 35	> Modern	−27.8 ± 0.4	16.2 ± 0.94
15–20 cm	0.622 ± 0.060	−383 ± 59	3895 ± 799	−28.9 ± 0.5	24.2 ± 5.1
30–40 cm	0.53 ± 0.053	−474 ± 53	5177 ± 774	−28.5 ± 0.1	17.4 ± 0.87
permafrost	0.515 ± 0.515	−490 ± 57	5383 ± 581	−28.1 ± 0.3	17.1 ± 1.4
Leachate DOC					
0–5 cm	1.042 ± 0.003	33 ± 2.5	> Modern	−27.3 ± 0.5	51.7 ± 15.8
15–20 cm	0.749 ± 0.048	−257 ± 47	2350 ± 526	−27.3 ± 0.1	101.5 ± 40.7
30–40 cm	0.652 ± 0.023	−353 ± 23	3447 ± 279	−27.2 ± 0.3	44.4 ± 20.0
permafrost	0.631 ± 0.022	−374 ± 21	3710 ± 274	−26.8 ± 0.2	26.4 ± 4.51
SPGW DOC	0.853 ± 0.046	−154 ± 45	1298 ± 421	−28.2 ± 0.2	20 ± 1.2

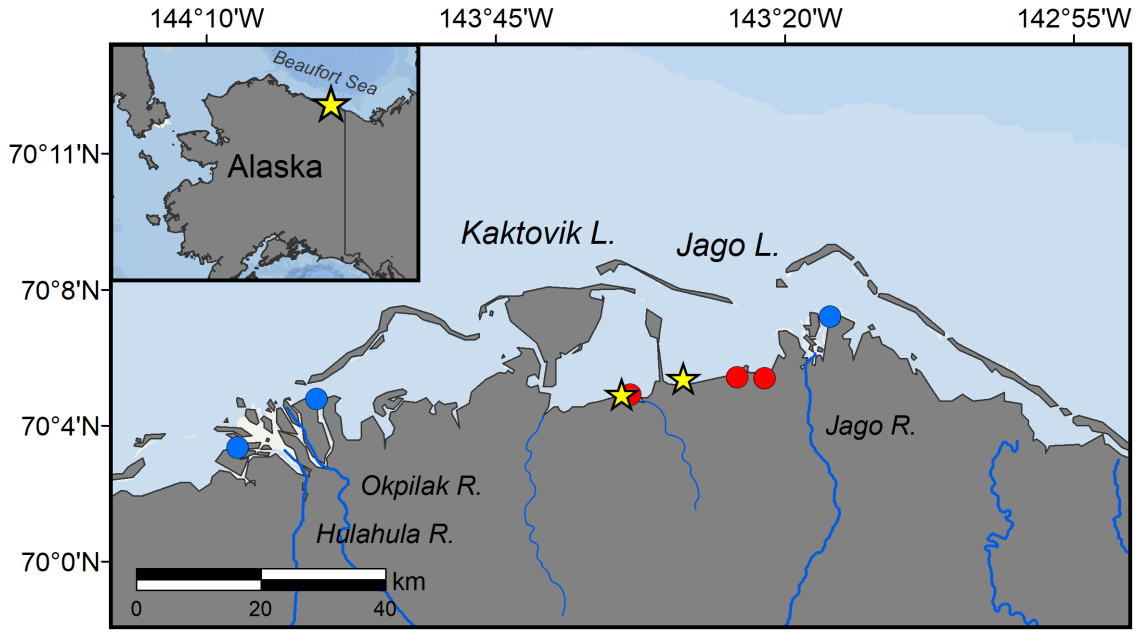

Figure 3.1. Map of the study sites along the eastern Alaska Beaufort Sea coast where samples were collected from soils (red circles), groundwater (yellow stars), and river water (blue circles).

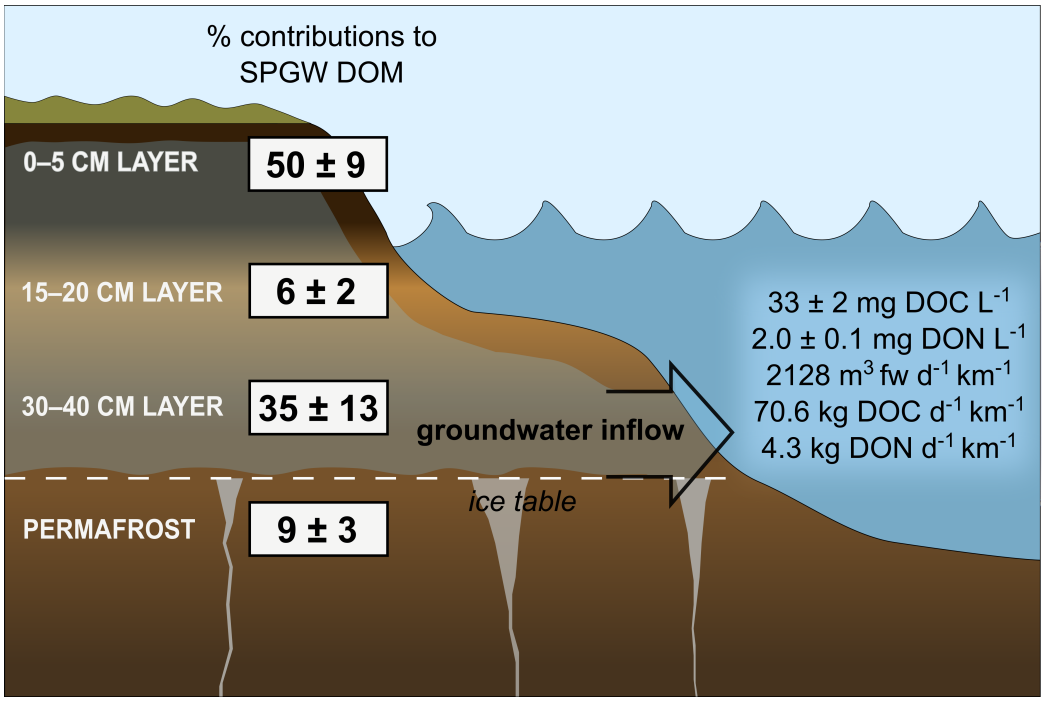

Figure 3.2. (left) Schematic of SPGW flow through the active layer during late summer with percent contributions of soil-DOM to SPGW DOM. Soil-DOM proportions were estimated from measurements of the 0–5 cm, 15–20 cm, 30–40 cm, and shallow permafrost sections. (right) SPGW concentrations of DOC and DON, and estimated upper range of fluxes of freshwater, DOC, and DON. Values are ± 1 standard error.

Chapter 4: Bioavailability of dissolved organic matter in groundwater inputs to Arctic coastal waters

ABSTRACT

In the Arctic, supra-permafrost groundwater inflow (SPGW) delivers appreciable quantities of dissolved organic matter (DOM) from land to nearshore coastal waters during the late summer. However, there are virtually no studies to date on the quality of this groundwater DOM and its potential to fuel biological production in Arctic coastal waters. Given SPGW inputs to nearshore coastal systems in the Arctic are anticipated to increase as permafrost thaws, this information is sorely needed to assess responses to and feedbacks with Arctic warming. Here we provide new results on the bioavailability, chemical composition, and reactivity of DOM in SPGW inputs to nearshore lagoons on the eastern Alaska Beaufort Sea coast. We conducted (1) biodegradable dissolved organic carbon (BDOC) experiments, (2) ultra-high resolution DOM composition analysis using Fourier transform ion cyclotron resonance mass spectrometry (FT-ICR MS), and (3) serial thermal oxidation via Ramped Pyrolysis Oxidation (RPO) coupled to measures of activation energy (*E)* and stable carbon and radiocarbon isotopes ($\delta^{13}C$ and $\Delta^{14}C$). These measurements were made on SPGW DOM samples as well as nearby river and lagoon water DOM for comparison. Our results reveal that SPGW, river water, and lagoon water DOM contains predominantly highly aromatic carbon compounds that are resistant to microbial degradation on the order of weeks to a few months. However, we found that microbial communities can effectively degrade an appreciable amount of this DOM in SPGW but not in river or lagoon water, indicating that SPGW contains a portion of bioavailable DOM that has already been degraded in river and lagoon waters during the late summer. Results of the reactivity structures of these DOM types indicates that SPGW contains a reactive component of DOM that is absent in river and lagoon water, while

lagoon water contains an unreactive component of DOM that is not in groundwater or river water. Together these results suggest that lagoon water DOM is influenced by soil-DOM sources carried by direct SPGW inputs as well as SPGW-fed river inputs that have been degraded. SPGW likely supplies an appreciable and previously unrecognized energy source for biological production in coastal waters of northern Alaska during late summer.

INTRODUCTION

Land-derived groundwater is a significant source of freshwater and nutrients to the coastal ocean worldwide (Zektser et al., 1993; Burnett et al., 2003; Moore, 2010; Sawyer et al., 2016) and yet, groundwater nutrient export to coastal waters is largely uncharacterized in the Arctic (Lecher, 2017). It has been demonstrated recently that supra-permafrost groundwater (SPGW) delivers appreciable quantities of dissolved organic matter (DOM), which includes dissolved organic carbon and nitrogen (DOC and DON), to coastal waters of northern Alaska during the late summer (Connolly et al., 2019a). SPGW inflow (i.e., groundwater flow through surficial soils above frozen permafrost) is firmly separated from sub-permafrost groundwater on the Arctic Coastal Plain, which flows beneath 200–600 m of permafrost and therefore circumvents the land-sea interface of nearshore coastal systems (Kane et al., 2013). In turn, SPGW is likely the principal form of groundwater inflow to nearshore coastal waters in the Arctic and a potentially large source of DOM for coastal biological production. SPGW DOM may be particularly important for food webs and the cycling of carbon and nitrogen in nearshore Arctic estuaries that rely heavily on inputs of terrestrial material (Dunton et al., 2006; Connelly et al., 2015; Harris et al., 2018). However, the realized importance of DOM as an energy source to metabolism is largely considered a function of its bioavailability for microbial consumption (Sobczak et al., 2010), which is inherently linked to its chemical composition and reactivity (Crump et al., 2003; Judd et al., 2006; Wickland et al., 2007; Fichot and Benner, 2014). Currently there is a lack of information on these properties of SPGW DOM that is needed to determine the role and importance of SPGW inputs for coastal ecological and biogeochemical processes in the Arctic.

The immediate threats of climate change adds urgency to this research need since Arctic warming is increasing groundwater discharge across the pan-Arctic (Smith et al., 2007; St. Jacques and Sauchyn, 2009; Walvoord et al., 2012; Rawlins et al., 2019), and liberating massive quantities of previously frozen and trapped stocks of organic matter in high-latitude soils and permafrost (Tarnocai et al., 2009; Schuur et al., 2013; Hugelius et al., 2014; Schädel et al., 2016). As permafrost thaws, anticipated increases in soil-DOM export via SPGW may constitute a positive feedback to warming through decomposition processes and the subsequent release of greenhouse gases (CO_2 and CH_4) (Frey and McClelland, 2009; Drake et al., 2015; Connolly et al., 2019a). Improved understanding of the composition and reactivity of SPGW DOM inputs to Arctic coastal waters is therefore also needed in order to predict responses to and feedbacks with warming in the Arctic.

Well over half of the Alaskan Beaufort Sea coast is framed by shallow lagoon systems (typically < 4 m) that are enclosed by barrier islands. These prominent estuarine features act as hotspots for biogeochemical cycling of organic matter and nutrients and support diverse assemblages of marine biological communities (Pedersen and Linn, 2005; von Biela et al., 2011; Dunton et al. 2012; Brown et al., 2012; Connelly, et al., 2015; Harris et al., 2018; Connolly et al., 2019b). While lagoons in northern Alaska are well recognized as highly valuable and productive ecosystems, scientific understanding forming the foundation of lagoon productivity is still growing. The consumption of biologically labile (biolabile) river-borne DOM delivered to lagoons during peak discharge in the late spring is one source of fuel for biological production (Holmes et al., 2008; Mann et al., 2012; McClelland et al., 2014). River inputs during the summer are also biologically relevant, but these inputs are much lower due to low river discharge and intense biological/photo-degradation that decreases surface water concentrations of DOC and DON (Striegl et al., 2005; McClelland et al., 2014; Fichot and Benner, 2014; Cory et

al., 2014). On the other hand, SPGW discharge increases during the summer with the thawing of the active layer (i.e., seasonally thawed surface soils above permafrost) and delivers appreciable quantities of DOM to lagoon ecosystems (Connolly et al., 2019a). Given that direct SPGW inputs are not exposed to sunlight before entering coastal waters and likely experience little biological degradation owing to water-logged soils and anoxic conditions (Frey and McClelland, 2009), SPGW may contain a higher proportion of biolabile and reactive DOM than river or lagoon DOM pools during the late summer.

Here we characterize the bioavailability, chemical composition, and reactivity of DOM in SPGW inflow to lagoons of the eastern Alaska Beaufort Sea coast during late summer. Our study also considers these DOM properties in neighboring river and lagoon waters during the same time period. We first assessed the bioavailability of DOM in SPGW, river water, and lagoon water from single-source bioincubation experiments that quantified the amount of microbial-mediated loss of DOC over a 28 day period. We also conducted these experiments using mixtures of SPGW and river water with lagoon water to identify potential priming effects of adding SPGW and river water DOM to the lagoon environment (Bianchi, 2011; Bianchi et al., 2015). Second, we linked the bioavailability of DOM to its chemical composition using ultra-high resolution electrospray ionization Fourier transform ion cyclotron resonance mass spectrometry (ESI-FT-ICR MS) to derive background DOM molecular compounds and subsequent changes in these compounds following bioincubation (Textor et al., 2018). Lastly, to compliment our assessment, we employed a regularized inverse method to relate DOC reactivity (i.e., activation energy, *E*) of SPGW, river water, and lagoon water to their stable carbon ($\delta^{13}C$) and radiocarbon isotopic ($\Delta^{14}C$) compositions using serial thermal oxidation (Ramped Pyrolysis Oxidation or RPO) (Hemingway et al., 2017a). This is the first study to use these three approaches

in concert to examine the bioavailability, chemical composition, and reactivity of DOM in SPGW, river water, and lagoon water in an Arctic coastal region.

MATERIALS AND METHODS

Water Sampling

A single SPGW composite was collected from 10 individual sampling locations using equal amounts of water along the beach of Jago Lagoon on 17 August 2017 (yellow star in Figure 4.1). On the same day, surface water samples were collected from the Jago River (blue circle in Figure 4.1) and from 2–3 m depth in Kaktovik Lagoon (red circle in Figure 4.1). River water was collected from the side of the mainstem channel near the delta and above tidal influence. Lagoon water was collected from Kaktovik Lagoon as opposed to Jago Lagoon because the water column of Jago Lagoon was entirely fresh during the sampling period. The salinity of our Kaktovik Lagoon water sample was 17–18, which is more representative of estuarine lagoon conditions over the summer (Harris et al., 2017). SPGW was extracted using piezometer wells that were installed to the depth of frozen ground (~1 m) running parallel to the shoreline. Samples from piezometers capture groundwater that has moved through the active layer to the lagoons without becoming channelized surface water flow. All water samples were collected using a peristaltic-pump attached with acid washed and Milli-Q rinsed Master-Flex tubing. Water samples were then dispensed into 10 L acid-washed and Milli-Q rinsed low-density polyethylene (LDPE) containers and transported in a cooler to the U.S. Fish & Wildlife Arctic National Wildlife Refuge (ANWR) facilities in Kaktovik, Alaska.

Biodegradable DOC Experimental Setup

The bioavailability of DOC is widely recognized as an important driver of microbial metabolism and has been studied in permafrost-influenced watersheds more recently to understand the potential degradation of vulnerable carbon pools (Holmes et al., 2008; Mann et al., 2012; Wickland et al., 2007, 2012; Abbott et al., 2014). Here we conducted biodegradable DOC (BDOC) experiments that quantified the amount of DOC loss over time using a standard experimental procedure for remote fieldwork reviewed in Vonk et al. (2015). Immediately following field collection, water samples were filtered through pre-combusted (450°C > 5 hr) GF/F glass microfiber filters (0.7 μm) into 125 mL acid-washed and Milli-Q rinsed polycarbonate bottles. Single-source experiments contained only groundwater, river water, and lagoon water, while mixing experiments contained a 50/50 mixture of groundwater with lagoon water and river water with lagoon water (60 mL of each source). BDOC experiments were initiated by incubating triplicate sets of each sample type in the dark at 20 °C for 0, 14, and 28 days. Bottle caps were loosely fitted to maintain oxygenated conditions. Samples for the 0 d time point were frozen after filtration and thus represent background DOC concentrations. At each subsequent time point, samples were re-filtered through a pre-combusted GF/F glass microfiber filters and immediately frozen to stop microbial activity. The bioincubation experiments were moved from Kaktovik to the University of Texas at Austin, Marine Science Institute (UTMSI) following fieldwork. To prevent the bioincubations from warming above 20 °C during their relocation, water samples were stored in cooler at ~4 °C for less than 48 hours. Therefore our estimates represent more conservative microbial-mediated changes over time than might occur if the samples were kept at a constant 20 °C. Concentrations of DOC were determined using high-temperature oxidation performed on a Shimadzu TOC analyzer at UTMSI. The amount of DOC consumed was calculated

as the difference between the initial and final DOC concentration (Δ DOC). The percent loss of DOC or percent of BDOC (% BDOC) was calculated from the Δ DOC/ $DOC_{initial}$ × 100. The decay rate was determined by Δ DOC/ time (in days).

Molecular Characterization of DOM using FT-ICR MS

FT-ICR MS allows for the determination of molecular formulae for thousands of DOM compounds (Sleighter and Hatcher, 2007). In recent studies, FT-ICR MS has been used to examine DOM composition and bioavailability in glacier and lake ecosystems (Stubbins et al., 2012; Spencer et al., 2014), temperate headwater streams, northern lakes, and coastal bays (Sleighter and Hatcher, 2008; Sleighter et al., 2010, 2014; Kellerman et al., 2015), and in Arctic watersheds (Spencer et al., 2015; Drake et al., 2018). Here we used FT-ICR MS to determine ultra-high resolution DOM molecular components in Arctic SPGW, river water, and lagoon water as well as in our groundwater and river water mixtures with lagoon water. Samples at times 0 d and 28 d were analyzed to assess which compound classes were used/transformed by microbial degradation. To prepare samples for FT-ICR MS, DOM was concentrated by solid phase extraction (SPE) using 100 mg Bond Elut PPL cartridges and methods described in Dittmar et al. (2008). Initial DOC concentrations were used to calculate the volume needed to achieve a target mass of 40 μg C mL^{-1} in 1-mL methanol elutions. An extraction efficiency of 65 % was assumed in our calculations. SPE-DOM extracts were stored at –20 °C before analysis on a 9.4 T FT-ICR MS at the National High Magnetic Field Laboratory (Tallahassee, Florida) with the instrument set to negative ion mode. FT-ICR MS spectra consist of thousands of individual molecular peaks and intensities that were evaluated in the mass range of 200–600 *m/z* (Koch and Dittmar, 2006). Molecular formulas calculated from *m/z* values were

assigned in PetroOrg software (Corilo, 2018) and included only elemental combinations of $C_{4-45}H_{4-200}N_{0-1}O_{0-25}S_{0-1}$ and mass errors less than 200 ppb, excluding noise (signals > 6 σ root mean square baseline; O'Donnell et al., 2016). Molecular formulas were categorized by specific compound classes based on their elemental stoichiometry and modified aromaticity indices (Al_{mod}) (Koch and Dittmar, 2006; Santi-Temkiv et al., 2013). These classes were determined from the following elemental and Al_{mod} boundaries: [i] unsaturated phenolic high oxygen, where Al_{mod} < 0.5, H/C < 1.5, O/C ≥ 0.5; [ii] unsaturated phenolic low oxygen, where Al_{mod} < 0.5, H/C < 1.5, O/C < 0.5; [iii] polyphenolic, where Al_{mod} 0.50–0.67; [iv] condensed aromatic, where Al_{mod} > 0.67; [v] aliphatic, where H/C ≥ 1.5, O/C < 0.9, N=0; and [vi] peptide-like, where H/C ≥ 1.5, O/C < 0.9, N ≥ 1 (O'Donnell et al., 2016). Compound classes were generated using Python software (Hemingway, 2017b). The contribution of each class to the DOM pool is based on the relative abundance (i.e., the number of molecular formulas assigned to each compound class). Changes in the relative abundances of these compound classes following bioincubation are used to represent shifts in DOM due to microbial utilization.

Reactivity Assessment of DOM using Ramped Pyrolysis Oxidation

Serial thermal oxidation using the RPO method involves heating an organic matter (OM) sample at a controlled rate while continuously quantifying and collecting CO_2, which is binned over user-defined time windows (termed "fractions"). Each fraction is then analyzed for its $\delta^{13}C$ and $\Delta^{14}C$ compositions (Rosenheim et al., 2008), allowing for the determination of various components of OM within a single bulk sample. RPO analysis has been recently applied to riverine sediments (Rosenheim and Galy, 2012; Rosenheim et al., 2013a; Bianchi et al., 2015), marine sediments (Rosenheim et al.,

2013b; Subt et al., 2016), temperate lake DOC (Zigah et al., 2017), and Arctic river particulate organic matter (POM) and coastal sediment (Schreiner et al., 2014; Zhang et al., 2017). New understanding of the reaction kinetics of the RPO technique allows us to make stronger interpretations of paired kinetic and isotope measurements, relating OM chemical composition, sources, and reactivity (Hemingway et al., 2017a).

Serial thermal oxidation was performed using SPE-DOM from SPGW, river water, and lagoon water samples (using the same methods as described above) on the RPO instrument at the Woods Hole Oceanographic Institution, National Ocean Sciences Accelerator Mass Spectrometry facility (WHOI/NOSAMS) (Rosenheim et al., 2008; Plante et al., 2013). A dried SPE-DOM sample in a combusted small 1 mm pyrex glass tube insert was transferred to a quartz reaction vessel, which was then placed in the top of the thermal analyzer. The thermal analyzer includes two coupled ovens, with the bottom oven set at a constant temperature of 800 °C and the top oven holding the sample reactor. The sample was thermally oxidized to CO_2 by gradually raising the top oven temperature with a ramped rate of 5 °C per minute to 800 °C, when all OC was oxidized. During oxidation, a mixed gas solution of ~8 % oxygen and 92 % helium flowed through the reactor at a rate of 35 mL per minute. The evolving gas was passed over a Pt/Ni/Cu twisted wire in the bottom oven to ensure complete oxidation of OC to CO_2. The evolving CO_2 was quantified downstream with an in-line Li-COR CO_2 analyzer and then cryogenically purified and collected using a series of flow-through glass traps. Five or six fractions were collected during serial oxidation where observable rising and falling CO_2 peaks were occurring, which can provide evidence of potential shifts in the types/sources of OM (Williams et al., 2014). $\Delta^{14}C$ and $\delta^{13}C$ measurements were made at NOSAMS using standard procedures (McNichol et al., 1994). Purified CO_2 gas samples were converted to graphite targets by reducing CO_2 with an iron catalyst under 1 atm H_2 at

550°C. Targets were subsequently analyzed for carbon isotopes ($\delta^{13}C$ ‰ and ^{14}C as fraction modern carbon). All $\Delta^{14}C$ data (in ‰) were corrected for isotopic fraction using measured $\delta^{13}C$ values that were quantified during the ^{14}C-AMS procedure. $\delta^{13}C$ values reported herein were determined separately using a VG Prism Stable Mass Spectrometer at NOSAMS. $\Delta^{14}C$ and radiocarbon age were determined from percent modern carbon using the year of sample analysis according to Stuiver and Polach (1977).

Measured RPO thermal profiles were plotted to compare the evolution of DOC oxidation to CO_2 with increases in temperature between SPGW, river water, and lagoon water samples. This provides a rudimentary first step in understanding similarities and differences in DOC chemical structure that affect thermal reactivity. As a second step, we determined DOC decay as a function *E,* the Arrhenius activation energy needed to transform DOC to CO_2 during serial thermal oxidation. *E* is an intrinsic property of the chemical bonding environment experienced by carbon atoms and is therefore a more suitable proxy for OC chemical composition and reactivity (Hemingway et al., 2017a). For each SPE-DOM sample, we determined the underlying *E* distribution leading to the observed thermal profiles (termed $p(0,E)$) as described by Hemingway et al., (2017a). This analysis was performed with the 'rampedpyrox' package in Python (Hemingway, 2017c). We calculated the temporal evolution of $p(0,E)$ to estimate the mean *E* values of DOC that decays within each RPO fraction. We then compared mean *E* values with ^{14}C (expressed as Fm) and $\delta^{13}C$ contents of the corresponding RPO fractions.

RESULTS AND DISCUSSION

Biodegradable DOC

SPGW DOC concentrations were on average over five times higher than that of nearby river water and lagoon water during the late summer (Table 4.1; Figure 4.2). This corroborates well with previous sites measurements of late summer DOC concentrations in SPGW, river water, and lagoon water (Connolly et al., 2018; Connolly et al., 2019a,b). Average DOC loss following the 28 d bioincubation was much higher in SPGW relative to river water and lagoon water (Table 4.1; Figure 4.2). The average percentage of BDOC (i.e., the biodegradable or microbial-utilized portion of DOC) following 28 days was more than double in SPGW relative to river water, and nearly an order of magnitude higher than in lagoon water (Table 4.1). These results suggest that direct SPGW inputs to coastal waters of northeastern Alaska contain a larger component of biolabile DOM than that of river water inputs and in the existing lagoon DOM pool during the late summer. Our results are comparable to other studies that measured analogous water types with the same experimental setup and over the summer (reviewed in Vonk et al., 2015). For example, values for Richardson Creek (< 250 km^2), a predominately groundwater-fed stream of the Yukon River watershed in Alaska, had a similar initial DOC concentration of 33 mg C L^{-1}, with a reported 4.3 % BDOC and 1.4 mg C L^{-1} DOC loss over 28 days (Vonk et al., 2015). Our river water results are comparable to ranges reported for the Yukon and Mackenzie rivers in North America and Kolyma River in Eurasia: initial DOC concentrations range from 3.4 to 7.6 mg C L^{-1}, with a reported 0 to 12.2 % BDOC and 0 to 0.56 mg C L^{-1} DOC loss over 28 days (Vonk et al., 2015; Spencer et al., 2015). However, our groundwater results are lower than the average of soil-leachates from surficial cores collected near Toolik Lake in northern Alaska: initial DOC concentration was 18 mg C L^{-1}, with a reported 26.7 % BDOC and 5.0 mg C L^{-1} DOC loss following 28

days (Vonk et al., 2015). The higher amount of BDOC in soil-leachates compared to SPGW DOM may be in part because soil-leachates contain highly biolabile DOM (e.g., from fresh plant growth inputs or root exudates; Marscher and Kalbitz, 2003) that could have already been degraded in SPGW DOM before entering coastal waters.

Average DOC concentration in our SPGW and lagoon water mixture was higher than in our river water and lagoon water mixture as expected (Table 4.1; Figure 4.2). Average DOC loss following the 28 d bioincubation nearly doubled in our groundwater and river water mixtures with lagoon water (Table 4.1). These results suggest that the addition of biolabile DOM in SPGW and river water could be enhancing the degradation of more stable DOM components in the existing lagoon DOM pool (i.e., facilitating a priming effect). On the other hand, the average DOC losses in groundwater and river water mixtures with lagoon water were markedly similar to the average DOC losses in background groundwater and river water experiments (Table 4.1). In other words, the decay rates between our 28 d single-source and mixing experiments were the same. The majority of DOC loss in our bioincubations occurred between 14 and 28 days, which might show more distinct decay rate differences; however, the average 14–28 d decay rates between background SPGW (0.092 ± 0.004 mg C L^{-1} day^{-1}) and river water (0.006 ± 0.001 mg C L^{-1} day^{-1}) were the same as their respective groundwater (0.090 ± 0.006 mg C L^{-1} day^{-1}) and river water (0.007 ± 0.001 mg C L^{-1} day^{-1}) mixtures with lagoon water. Since very little DOC was consumed in our background lagoon water bioincubation, then it could be the case that microbial communities in our mixtures were simply degrading solely SPGW and riverine DOC with similar rates than those found in our background experiments. A priming effect would be evident if the amount of DOC utilized by microorganisms was higher in our mixtures than in our background experiments. The absence of a strong priming signal is consistent with other studies demonstrating that

priming causes a weak or no effect on the degradation of DOC within aquatic systems (Dorado-Garcia et al., 2016; Blanchet et al., 2017; Bengtsson et al., 2018; Textor et al., 2018). On the other hand, these results do suggest that mixing effects between SPGW and lagoon water (such as flocculation or shifts in ionic conditions) do not hinder the ability of microorganisms to degrade SPGW DOM.

DOM Composition and Microbial Utilization

Ultra-high resolution FT-ICR MS characterization revealed that the composition of DOM in SPGW, river water, and lagoon water samples are all similarly dominated by a high relative abundance of unsaturated phenolic high and low O/C compounds (Table 4.2; T0 in Figures 4.3 and 4.4). We found similar proportions of the other compound classes within these background DOM sample, with moderate relative abundances of polyphenolics, low condensed aromatics and aliphatics, and very low peptide-like and sugar compounds. The overwhelming unsaturated phenolic and polyphenolic signal is evident in our van Krevelen diagrams (T0 in Figure 4.3), where we see high relative abundances in regions associated with lignin and tannin-like compounds (Sleighter and Hatcher, 2007). These results suggest that highly aromatic vascular plant material makes up the majority of DOM in SPGW, river water, and lagoon water in northeastern Alaska. On the contrary, compounds have lower relative abundances in regions associated with combusted terrestrial material or degraded lignin (i.e., condensed aromatics), as well as energy-rich sources such as lipids and microbial products (i.e., aliphatics) and proteins and carbohydrates (i.e., peptide-like and sugars) (T0 in Figure 4.3).

A strong linkage between soil leachates and DOM in aquatic networks can help explain the observed marked similarity in DOM composition between SPGW, river

water, and lagoon water during late summer. More specifically, their compositions strongly resemble that of DOM derived from organic-rich surface soils (i.e., the organic mat) and from thawing permafrost organic matter (Ward and Cory, 2015), which are subject to leaching with soil thawing during the summer. A convergence of soil-DOM sources in SPGW, local river water, and lagoon water is supported by a recent line of evidence suggesting that [1] DOM in lagoon water (~half strength seawater) is inherently terrestrial-freshwater during the summer (Connolly et al., 2019b); [2] summer DOM in rivers draining into lagoons are strongly influenced by SPGW sources (Connolly et al., 2019a); and [3] SPGW contains highly leachable soil-DOM sources primarily from organic-rich surface soils and deeper soil horizons that potentially extend into thawing permafrost (Connolly et al., 2019a). This would suggest that lagoon DOM during the late summer is strongly influenced by direct SPGW inputs and (SPGW-fed) river inputs.

The similarity in composition between SPGW, river water, and lagoon water DOM could also potentially arise from the loss of biolabile compounds in SPGW before entering coastal waters, the inability of microorganisms to utilize highly aromatic carbon compounds, and/or the effects of photo-degradation on surface water DOM. It has been shown that microbial communities in Arctic surface waters prefer energy-rich aliphatic, peptide-like, and sugar compounds (Spencer et al., 2015). These compounds are abundant in DOM derived from recently produced litter and soil leachates and thus account for a significant portion of BDOC observed in aquatic environments (Holmes et al., 2008; Wickland et al., 2012; Mann et al., 2012; Kellerman et al., 2015; O'Donnell et al., 2016; Textor et al., 2018). Likewise, highly biolabile aliphatic compounds are abundant in DOM derived from thawing permafrost (Ward and Cory, 2015; Spencer et al., 2015; Drake et al., 2018). Here we found a lower than expected relative abundance of aliphatic, peptide-like, and sugar compounds in SPGW DOM given that SPGW contains leachates

from organic-rich soils in the active layer, which may include thawed permafrost organic matter (Connolly et al., 2019a). This may be due to microbial degradation of these leachate-derived compounds as SPGW moves laterally towards lagoons, which can take weeks to months during the summer (Wales et al., 2019). The lack of aliphatic, peptide-like, and sugar compounds explains the low amounts of BDOC in our experiments.

In general, we found little microbial-mediated change in DOM composition between initial (T0) and final (T28) samples in our single-source and mixing experiments (Figures 4.3 and 4.4). This may be due to their high relative abundance of phenolic and polyphenolic compounds, which are more resistant to biological degradation and may even inhibit bacterial respiration (Freeman et al., 2001; Mann et al., 2014). On the other hand, we did find an observable decrease in the relative abundance of these compounds in SPGW DOM, but not in river water or lagoon water DOM (Figure 4.3). This suggests that microbial communities are able to effectively degrade aromatic DOM in SPGW, but to a lesser degree in that of river and lagoon water over the course of weeks to months. This could in part be explained by the photo-degradation of highly aromatic DOM in surfaces waters that does not occur in SPGW during the summer (Cory et al., 2014).

DOM Reactivity Assessment

Results of serial thermal DOM oxidation to CO_2 in RPO thermoprofiles revealed that SPGW and riverine DOM oxidize over the same range of temperatures, with the vast majority of DOM oxidized between ~200–550 °C and peaks at 458 °C and 510 °C, respectively (Figure 4.5). Lagoon water DOM oxidizes over a broader temperature range, with most of the DOM oxidized between ~200–700 °C and with two discernable peaks at 524 °C and 578 °C. Comparisons of these thermoprofiles suggests that SPGW and river

water have similar thermally reactive chemical structures/ bond strengths. Interestingly, the oxidation of SPGW DOM peaks at a slightly lower temperature than river water DOM. Together this support the idea that SPGW and river water DOM share similar compositions and soil-DOM sources, but SPGW contains some compounds that are more thermally reactive. We see that a component of lagoon water DOM is reactive over a similar temperature range as SPGW and river water DOM, peaking at a temperature that is similar to riverine DOM. However unlike SPGW and river water, lagoon water seems to contain some portion of less reactive DOM that oxidizes at higher temperatures.

Given that activation energy (*E*) is an intrinsic property of the sample type and does not depend on experimental conditions (such as temperature ramp rate), it serves as a better proxy for understanding OC bond strength/ chemical composition and thus potential OC biolability (Hemingway et al., 2017a). Organic matter pools that integrate a diversity of sources, including recently assimilated biomass, organic matter that has been transformed, or stabilized pre-aged material typically exhibit a broader and more complex distribution of *E* (Hemingway et al., 2017a). Thus comparing mean *E* values and *p*(0,E) profiles with isotopic measurements during serial oxidation can be helpful for examining how OM reactivity relates to variability in OM sources. Here we quantified *p*(0,E) profiles and the relationships between mean *E* distributions and their corresponding $\delta^{13}C$ and $\Delta^{14}C$ values (expressed as Fm) of RPO fractions collected from SPGW, river water, and lagoon water SPE-DOM samples according to Hemingway et al. 2017a (Table 4.3; Figure 4.6). The reactivity structures (revealed by *p*(0,E) profiles) in SPGW, river water, and lagoon water DOM are markedly similar between an *E* of 100–200 kJ mol^{-1} (Figure 4.6; top). We do see a higher *p*(0,E) peak in SPGW relative to river and lagoon water DOM when *E* = ~172 kJ mol^{-1}, whereas we see a lower *p*(0,E) peak in lagoon water relative to SPGW and river water DOM when *E* = ~180–190 kJ mol^{-1}. Unlike SPGW and

river water DOM, we see a broader distribution of *E* in lagoon water DOM, where *p*(0,E) additionally peaks when *E* = ~202 kJ mol^{-1}. These results suggest that SPGW, river water, and lagoon water DOM have similar underlying chemical compositions/ bond strengths, but that [1] SPGW DOM contains a reactive component when *E* = ~172 kJ mol^{-1} that is absent in river and lagoon water DOM; [2] both SPGW and river water DOM contain a reactive component when *E* = ~180–190 kJ mol^{-1} that is absent in lagoon water; and [3] lagoon water DOM contains a reactive component at an higher *E*= ~202 kJ mol^{-1} that is absent in SPGW and river water DOM.

When we compare the distribution of mean *E* values with their respective isotopic values in RPO fractions, we find that SPGW, river water, and lagoon water DOM are all predominately made up of terrestrial carbon (i.e., they have depleted $\delta^{13}C$ values) (Figure 4.6; bottom). Interestingly, we see slightly more enriched $\delta^{13}C$ values in lagoon water DOM, which increase as *E* increases. This could arise if lagoon water contains a small component of aged and unreactive marine-derived DOM from polar mixed layer water (Druffel et al., 2017). We also found that SPGW and lagoon water have a similar Fm age distribution among RPO fractions, whereas river water DOM fractions are typically modern and decrease in age with increasing *E* (Figure 4.6; middle). These results suggest that river water can contain DOM leachates predominately from shallow soil horizons (< 10 cm) and that the composition of leached DOM from older and deeper soil horizons are similar despite a difference in age by ~1,000 years (Connolly et al., 2019a). More importantly, the similar ^{14}C-DOC ages between SPGW and lagoon water suggests that direct SPGW DOM inputs may make up a significant portion of lagoon DOM.

CONCLUSIONS

In this study, we demonstrate that direct SPGW inputs to lagoons along the Alaska Beaufort Sea coast contain a portion of bioavailable DOM that is absent in river and lagoon waters during the late summer. The observed low percentages of BDOC in our samples can be attributed to potentially large amounts of highly aromatic carbon from leached soil organic matter. While we found little change in the relative abundances of DOM compound classes over the course of 28 d bioincubation experiments, there was an observable microbial-mediated loss of phenolic and polyphenolic compounds in SPGW. This suggests that SPGW DOM contains aromatic material (e.g., from soil leachates) that can be effectively degraded by microbial communities. The observed low amounts of BDOC and low DOC concentrations in river and lagoon waters may be due to intense photo-degradation that removes aromatic DOM compounds over the summer. These results corroborate well with new understanding of the reactivity structures of SPGW, river water, and lagoon water DOM, which indicates that SPGW contains a component of reactive DOM that is not present in river and lagoon water, while lagoon water contains a portion of unreactive DOM that is absent in SPGW or river water. Together these results suggest that lagoon DOM is influenced by SPGW and SPGW-fed river water that has undergone intense degradation and in turn, results in low concentrations of stable lagoon DOM during late summer. Arctic coastal regions are already being impacted by climate-linked changes in hydrology and thawing permafrost, which are anticipated to increase SPGW DOM inputs to Arctic coastal waters. The introduction of permafrost organic matter to SPGW may change its bioavailability, composition, and reactivity. Studies are needed to assess how shifts in the properties of SPGW DOM as permafrost thaws will alter coastal ecological and biogeochemical processes in the Arctic. For instance, future efforts should focus on improving mechanistic understanding of the relationship between

land-derived freshwater inflows, such as SPGW and river water inputs, and food web structure and function in nearshore estuarine ecosystems in northern Alaska.

Table 4.1. Concentrations of DOC at the start of the bioincubation experiments (initial DOC), the amount of DOC consumed following a 28 day incubation (Δ DOC), and the percentage of DOC loss or biodegradable DOC (BDOC). Values are averages ± 1 standard error

Sample	Initial DOC (mg C L^{-1})	Δ DOC (mg C L^{-1})	BDOC (%)
SPGW	28.29 ± 0.09	1.28 ± 0.05	4.5 ± 0.2
river water	5.03 ± 0.01	0.09 ± 0.01	1.8 ± 0.2
lagoon water	2.34 ± 0.03	0.01 ± 0.06	0.6 ± 2.8
SPGW + lagoon water	14.89 ± 0.11	1.26 ± 0.08	8.5 ± 0.5
river water + lagoon water	4.06 ± 0.01	0.11 ± 0.02	2.7 ± 0.6

Table 4.2. Chemical composition of DOM in background SPGW, river water, and lagoon water samples revealed by FT-ICR MS. The total *n* of molecular formulas is indicated. For each compound class, the relative abundances (i.e., the number of molecular formulas of the total) as well as the % relative abundance in parenthesis are shown.

Compound Class	Relative Abundance		
	SPGW (n = 4654)	River water (n = 6902)	Lagoon water (n = 7915)
Unsaturated phenolic high O/C	2945 (63.3)	4201 (60.9)	4623 (58.4)
Unsaturated phenolic low O/C	829 (17.8)	1716 (24.9)	2019 (25.5)
Polyphenolic	555 (11.9)	604 (8.8)	666 (8.4)
Condensed aromatic	127 (2.7)	119 (1.7)	175 (2.2)
Aliphatic	140 (3.0)	212 (3.1)	366 (4.6)
Peptide-like	10 (0.2)	14 (0.2)	45 (0.6)
Sugars	47 (1.0)	36 (0.5)	21 (0.3)

Table 4.3. Temperature range, activation energy (E), and isotopic data for each RPO fraction (f) collected from SPE-DOM samples. Values for E are the mean ± 1 standard deviation. Analytical error for $\delta^{13}C$ is ± 0.15 (1 standard deviation). Analytical error in ^{14}C measurements is very small so and was not included in the table.

Sample	f	Temperature Range (°C)	E (kJ mol^{-1})	^{14}C Age (yr BP)	Fraction Modern	$\delta^{13}C$ (‰)
SPGW	1	103–295	127 ± 10	1020	0.881	−28.5
	2	295–382	152 ± 11	750	0.911	−29.6
	3	382–458	172 ± 7	700	0.917	−29.0
	4	458–510	180 ± 4	640	0.923	−28.8
	5	510–539	183 ± 2	685	0.918	−29.7
river water	1	102–243	119 ± 8	440	0.948	−30.0
	2	243–401	151 ± 15	modern	1.087	−29.6
	3	401–451	172 ± 7	modern	1.072	−29.0
	4	451–510	182 ± 6	modern	1.086	−28.8
	5	510–564	186 ± 2	modern	1.130	−29.5
lagoon water	1	110–283	126 ± 9	745	0.916	−28.2
	2	283–411	154 ± 12	995	0.884	−27.7
	3	411–460	173 ± 10	955	0.889	−27.6
	4	460–524	190 ± 8	875	0.897	−27.4
	5	524–577	200 ± 7	940	0.890	−26.5
	6	577–682	210 ± 7	915	0.893	−27.0

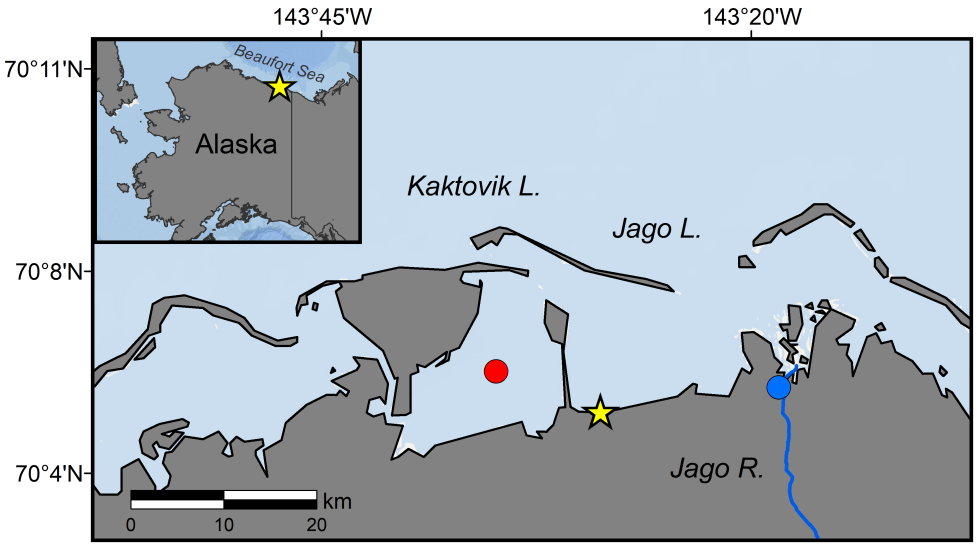

Figure 4.1. Study sites along the eastern Alaska Beaufort Sea coast where samples were collected for SPGW (yellow star), and river water (blue circle), and lagoon water (red circle).

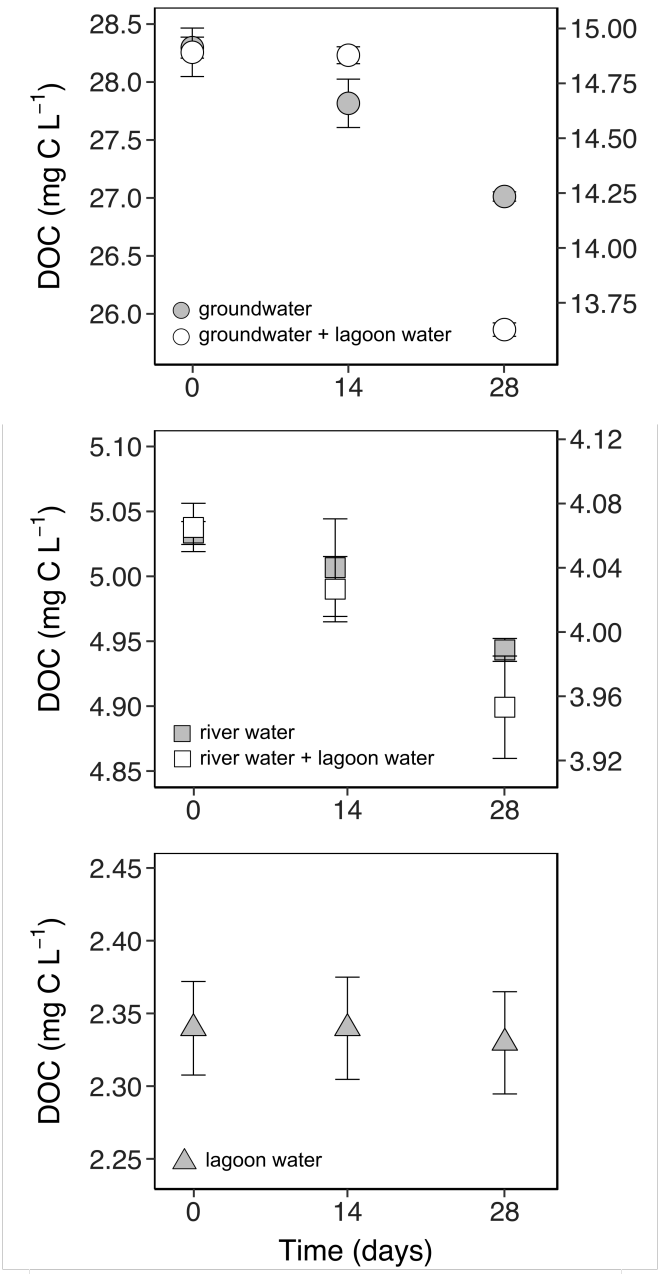

Figure 4.2. DOC loss in single-source and mixing 28 day bioincubation experiments. Top: SPGW (labeled as groundwater; dark circles) and SPGW plus lagoon water (white circles). Middle: river water (dark squares) and river water plus lagoon water (white squares). Bottom: lagoon water (dark triangles). The left y-axis corresponds to DOC of the single-source experiments, while the right y-axis corresponds to DOC of the mixing experiments. Points are the average of three replicates. Error bars are ± 1 standard error of the mean.

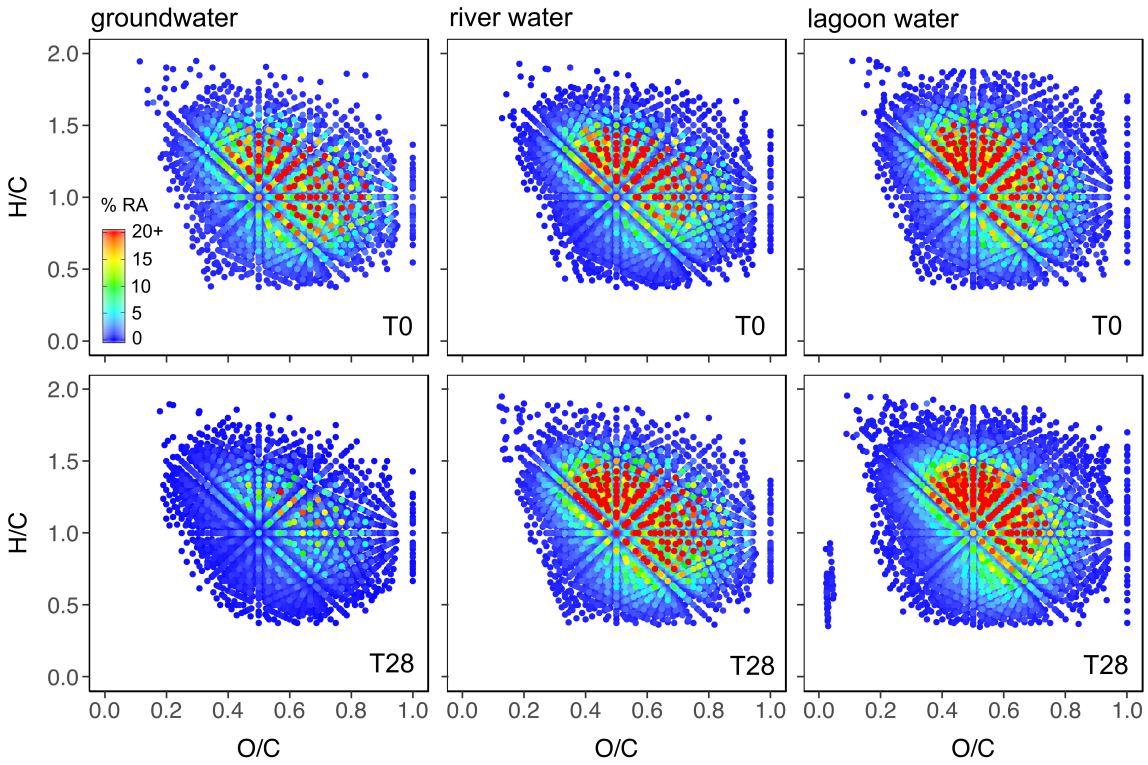

Figure 4.3. van Krevelen diagrams of elemental DOM composition derived from FT-ICR MS. The color scale represents a gradient of increasing relative abundance (% of molecular formulas assigned) from 0 to ≥ 20 %. Plots show changes in the relative abundance of molecular formulas between initial (T0) and final (T28) background SPGW (labeled as groundwater), river water, and lagoon water samples.

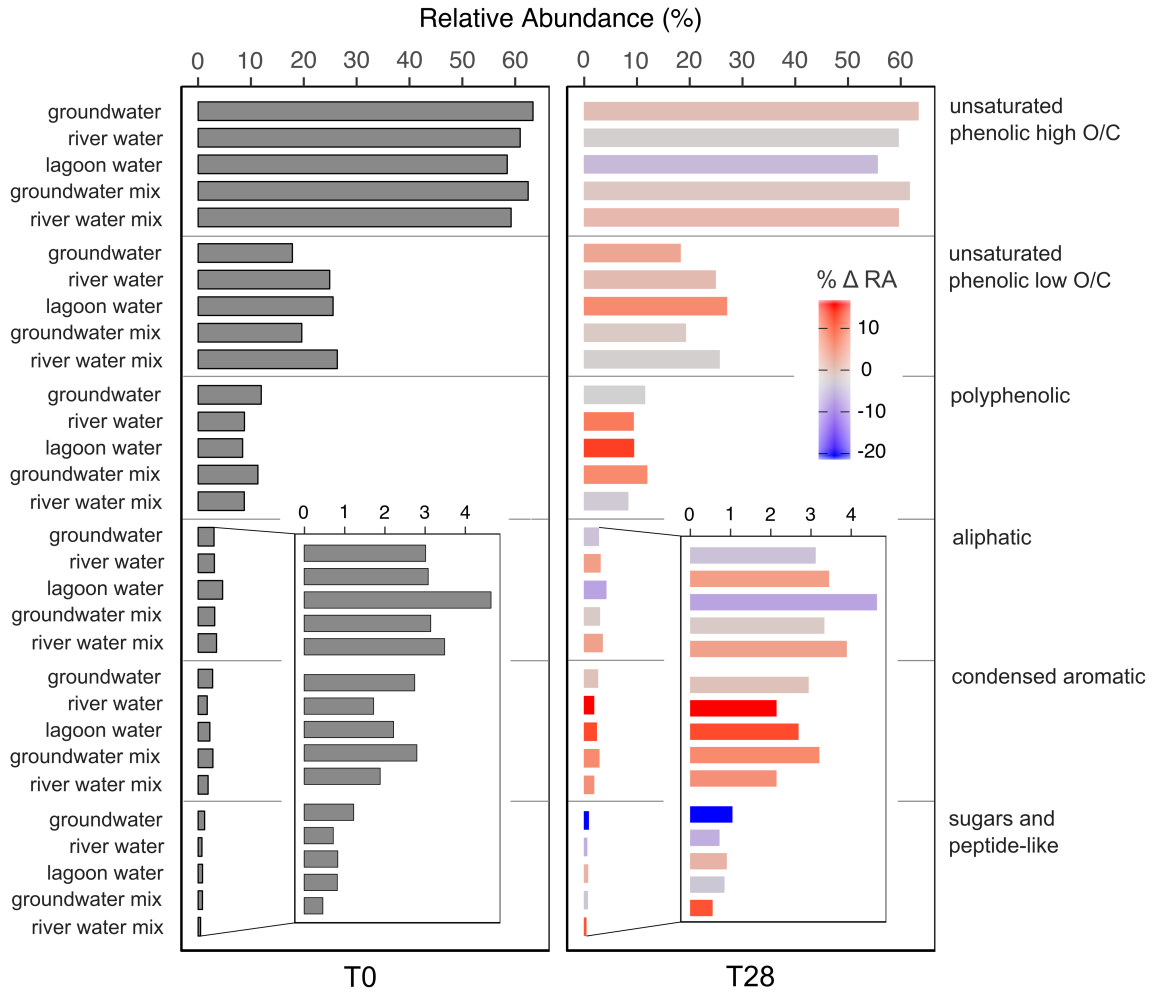

Figure 4.4. Chemical composition of DOM revealed by FT-ICR MS in initial (T0) and final (T28) background SPGW (labeled as groundwater), river water, and lagoon water samples as well as in samples of SPGW and river water mixed with lagoon water. Bars represent the relative abundance (% of molecular formulas assigned) of different compound classes. The color gradient for T28 samples represents the change in relative abundance of compound classes as an increase (in red) or decrease (in blue). Increases did not exceed 16 %, while decreases did not exceed −21 %.

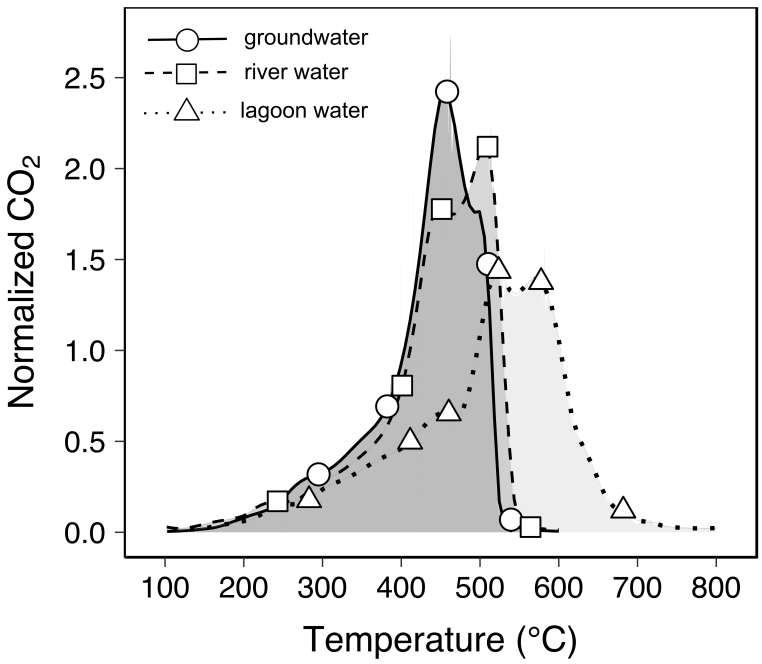

Figure 4.5. RPO thermoprofiles of SPE-DOM from river water (dashed lined), SPGW (labeled as groundwater; solid line), and lagoon water (dotted line). Five or six CO_2 fractions were collected during serial thermal oxidation from ~100 to 800 °C. Shapes indicate the max temperatures where individual CO_2 fractions were collected.

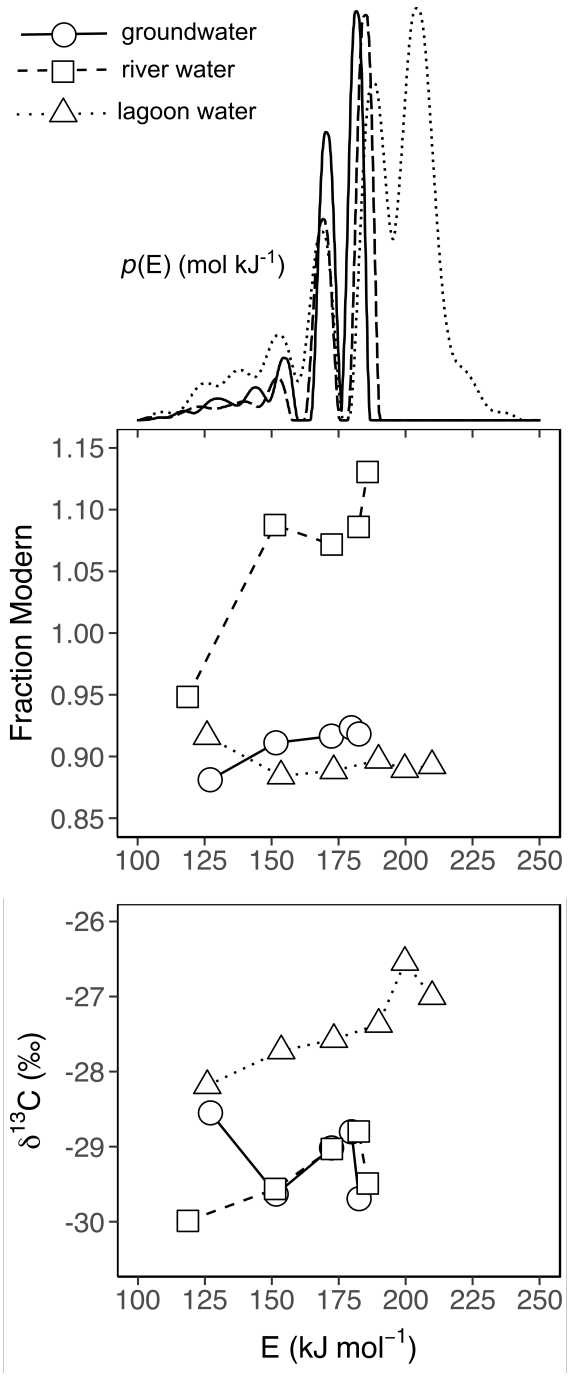

Figure 4.6. Top: regularized $p(0,E)$ distributions from SPE-DOM of river water (dashed line), SPGW (labeled as groundwater; solid line), and lagoon water (dotted line). Middle and bottom: plots of mean E values vs. Fm and fractionation-corrected $\delta^{13}C$.

Overall Conclusions

The results of the studies contained in this dissertation provide new understanding of DOM characteristics that link watershed export and Arctic coastal environments, and how Arctic land-ocean systems will respond to the immediate threats of climate change. While river inputs of DOM are essential to coastal ecosystem function, our understanding of these inputs is still limited in many remote regions of the Arctic (Holmes et al., 2013). Watershed slope is a promising indicator of variations in fluvial DOM that can be used to infer concentrations in high-latitude catchments where field-data collection is prohibitive (Harms et al., 2016; Khosh et al., 2017). However, relationships between watershed slope and fluvial concentrations of DOC and DON have not been generalized for the full range of catchment sizes and geographic locations that is representative of the pan-Arctic. Chapter 1 reveals that watershed slope is an excellent predictor of spring and summer fluvial concentrations of DOC and DON among pan-Arctic rivers, and that slope-concentration relationships do not vary by scale or region. These patterns are linked to variations in soil organic matter contents, which are related to catchment coverage by organic-rich coastal plain versus organic-poor mountainous terrain. Concentrations of DOC and DON from slope-derived relationships were paired with discharge data to estimate annual DOM fluxes from five Eurasian rivers in data-poor regions. These fluxes serve as updates from previously reported values and thus contribute new understanding of DOM inputs from pan-Arctic watersheds where export estimates are limited. Tracking long-term changes in these relationships in the future can help us to identify the impacts of thawing permafrost and associated shifts in hydrology as the Arctic warms.

Seasonality is a defining feature of physicochemical conditions in Arctic coastal waters, but fundamental knowledge of temporal patterns in DOM within productive nearshore estuaries, such as lagoon systems along the Alaskan Beaufort Sea coast, are

lacking to date. Chapter 2 provides baseline understanding of temporal variations in the quantities and sources of DOM within lagoons along the eastern Alaska Beaufort Sea coast, thereby improving knowledge of the links between watershed nutrient export, biogeochemical cycling, and biological production in Arctic coastal waters on seasonal timeframes. Lagoon DOM in the spring (late June) is strongly influenced by river inputs that inundate the Beaufort Sea coastline following the snowmelt-driven peak discharge period. Lagoon DOM over the summer (August) reflects the mixing of freshet-derived DOM with marine-sourced DOM from the Beaufort Sea. The quantities of summer lagoon DOM do deviate from conservative mixing behavior, which can be attributed to variability in the magnitude of riverine DOM inputs during the late spring and summer months as well as variability in lagoon geomorphology that affects the exchange of water with the open ocean. Lagoon DOM during the winter (April) is predominately sourced from the polar mixed layer, but there is evidence that inputs from regenerated benthic material and/or degrading POM contribute to lagoon DOM pools during this time. While mixing of freshwater and marine DOM is a primary driver of temporal changes in the quantities of lagoon DOM between the spring and winter periods, processing effects by microbial and photo-degradation may also be important. Overall, Chapter 2 demonstrates that distinct seasonal transition in ice-coverage, runoff from land, and connectivity with the open ocean are coupled to dynamics changes in the sources and quantities of DOM in Arctic lagoons, which in turn, can help explain the timing and magnitude of biological production. This study provides new understanding of seasonal patterns in lagoon DOM that are needed to assess the impacts of Arctic warming, which are already affecting the landward and ocean margins of lagoons in northern Alaska (Lantuit et al., 2011).

Groundwater will become an increasingly important source of freshwater and nutrients to aquatic ecosystems as permafrost thaws in the Arctic (Frey and McClelland,

2009). While it is known that SPGW flow increases with the seasonal thawing of the active layer and represents a major source of DOM to fluvial networks in the summer (Walvoord et al., 2012; Neilson et al., 2018), few studies have attempted to characterize SPGW inputs to Arctic coastal waters. In Chapter 3, we found that late summer SPGW supplies an appreciable quantity of freshwater, DOC, and DON to lagoon ecosystems of the eastern Alaska Beaufort Sea coast and to Arctic coastal waters more generally. SPGW DOM inputs thus provide a potentially important source of energy for lower trophic productivity, especially in coastal regions without river inputs. This groundwater DOM is sourced from organic-rich soils that span the entire thawed soil profile, but primarily from highly leachable soils near the surface and deeper soil horizons, including shallow permafrost. The export of SPGW DOM to Arctic coastal waters will likely increase in the future as thawing permafrost liberates massive stores of soil organic matter.

While SPGW is a major input of DOM to Arctic coastal waters during the late summer, knowledge of the composition and bioavailability of this DOM is inherent to understanding its use as a food source by lagoon consumers. In Chapter 4, biodegradable DOC experiments showed that there is little microbial-mediated loss of DOC in SPGW, river water, and lagoon water over 28 days. This can be attributed to their high relative abundance of aromatic carbon compounds, which tend to be more resistant to biological degradation than higher energy-yielding compounds such as aliphatics (Freeman et al., 2001; Mann et al., 2014; Spencer et al., 2015). In contrast, the experimental results do suggest that microbial communities consume an appreciable amount of DOM compounds in SPGW that appear to have already been degraded in riverine and lagoon water. One possible explanation is that SPGW contains fresh and recently produced soil-DOM that has seen less prior biological and photo-degradation. This is supported by results of the reactivity structures of DOM in SPGW, river water, and lagoon water during the late

summer. These results show that SPGW contains a component of reactive DOM that is not present in river and lagoon water, while lagoon water contains a portion of unreactive DOM that is absent in SPGW and river water inputs.

Groundwater is a globally significant source of nutrients for coastal environments that has only recently gained attention in the Arctic (Moore, 2010; Dimova et al., 2015; Lecher, 2017). However, the importance of SPGW DOM inputs to coastal lagoons in northern Alaska, and the role that SPGW plays in ecosystem function as well as the cycling of carbon and nitrogen has not been fully realized. As Chapters 3 and 4 reveal, SPGW is a major terrestrial source of DOM to Arctic coastal waters during the late summer and may provide an important carbon subsidy for lagoon food webs that rely heavily on land-derived material throughout the year (Dunton et al., 2006; Connelly et al., 2015; Harris et al., 2018). As Chapters 1 and 2 reveal, landscape features and seasonal changes in surface hydrology are primary drivers of watershed DOM export to Arctic coastal waters across spatial and temporal scales. Future studies characterizing spatial and seasonal variations in SPGW DOM inputs would improve our understanding of linkages among watershed nutrient export, biological production, and biogeochemical cycling in Arctic coastal waters. While our experimental studies on the bioavailability of DOM in SPGW versus river and lagoon water provide useful information on the potential importance of these sources, further investigation on the use of these DOM types by lagoon consumers is needed. Perhaps most importantly, SPGW DOM export serves as a direct pathway for the movement of organic matter in thawing permafrost from land to Arctic coastal environments. Future studies that characterize the relationships between thawing permafrost, groundwater hydrology, and biogeochemical cycling in Arctic coastal systems are urgently needed in order to assess their response to and forecast feedbacks with current and on-going warming in the Arctic.

Appendices

Appendix A: Chapter 1 Supplementary Material

This supplementary material provides the procedures for sample collection and analysis for rivers east of the Sagavanirktok along the North Slope of Alaska; details on watershed delineation, watershed slope, and soil organic carbon content estimation; and regression coefficients for relationships between watershed slope and concentrations of DOC, DON, and NO_3^-.

In this section we describe the procedures for sample collection and analysis for the eastern North Slope rivers. Water samples from the Kavik, Canning, Hulahula, Okipilak, Jago, Aichilik, Kongakut, and Turner rivers were collected from a wide range of catchments, including sites in the headwaters of the Brooks Mountain Range, along river main stems, in low-lying tundra tributaries, and at downstream locations near the river deltas. Sampling was largely performed by citizen scientists and researchers from the Arctic National Wildlife Refuge (a branch of the U.S. Fish and Wildlife Service), the United States Geological Survey, and the University of Alaska, Fairbanks. This necessitated development of a lightweight, portable, easily operable sampling procedure. In the field, surface water samples for dissolved constituents were collected using acid washed pre-leached 140 mL polypropylene syringes. Samples were then immediately filtered using 33 mm diameter 0.45 μm polyethersulfone membrane syringe tip filters into acid washed pre-leached polycarbonate bottles. Following filtration, samples were acidified for preservation (final pH < 2) using ultra-pure hydrochloric acid. Samples were analyzed for DOC and total dissolved nitrogen (TDN) at the University of Texas Marine Science Institute (UTMSI) on a Shimadzu TOC/TN analyzer. NO_3^- was also measured from collected samples at UTMSI using a cadmium reduction method modified for a BioTek μQuant microplate spectrophotometer (Jones, 1984). Ammonium (NH_4^+) data were not measured for most collection sites; therefore, DON was calculated from TDN minus NO_3^- alone. Although missing NH_4^+ values add some uncertainty to estimates of DON concentrations, rivers draining Alaska's North Slope typically have low NH_4^+ concentrations and uncertainties introduced by not accounting for the contribution of NH_4^+ are minor (Townsend-Small et al., 2011; Khosh et al., 2017).

Here we describe our approach to define watershed boundaries. Watershed areas upstream of sampling locations on the six largest rivers (Ob', Yenisey, Lena, Kolyma,

Yukon, and Mackenzie) were delineated with ESRI ArcGIS version 10.2 software (North Pole Lambert Equal Area Projection) using a 1 km digital elevation model (Hydro 1K DEM). Exact coordinates of sampling locations were used for the Yukon, Mackenzie, Ob', Yenisey, and Kolyma delineations. The Lena was delineated from a point 40 km upstream of the sampling location due to ambiguities in DEM resolution for this site. Watershed areas upstream of the Pechora at Ust-Tsilma, Mezen at Malonisogorskoye, Severnaya Dvina at Ust-Pinega, Olenek 7.5 km downstream from Buur's offing, and Yana at Ubileynaya were delineated using the same approach. Watershed areas for Alaska's North Slope rivers were delineated using the same software, but with a 40 m DEM (USGS National Elevation Dataset). Watershed slope (%) was estimated from each delineated area using Google Earth Engine for the larger pan-Arctic rivers and ArcGIS for the smaller North Slope rivers. Although these software packages are different, their areal extrapolation methods to calculate watershed slope are similar. Refer to Burrough and McDonell (1998) for more details on how watershed slope is calculated. Watershed area and slope calculations for the Ob' excluded a large endorheic basin (an internal drainage area with no connection to the rest of the river network) of ~245,277 km^2 that lies within the southern region of the watershed. Likewise, a smaller endorheic zone (7,693 km^2) was excluded from the southern region of the Yensiey watershed. Average soil organic carbon content (SOCC kg m^{-2}) was calculated within delineated catchment boundaries for each sampling location in this study using the soil organic matter dataset (100 cm) from the Northern Circumpolar Soil Carbon Database (NCSCD) (Hugelius et al., 2013). The NCSCD raster dataset includes gridded SOCC values for the entire pan-Arctic that can be used for estimating watershed means. The highest spatial resolution dataset (0.012°) was used for all watersheds, except for the Yenisey where a 0.05° resolution dataset covered a greater extent of the watershed. The Ob' watershed is not

included because a large portion of the watershed was missing in the NCSCD dataset. Average SOCC and watershed slope values for each catchment in this study were used to develop a natural log-linear regression relationship between these two variables.

Table A.1. Regression coefficients for relationships between watershed slope values (%) and fluvial constituent concentrations (mg L^{-1}). Results are provided for analyses using all available data as well as balanced datasets (i.e., equal spring and summer representation of data). 95 % confidence intervals (CI) are reported below coefficient values. Values and CIs in bold indicate a significant difference (α set at 0.05) between spring and summer coefficients from an analysis of covariance (ANCOVA) test. For DOC and DON, the regression models take the form of y = mln(x) + b. The NO_3^- models take the form of y = m(x) + b.

	DOC				DON				NO_3^-			
	Intercept	Slope	R^2	*n*	Intercept	Slope	R^2	*n*	Intercept	Slope	R^2	*n*
Unbalanced												
Spring												
Value	15.1	−3.64	0.75	35	0.421	−0.091	0.70	33	0.049	**0.0001**	0.002	33
CI	13.9 to 16.3	−4.01 to −3.27			0.387 to 0.455	−0.101 to −0.080			0.033 to 0.066	**−0.0004 to 0.0006**		
Summer												
Value	12.3	−2.94	0.62	52	0.503	−0.120	0.65	44	0.009	**0.0022**	0.16	44
CI	11.3 to 13.4	−3.27 to −2.61			0.460 to 0.545	−0.134 to −0.106			−0.017 to 0.035	**0.0014 to 0.0029**		
Balanced												
Spring												
Value	**14.7**	−3.39	0.67	22	0.395	−0.081	0.67	20	0.051	**0.0004**	0.017	20
CI	**13.1 to 16.2**	−3.92 to −2.86			0.358 to 0.433	−0.095 to −0.068			0.032 to 0.070	**−0.0003 to 0.0010**		
Summer												
Value	**10.8**	−2.54	0.70	22	0.365	−0.082	0.73	20	0.002	**0.0044**	0.41	20
CI	**9.7 to 11.8**	−3.63 to −1.45			0.331 to 0.398	−0.093 to −0.070			−0.034 to 0.038	**0.0031 to 0.0056**		

APPENDIX B: CHAPTER 2 SUPPLEMENTARY MATERIAL

This supplementary material section provides a figure comparing lagoon DOC concentrations and C:N ratios with their associated stable oxygen isotope ($\delta^{18}O$) values for a subset of low-salinity (salinity < 5) lagoon water samples collected in June. $\delta^{18}O$ data was collected from Harris et al. (2017).

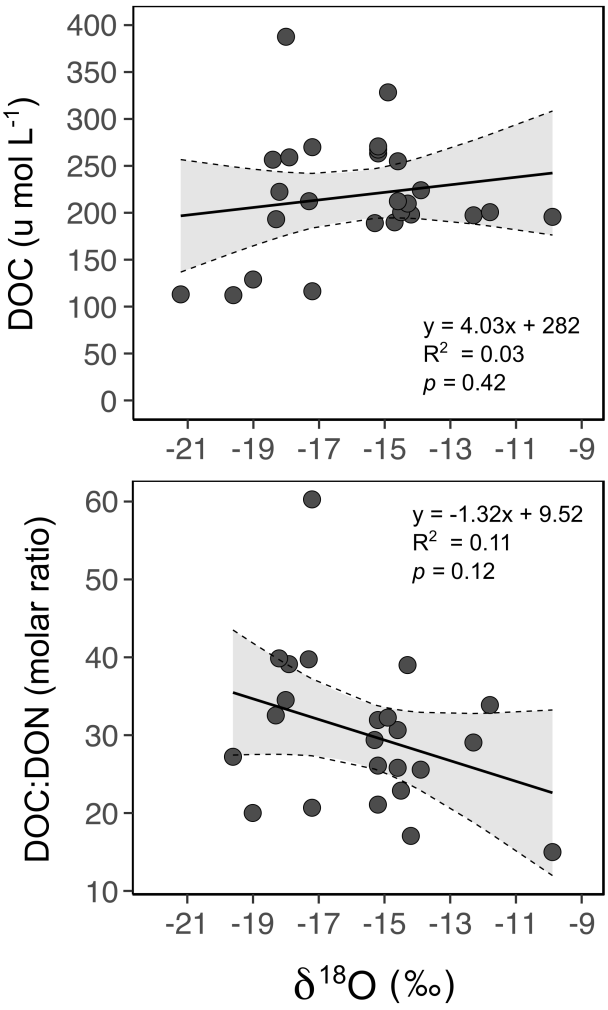

Figure B.1. Relationships between DOC concentration and C:N ratios versus $\delta^{18}O$ values for lagoon water samples collected in June. All samples had salinities < 5. The gray shaded areas and dashed lines mark the upper and lower limits of the 95 % confidence interval bands.

APPENDIX C: CHAPTER 3 SUPPLEMENTARY MATERIAL

This supplementary information material provides a figure depicting boat-towed measurements of radon (^{222}Rn) in Kaktovik Lagoon, a more detailed description of the steady-state radon ^{222}Rn isotope box model, and discussion of the uncertainty in our modeled supra-permafrost groundwater (SPGW) discharge and DOM fluxes.

In this section we provide a step-by-step description of the steady-state Rn isotope box model calculations that were used to estimate total groundwater discharge to Kaktovik Lagoon. This model uses the same mass balance approach described in a number of other studies (e.g., Cable et al., 1996; Corbett et al., 2000; Dimova and Burnett, 2011; Dimova et al., 2013). In particular, our model adopts a framework for lake systems in Kluge et al. (2007).

Assuming that Kaktovik Lagoon is well mixed and that lagoon Rn activity is at a steady state (i.e., $dC_{la}/dt = 0$), then only the following quantities need to be determined for the model: the mean Rn activity concentration of lagoon water $C_{la\text{-}Rn}$, a representative Rn activity concentration of SPGW inflow C_{gw}, the radium (^{226}Ra) activity concentration of the lagoon water $C_{la\text{-}Ra}$, a representative value for the Rn sediment flux F_{sed}, and the gas exchange flux of Rn from the lagoon surface to the atmosphere F_{atms}. We assume that the lagoon water level remained the same during the sampling period (21 & 21 August 2017) and so we can treat the total lagoon volume (V) and exchange with groundwater as constant. We also assume that lagoon Rn activity concentrations do not change over time. This assumption is reasonable because of the shallow and largely enclosed nature of Kaktovik Lagoon, which is expected to cause a relatively long residence time of water over the summer (Delesalle and Sournia, 1992). Given the assumptions, the Rn mass balance equation is thus:

$$(1) \qquad Q_{gw}\,(C_{gw} - C_{la\text{-}Rn}) + F_{sed}\,A_{sed} - F_{atms}\,A_{surf} - \lambda_{Rn}\,V\,(C_{la\text{-}Rn}) + \lambda_{Ra}\,V\,(C_{la\text{-}Ra}) = 0$$

Q_{gw} is the unknown volumetric groundwater inflow ($m^3\ d^{-1}$), which can be calculated when all other inputs, outputs, and sinks/sources are known: the input of Rn from lagoon sediments $F_{sed}\ A_{sed}$, the loss of lagoon Rn to the atmosphere $F_{atms}\ A_{surf}$, the

loss of lagoon Rn to natural decay λ_{Rn} V ($C_{la\text{-}Rn}$), and the introduction of Rn to lagoon water through Ra decay λ_{Ra} V ($C_{la\text{-}Ra}$).

C_{gw} (Bq m^{-3}) was estimated from the average of three SPGW samples (222.5 Bq m^{-3}). The discrete groundwater samples were analyzed using 250 mL volumes following the Wat250 protocol for the RAD7 radon-in-air monitor (Durridge Company, Inc.). Each Rn measurement was corrected for ^{222}Rn that has decayed during the time elapsed between sample collection and measurement in the field following:

(2) $$C_{gw\text{-}initial} = C_{gw\text{-}final} / e^{-\lambda Rn\, t}$$

$C_{gw\text{-}final}$ (Bq m^{-3}) is the measured groundwater Rn concentration following sample collection. λ_{Rn} is the decay constant of ^{222}Rn (0.181) with a half-life of 3.83 days. t (in days) is the time elapsed between each sample collection and sample Rn measurement.

$C_{la\text{-}Rn}$ (Bq m^{-3}) is the average of boat-towed Rn measurements collected over the course of 21 and 22 August 2017 (32.4 Bq m^{-3}). The measurements were done *in-situ* using the RAD-AQUA accessory (or water degassing chamber). Water from approximately 2–3 feet depth was pumped continuously into the RAD-AQUA accessory. The gas in the chamber was sent to three separate RAD7 units following the approach of Dulaiova et al. (2005). The RAD7 monitors each measured Rn every 30 minutes but each unit was started 10 minutes apart. With the boat moving at 1–2 knots, this allowed for traversing Kaktovik Lagoon over two days. The Rn measurements shown in the map are located at the mid-point of a 30-minute long traverse preceding each Rn measurement.

A_{surf} is the area of the lagoon surface and A_{sed} is the area of the lagoon sediment surface, which are assumed to be the same. A_{sed} and A_{surf} (2.47×10^7 m^2) were estimated from the perimeter of Kaktovik Lagoon (2.88×10^4 m) using the Google Earth polygon

tool. A small embayment near a stream outlet on the eastern side of Kaktovik Lagoon was not included in this area estimate.

λ_{Ra} is the decay constant of ^{226}Ra (1.19×10^{-6}) with a half-life of 1,577 years.

$C_{la\text{-}Ra}$ (Bq m^{-3}) is the Ra concentration of Kaktovik Lagoon (5.93 Bq m^{-3}). We did not directly measure ^{226}Ra in this study and so we used an estimate of late summer Ra concentration in Elson Lagoon on the western side of the Alaskan Beaufort Sea coast from Dimova et al. (2015) (35.6 +/− 5.8 dpm per 100 L converted to Bq m^{-3}). Kaktovik and Elson lagoons are functionally similar, so we assume that Ra concentrations are the same during this time period.

V of Kaktovik Lagoon (6.15×10^7 m^3) was estimated from A_{surf} and the average lagoon depth (2.5 m), which was calculated from a NOAA bathymetric map.

The other terms for the Rn box model were calculated from the following series of equations:

$$(3) \qquad F_{sed} = (D_s \lambda_{Rn})^{0.5} \times (C_{sed} - C_{la\text{-}Rn})$$

F_{sed} (Bq m^2 day^{-1}) is the flux of Rn from lagoon benthic sediments. D_s (m^2 day^{-1}) is the wet bulk sediment diffusion coefficient. Here we assume a D_s value of 4.22×10^{-5} m^2 day^{-1} for Kaktovik Lagoon, which is derived from the 154 cm^2 yr^{-1} estimate for benthic sediments at 0–1 cm depth in Toolik Lake, Alaska reported by Cornwell and Banahan (1992). The diffusive conditions in benthic sediments of Toolik Lake are likely similar to that in Kaktovik Lagoon because their surrounding environments are very similar. C_{sed} (Bq m^{-3}) is the equilibrium activity of Rn measured from wet lagoon benthic sediments. C_{sed} was estimated from the average of seven lagoon sediment samples collected in late August 2017 (2,932 Bq m^{-3}). Each sediment sample was dried and

measured for Rn activity in a bulk emissions chamber. Rn concentrations were then converted to the expected Rn activity from wet lagoon sediments using the equation:

(4) $C_{sed} = Mn_{Rn\text{-}box} / V_w$

C_{sed} (Bq m^{-3}) is the expected Rn activity concentration from wet lagoon sediments in the bulk emissions chamber given a sediment porosity (ϕ_{sed}) of 0.25 and particle density of quartz; this porosity was assumed and is typical of silty sand such as those present in Kaktovik Lagoon. $Mn_{Rn\text{-}box}$ (Bq) is the measured Rn production from a known mass of dry sediment. V_w (m^3) is the volume of water or air in the bulk emissions chamber (2,800 cm^3).

F_{atms} (Bq m^2 day^{-1}) is the loss of Rn to the atmosphere from the lagoon water-air interface. F_{atms} is calculated from the following series of equations:

(5) $F_{atms} = k(600) \times (C_{la\text{-}Rn} - \alpha\, C_{air})$

k(600) (m day^{-1}) is the gas transfer coefficient and C_{air} (Bq m^{-3}) is the Rn concentration in the air, which is assumed to be 0.10. α is the Ostwald's solubility coefficient. k(600) was estimated using the following equations (Macintyre et al., 1995):

(6) $k(600) = 0.45\ (u10^{1.6}) \times (Sc/600)^{-b}$

u10 (m sec^{-1}) is the wind speed at 10 m above ground and b is 0.5 for wind speeds > 3.6 m/s or = 0.667 for wind speeds < 3.6 m/s. Average wind speed above

Kaktovik Lagoon (0.002 m sec^{-1}) was acquired from wunderground.com for 21 and 22 August 2017. Sc is the Schmidt number, which is calculated by the following equation:

(7) $Sc = v / D_m$

v is the kinematic viscosity (cm^2 sec^{-1}) and D_m is the Rn molecular diffusion coefficient. v is solved by:

(8) $v = \mu / \rho$

μ (kg m^{-1} sec^{-1}) is the absolute viscosity and ρ (kg m^{-3}) is the density of lagoon water with a water temperature of the 9.68 °C and salinity of 20.4 PSU. Temperature and salinity were not measured throughout Kaktovik Lagoon during the study period. Rather, these values were calculated from 15 August 2012 data reported in Harris et al. (2017). Therefore we assume that these values represent ambient lagoon conditions during our sampling period. In step (7), D_m is calculated by:

(9) $D_m = 10^{-(980/T)} + 1.59$

where T is the temperature of lagoon water in Kelvin (282.83 K). In step (5), α is given by:

(10) $\alpha = 0.105 + 0.405\ e^{-0.0502\ T}$

where T is the average air temperature on 21 and 22 August (6.67 °C) acquired from wunderground.com.

In the proceeding section we quantify uncertainty in total groundwater discharge by propagating standard errors (SE) for the main components of the Rn box model. These SEs reflect variability between Rn measurements as opposed to analytical uncertainty. Analytical uncertainties for Rn measurements are typically 10–15 % using these methods (Dimova et al., 2013). These components and their associated mean Rn concentrations ± 1 SE are: land-derived SPGW inputs (223 ± 20 Bq m^{-3}), lagoon sediment inputs (2,932 ± 650 Bq m^{-3}), and lagoon water (32.4 ± 3.9 Bq m^{-3}). Propagating error from individual end-member values show (1) a 12 % increase and 10 % decrease in discharge associated with error in our groundwater Rn value; (2) a 27 % increase and decrease in discharge associated with error in our lagoon sediment Rn value; and (3) a 29 % increase and 28 % decrease in discharge associated with error in our lagoon water Rn value. Using the average Rn end-member values, our modeled groundwater discharge to Kaktovik Lagoon was 8.56×10^5 m^3 day^{-1}. The potential minimum and maximum groundwater discharge when propagating error from all three end-members is 3.50×10^5 m^3 day^{-1} and 1.51×10^6 m^3 day^{-1}. Maximum discharge results from a propagation of error associated with the mean groundwater Rn value – 1 SE (202 Bq m^{-3}), the mean lagoon sediment Rn value – 1 SE (2281 Bq m^{-3}), and the mean lagoon water value + 1 SE (36. 2 Bq m^{-3}), while the opposite will result in the estimated minimum groundwater discharge.

Using the average end-member Rn values and the assumption that 5 % of total groundwater discharge measured by our Rn box model is land-derived freshwater, we estimated that SPGW exports 2,128 m^3 of freshwater, 70.6 kg of DOC, and 4.3 kg of DON per day per km shoreline. Scaled to the Alaska Beaufort Sea coastline, SPGW delivers an estimated 4.2×10^6 m^3 freshwater day^{-1}, 138 Mg DOC day^{-1}, and 8.4 Mg

DON day^{-1}. After accounting for error propagation, we estimate at a minimum SPGW exports 871 m^3 of freshwater, 28.9 kg of DOC, and 1.8 kg of DON per day per km shoreline. Scaled to the Alaska Beaufort Sea coastline, this equates to 1.7×10^6 m^3 freshwater day^{-1}, 56.5 Mg DOC day^{-1}, and 3.4 Mg DON day^{-1}. We estimate at a maximum SPGW exports 3,753 m^3 of freshwater, 125 kg of DOC, and 7.5 kg of DON per day per km shoreline. Scaled up to the Alaska Beaufort Sea coastline, this equates to 7.3×10^6 m^3 freshwater day^{-1}, 244 Mg DOC day^{-1}, and 14.7 Mg DON day^{-1}.

This analysis demonstrates that we can expect an uncertainty in SPGW discharge and DOM fluxes that ranges from 76 % higher and 59 % lower than average estimates.

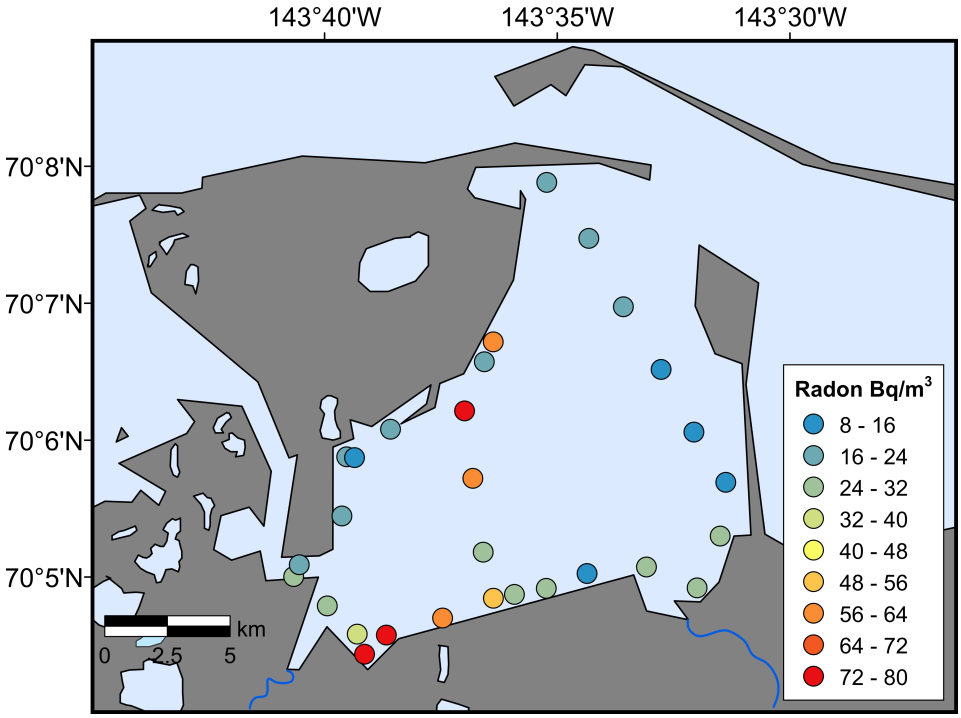

Figure C.1. Boat-towed measurements of ^{222}Rn concentrations around Kaktovik Lagoon conducted on August 21st and 22nd 2017.

References

Aagaard, K. & Carmack, E. C. (1989). The role of sea ice and other fresh water in the Arctic circulation. *Journal of Geophysical Res*earch*: Oceans,* 94 (C10), 14485–14498. doi:10.1029/JC094iC10p14485

Aarnos, H., Ylöstalo, P., & Vähätalo, A. V. (2012). Seasonal phototransformation of dissolved organic matter to ammonium, dissolved inorganic carbon, and labile substrates supporting bacterial biomass across the Baltic Sea. *Journal of Geophysical Research Biogeoscience*, 117, G01004. doi:10.1029/2010jg001633

Abbott, B. W., Jones, J. B., Godsey, S. E., Larouche, J. R., & Bowden, W. B. (2015). Patterns and persistence of hydrologic carbon and nutrient export from collapsing upland permafrost. *Biogeosciences*, 12, 3725–3740. https://doi.org/10.5194/bg-12-3725-2015

Abbott, B. W., Larouche, J. R., Jones, J. B., Bowden, W. B., & Balser, A. W. (2014). Elevated dissolved organic carbon biodegradability from thawing and collapsing permafrost. *Journal of Geophysical Research: Biogeosciences*, 119, 2049–2063. doi:10.1002/2014JG002678

Ågren, A., Buffam, I., Berggren, M., Bishop, K., Jansson, M., & Laudon, H. (2008). Dissolved organic carbon characteristics in boreal streams in a forest wetland gradient during the transition between winter and summer. *Journal of Geophysical Research*, 113, G03031. doi:10.1029/2007JG000674

Aiken, G. R., Spencer, R. G. M., Striegl, R. G., Schuster, P. F., & Raymond, P. A. (2014). Influences of glacier melt and permafrost thaw on the age of dissolved organic carbon in the Yukon River basin. *Global Biogeochemical Cycles*, 28, 525–537. doi:10.1002/2013GB004764

Alkire, M. B. & Trefry, J. H. (2006). Transport of spring floodwater from rivers under ice to the Alaskan Beaufort Sea, *Journal of Geophysical Research*, 111, C12008. doi:10.1029/2005JC003446

Amon, R. M. W. (2004) The Role of Dissolved Organic Matter for the Organic Carbon Cycle in the Arctic Ocean. In: Stein R., MacDonald R.W. (eds) The Organic Carbon Cycle in the Arctic Ocean. Springer, Berlin, Heidelberg. https://doi.org/10.1007/978-3-642-18912-8_4

Amon, R. M. W. & Meon, B. (2004). The biogeochemistry of dissolved organic matter and nutrients in two large Arctic estuaries and potential implications for our understanding of the Arctic Ocean system. *Marine Chemistry,* 92(1-4), 311–330. doi:10.1016/j.marchem.2004.06.034

Barnes, R. T., Butman, D. E., Wilson, H. F., & Raymond, P. A. (2018). Riverine Export of Aged Carbon Driven by Flow Path Depth and Residence Time, *Environmental Science & Technology*, 52 (3), 1028–1035. doi:10.1021/acs.est.7b04717

Beaupré, S. R., Druffel, E. R. M., & Griffin, S. (2007). A low-blank photochemical extraction system for concentration and isotopic analyses of marine dissolved organic carbon. *Oceanography Methods*, 5, 174–184. https://doi.org/10.4319/lom.2007.5.174

Bengtsson, M. M., Attermeyer, K., & Catalán, N. (2018). Interactive effects on organic matter processing from soils to the ocean: Are priming effects relevant in aquatic ecosystems? *Hydrobiologia*, 822(1), 1–17. https://doi.org/10.1007/s10750-018-3672-2

Benner, R., Benitez-Nelson, B., Kaiser, K., & Amon, R. M. W. (2004). Export of young terrigenous dissolved organic carbon from rivers to the Arctic Ocean. *Geophysical Research Letters,* 31(5), L05305. doi:10.1029/2003GL019251

Bianchi, T. S. (2011). The role of terrestrially derived organic carbon in the coastal ocean: A changing paradigm and the priming effect. *Proceedings of the National Academy of Sciences*, 108(49), 19473–19481. https://doi.org/10.1073/pnas.1017982108

Bianchi, T. S., Galy, V. V., Rosenheim, B. E., Shields, M., Cui, X., & Van Metre, P. (2015). Paleoreconstruction of organic carbon inputs to an oxbow lake in the Mississippi River watershed: effects of dam construction and land use change on regional inputs. *Geophysical Research Letters* 42, 7983–7991. https://doi.org/10.1002/2015GL065595

Blanchet, M., Pringault, O., Panagiotopoulos, C., Lefèvre, D., Charrière, B., Ghiglione, J. F., et al. (2017). When riverine dissolved organic matter (DOM) meets labile DOM in coastal waters: Changes in bacterial community activity and composition. *Aquatic Sciences*, 79(1), 27–43. https://doi.org/10.1007/s00027-016-0477-0

Boehm, A. B., Paytan, A., Shellenbarger, G. C., & Davis, K. A. (2006). Composition and flux of groundwater from a California beach aquifer: Implications for nutrient supply to the surf zone. *Continental Shelf Research*, 26(2), 269–282. https://doi.org/10.1016/j.csr.2005.11.008

Borges, A. V. & Abril, G. (2011). Carbon dioxide and methane dynamics in estuaries. In: *treatise on Estuarine and Coastal Science*, Elsevier Inc. p. 119–162.

Bowden, W. B., Gooseff, M. N., Balser, A., Green, A., Peterson, B. J., & Bradford, J. (2008). Sediment and nutrient delivery from thermokarst features in the foothills of the North Slope, Alaska: Potential impacts on headwater stream ecosystems. *Journal of Geophysical Research*: *Biogeosciences,* 113, G02026. doi:02010.01029/02007JG000470

Brown, J., Jorgenson, M. T., Smith, O. P., & Lee, W. (2003). Long-term rates of coastal erosion and carbon input, Elson Lagoon, Barrow, Alaska. In *Eighth International Conference on Permafrost*, p. 21—25.

Brown, S., Kendall, S., Churchwell, R., Taylor, A., & Anna-Marie, B. (2012). Relative shorebird densities at coastal sites in the Arctic National Wildlife Refuge. *Waterbirds,* 35, 546–554. https://doi.org/10.1675/063.035.0405

Burnett, W., Bokuniewicz, H., Huettel, M., Moore, W., & Taniguchi, M. (2003). Groundwater and Pore Water Inputs to the Coastal Zone. *Biogeochemistry,* 66(1/2), 3–33. https://www.jstor.org/stable/1469879

Burrough, P. A. & McDonell, R. A., (1998). Principles of Geographical Information Systems (Oxford University Press, New York), 190 pp.

Cable, J. E., Burnett, W. C., Chanton, J. P., & Weatherly, G. L. (1996). Estimating groundwater discharge into the northeastern Gulf of Mexico using radon-222. *Earth and Planetary Science Letters*, 143, 591–604. https://doi.org/10.1016/S0012-821X (96)00173-2

Carmack, E. & Wassmann, P. (2006). Food webs and physical-biological coupling on pan-Arctic shelves: Unifying concepts and comprehensive perspectives. *Progress in Oceanography*, 71, 446–477. https://doi.org/10.1016/j.pocean.2006.10.004

Casper, A. F., Rautio, M., Martineau, C., & Vincet, W. F. (2014). Variation and assimilation of Arctic riverine seston in the pelagic food web of the Mackenzie River delta and Beaufort Sea transition zone. *Estuaries and Coasts*, 38(5), 1656–1663. https://doi.org/10.1007/s12237-014-9917-z

Cauwet, G. & Sidorov, I. (1996). The biogeochemistry of the Lena River: organic carbon and nutrients distribution. *Marine Chemistry*, 53, 211–227. https://doi.org/10.1016/ 0304-4203(95)00090-9

Churchwell, R. T., Kendall, S. J., Blanchard, A. L., Dunton, K. H., & Powell, A. N. (2015). Natural disturbance shapes benthic intertidal macroinvertebrate communities of high latitude river deltas. *Estuaries and Coasts*, 39, 798. https://doi.org/10.1007/ s12237-015-0028-2

Connelly, T. L., McClelland, J. W., Crump, B. C., Kellogg, C. T. E., & Dunton, K. H. (2015). Seasonal changes in quantity and composition of suspended particulate organic matter in lagoons of the Alaskan Beaufort Sea. *Marine Ecology Progress Series*, 527, 31–45. https://doi.org/10.3354/meps11207

Connolly, C. T., Burkart, G., Cardenas, M. B., Spencer, R. G. M, & McClelland, J. W. (2019a). Groundwater as a major source of dissolved organic matter to Arctic coastal waters. In progress.

Connolly, C. T., Kellogg, C. T. E., Dunton, K. H., Crump, B. C., & McClelland, J. W. (2019b). Seasonality of dissolved organic matter in lagoon ecosystems along the eastern Alaska Beaufort Sea coast. In progress.

Connolly, C. T., Khosh, M. S., Burkart, G. A., Douglas, T. A., Holmes, R. M., Jacobson, A. D., Tank, S. E., McClelland, J. W. (2018). Watershed slope as a predictor of fluvial dissolved organic matter and nitrate concentrations across geographical space

and catchment size in the Arctic. *Environmental Research Letters*, 13(10), 104015. https://doi.org/10.1088/1748-9326/aae35d

Corbett, D. R., Dillon, K., Burnett, W. C., & Chanton, J. P. (2000). Estimating the groundwater contribution into Florida Bay via natural tracers, Rn-222 and CH4. *Limnology and Oceanograpy*, 45, 1546–1557. https://doi.org/10.4319/lo.2000.45.7.1546

Corilo, Y. (2018). PetroOrg Software, Florida State University.

Cornwell, J. C. & Banahan, S. (1992). A silicon budget for an Alaskan arctic lake. *Hydrobiologia*, 240, 37–44. https://doi.org/10.1007/BF00013450

Cory, R. M., Ward, C. P., Crump, B. C., & Kling, G. W. (2014). Sunlight controls water column processing of carbon in arctic fresh waters. *Science,* 345, 925–928. doi:10.1126/science.1253119

Creed, I. F. & Beall, F. D. (2009). Distributed topographic indicators for predicting nitrogen export from headwater catchments. *Water Resources Research*, (45), W10407. doi:10.1029/2008WR007285

Creed, I. F., Beall, F. D., Clair, T. A., Dillon, P. J., & Hesslein, R. H. (2008). Predicting export of dissolved organic carbon from forested catchments in glaciated landscapes with shallow soils. *Global Biogeochemical Cycles*, (22), GB4024. doi:10.1029/2008GB003294

Creed, I. F., Sanford, S. E., Beall, F. D., Molot, L. A., & Dillon, P. J. (2003). Cryptic wetlands: Integrating hidden wetlands in regression models of export of dissolved organic carbon from forested landscapes. *Hydrologic Processes*, 17, 3629– 3648. doi:10.1002/hyp.1357

Crump, B., Kling, G., Bahr, M., & Hobbie, J. (2003). Bacterioplankton community shifts in an arctic lake correlate with seasonal changes in organic matter source. *Applied and Environmental Microbiology*, 69, 2253–2268. doi:10.1128/AEM.69.4.2253-2268.2003

D'Amore, D. V., Edwards, R. T., & Biles, F. E. (2016). Biophysical controls on dissolved organic carbon concentrations of Alaskan coastal temperate rainforest estimates. *Aquatic Sciences*, 78, 381–393. doi:10.1007/s00027-015-0441-4

Darnis, G. & Fortier, L. (2012). Zooplankton respiration and the export of carbon at depth in the Amundsen Gulf (Arctic Ocean). *Journal of Geophysical Research*, 117, C04013. doi:10.1029/ 2011-JC007374

Dean, K. G., Stringer, W. J., Ahlns, K., Searcy, C., & Weingartner, T. (1994). The influence of river discharge on the thawing of sea ice, Mackenzie River Delta: albedo and temperature analysis. *Polar Research*, 13, 83–94. https://doi.org/10.3402/polar.v13i1.6683

Delesalle, B. & Sournia, A. (1992). Residence time of water and phytoplankton biomass in coral reef lagoons. *Continental Shelf Research*, 12, 939–949. https://doi.org/10.1016/0278-4343(92)90053-M

Dillon, P. J. & Molot, L. A. (1997). Effect of landscape form on export of dissolved organic carbon, iron, and phosphorus from forested stream catchments. *Water Resources Research*, 33, 2591–2600. doi:10.1029/97WR01921

Dimova, N. T. & Burnett, W. C. (2011). Evaluation of groundwater discharge into small lakes based on the temporal distribution of radon-222. *Limnology and* Oceanography, 56(2), 486–494. https://doi.org/10.4319/lo.2011.56.2.048

Dimova, N. T., Burnett, W. C., Chanton, J. P., & Corbett, J. E. (2013). Application of radon-222 to investigate groundwater discharge into small shallow lakes. *Journal of Hydrology*, 486, 112–122. doi:10.1016/j.jhydrol.2013.01.043

Dimova, N., Paytan, A., Kessler, J. D., Sparrow, K. J., Kodovska, F. G-T., Lecher, A., L., Murry, J., & Tulaczyk, S. (2015). Current magnitude and mechanisms of groundwater discharge in the Arctic: a case study from Alaska. *Environmental Science and Technology*, 49(20), 12036–12043. doi:10.1021/acs.est.5b02215

Dittmar, T. & Kattner, G. (2003). The biogeochemistry of the river and shelf ecosystem of the Arctic Ocean : A review. *Marine Chemistry*, 83(3-4), 103–120. https://doi.org/10.1016/S0304-4203(03)00105-1

Dittmar, T., Koch, B., Hertkorn, N., & Kattner, G. (2008). A simple and efficient method for the solid-phase extraction of dissolved organic matter (SPE-DOM) from seawater. *Limnology and Oceanography Methods*, 6, 230–235. https://doi.org/10.4319/lom.2008.6.230

Dorado-García, I., Syvaranta, J., Devlin, S. P., Medina-Sánchez, J. M., & Jones, R. I. (2016). Experimental assessment of a possible microbial priming effect in a humic boreal lake. *Aquatic Sciences*, 78, 191–202. https://doi.org/10.1007/s00027-015-0425-4

Dornblaser, M. M. & Striegl, R. G. (2007). Nutrient (N, P) loads and yields at multiple scales and subbasin types in the Yukon River basin, Alaska. *Journal of Geophysical Research*: *Biogeosciences*, 112, G04S57. doi:10.1029/2006JG000366

Dou, F., Ping, C., Guo, L., & Jorgenson, T. (2008). Estimating the Impact of Seawater on the Production of Soil Water-Extractable Organic Carbon during Coastal Erosion. *Journal of Environmental Quality*, 37, 2368–2374. doi:10.2134/jeq2007.0403

Douglas, T. A., Fortier, D., Shur, Y. L., Kanevskiy, M. Z., Guo, L., Cai, Y., & Bray, M. T. (2011). Biogeochemical and geocryological characteristics of wedge and thermokarst cave ice in the CRREL permafrost tunnel, Alaska. *Permafrost Periglacial Processes*, 22, 20–128. doi:10.1002/ppp.709

Drake, T. W., Guillemette, F., Hemingway, J. D., Chanton, J. P., Podgorski, D. C., Zimov, N. S., & Spencer, R. G. M. (2018). The ephemeral signature of permafrost

carbon in an Arctic fluvial network. *Journal of Geophysical Research: Biogeosciences*, 123, 1475–1485. https://doi.org/10.1029/2017JG004311

Drake, T. W., Wickland, K. P., Spencer, R. G. M., McKnight, D. M., & Striegl, R. G. (2015). Ancient low–molecular-weight organic acids in permafrost fuel rapid carbon dioxide production upon thaw. *Proceedings of the National Academy of Sciences*, 112 (45) 13946–13951. https://doi.org/10.1073/pnas.1511705112

Druffel, E. R. M., Griffin, S., Glynn, C. S., Benner, R., & Walker, B. D. (2017). Radiocarbon in dissolved organic and inorganic carbon of the Arctic Ocean. *Geophysical Research Letters*, 44, 2369–2376. doi:10.1002/2016GL072138

Dulaiova, H., Peterson, R., Burnett, W. C., & Smith, D. L. (2005). A Multi-Detector Continuous Monitor for Assessment of ^{222}Rn in the Coastal Ocean. *Journal of Radioanalytical and Nuclear Chemistry,* 263(2), 361–365. https://doi.org/10.1007/s10967-005-0595-y

Dunton, K. H. & Crump, B. C. (2014). Collaborative Research: Terrestrial Linkages to Microbial and Metazoan Communities in Coastal Ecosystems of the Beaufort Sea. Arctic Data Center. urn:uuid:a8a80b4d-6170-4f12-bf62-37a0bcda9e5e

Dunton, K. H., Schonberg, S. V., & Cooper, L. W. (2012). Food web structure of the Alaskan nearshore shelf and estuarine lagoons of the Beaufort Sea. *Estuaries and Coasts,* 35(2), 416–435. https://doi.org/10.1007/s12237-012-9475-1

Dunton, K. H., Weingartner, T. & Carmack, E. C. (2006). The nearshore western Beaufort Sea ecosystem: circulation and importance of terrestrial carbon in arctic coastal food webs. *Progress in Oceanography*, 71, 362–378. https://doi.org/10.1016/j.pocean.2006.09.011

Eimers, M. C., Watmough, S. A., & Buttle, J. M. (2008). Long-term trends in dissolved organic carbon concentration: a cautionary note. *Biogeochemistry*, 87, 71–81. doi:10.1007/s10533-007-9168-1

Fichot, C. G. & Benner, R. (2012). The spectral slope coefficient of chromophoric dissolved organic matter ($S_{275–295}$) as a tracer of terrigenous dissolved organic carbon in river-influenced ocean margins. *Limnology and Oceanography*, 57. doi:10.4319/lo.2012.57.5.1453

Fichot, C. G. & Benner, R. (2014). The fate of terrigenous dissolved organic carbon in a river-influenced ocean margin. *Global Biogeochemical Cycles*, 28, 300–318. doi: 10.1002/2013GB004670

Finlay, J. C., Neff, J. C., Zimov, S. A., Davydova, A., & Davydov, S. (2006). Snowmelt dominance of dissolved organic carbon in high-latitude watersheds: Implications for characterization and flux of river DOC. *Geophysical Research Letters,* 33(10), L10401. doi:10.1029/2006GL025754.

Forbes, D. L. (editor). 2011. State of the Arctic Coast 2010–Scientific Review and Outlook. International Arctic Science Committee, Land-Ocean Interactions in the

Coastal Zone, Arctic Monitoring and Assessment Programme, International Permafrost Association. HelmholtzZentrum, Geesthacht, Germany, 178 p. http://arcticcoasts.org

Freeman, C., Ostle, N., & Kang, H. (2001). An enzymic "latch" on a global carbon store. *Nature*, 409, 149–150. doi:10.1038/35051650

Frey, K. E. & McClelland, J. W. (2009). Impacts of permafrost degradation on arctic river biogeochemistry. *Hydrological Processes,* 23*,* 169–182. doi:10.1002/hyp.7196

Frey, K. E., Siegel, D. I., & Smith, L. C. (2007). Geochemistry of west Siberian streams and their potential response to permafrost degradation. *Water Resources Research,* 43(3), W03406. doi:10.1029/2006WR004902

Frey, K. E. & Smith, L. C. (2005). Amplified carbon release from vast West Siberian peatlands by 2100. *Geophysical Research Letters*, 32(9), L09401. doi:10.1029/2004 GL022025.

Fritz, M., Opel, T., Tanski, G., Herzschuh, U., Meyer, H., Eulenburg, A., & Lantuit, H. (2015). Dissolved organic carbon (DOC) in Arctic ground ice. *The Cryosphere*, 9, 737–752. https://doi.org/10.5194/tc-9-737-2015

Gallagher, D. L., Dietrich, A. M., Reay, W. G., Hayes, M. C., & Simmons, G. M. Jr. (1996). Ground water discharge of agricultural pesticides and nutrients to estuarine surface water. *Groundwater Monitoring and Remediation*, 16(1), 118–129. https://doi.org/10.1111/j.1745-6592.1996.tb00579.x

Garneau, M. E., Vincent, W. F., Alonso-Sáez, L., Gratton, Y., & Lovejoy, C. (2006). Prokaryotic community structure and heterotrophic production in a river-influenced coastal Arctic ecosystem. *Aquatic Microbial Ecology*, 42, 27–40. doi:10.3354/ ame042027

Gergel, S. E., Turner, M. G., & Kratz, T. K. (1999). Dissolved organic carbon as an indicator of the scale of watershed influence on lakes and rivers. *Ecological Applications*, 9, 1377–1390. doi:10.1890/1051-0761(1999)009[1377:DOCAAI]2.0. CO;2

Gersper, P. L., Alexander, V., Barkley, S. A., Barsdate, R. J., & Flint, P. S. (1980). *An Arctic ecosystem: The Coastal Tundra at Barrow, Alaska*, edited by J. Brown, P. C. Miller, L. L. Tieszan, and F. L. Bunnell, Dowden, Hutchinson & Ross, Stroudsburg, Pennsylvania, United States of America.

Gibbs, A. E. & Richmond, B. M. (2015). National assessment of shoreline change—Historical shoreline change along the north coast of Alaska, U.S.—Canadian border to Icy Cape: U.S. Geological Survey Open-File Report 2015—1048, 96 pp., doi:10.3133/ofr20151048.

Giblin, A. E., Hopkinson Jr. C. S., & Tucker, J. (1997). Benthic metabolism and nutrient cycling in Boston Harbor, Massachusetts. *Estuaries*, 20, 346–364. https://www. jstor.org/stable/1352349

Gordeev, V. V., Martin, J. M., Sidorov, I. S., & Sidorova, M. V. (1996). A reassessment of the Eurasian river input of water, sediment, major elements, and nutrients to the Arctic Ocean. *American Journal of Science*, 296, 664–691. doi:10.2475/ajs.296.6.664

Gorham, E., Underwood, J., Janssens, J., Freedman, B., Maass, W., Waller, D., & Ogden, J. (1998). The chemistry of streams in southwestern and central Nova Scotia, with particular reference to catchment vegetation and the influence of dissolved organic carbon primarily from wetlands. *Wetlands*, 18, 115–132. https://doi.org/10.1007/BF03161449

Guo, L. & Macdonald, R. W. (2006). Sources and transport of terrigenous organic matter in the upper Yukon River: Evidence from isotope ($\delta^{13}C$, $\Delta^{14}C$, and $\delta^{15}N$) composition of dissolved, colloidal, and particulate phases. *Global Biogeochemical Cycles*, 20, GB2011. doi:10.1029/2005GB002593

Guo, L., Ping, C.-L., & Macdonald, R. W. (2007). Mobilization pathways of organic carbon from permafrost to arctic rivers in a changing climate. *Geophysical Research Letters*, 34(13), 1–5. doi:10.1029/2007GL030689

Hardison, A., McTigue, N. D., Gardner, W. S., & Dunton, K. H. (2017). Arctic shelves as platforms for biogeochemical activity: nitrogen and carbon transformations in the Chukchi Sea, Alaska. *Deep-Sea Research II*, 144, 78–91. https://doi.org/10.1016/j.dsr2.2017.08.004

Harms, T. K., Edmonds, J. W., Genet, H., Creed, I. F., Aldred, D., Balser, A., & Jones, J. B. (2016). Catchment influence on nitrate and dissolved organic matter in Alaskan streams across a latitudinal gradient. *Journal of Geophysical Research: Biogeosciences*, 121(2), 350–369. http://doi.org/10.1002/2015JG003201

Harms, T. K. & Jones, J. B. (2012). Thaw depth determines reaction and transport of inorganic nitrogen in valley bottom permafrost soils. *Global Change Biology,* 18(9), 2958–2968. doi:10.1111/j.1365-2486.2012.02731.x

Harris, C. M., McClelland, J. W., Connelly, T. L., Crump, B. C., & Dunton, K. H. (2017). Salinity and temperature regimes in eastern Alaskan Beaufort Sea lagoons in relation to source water contributions. *Estuaries and Coasts*, 40, 50–62. https://doi.org/10.1007/s12237-016-0123-z

Harris, C. M., McTigue, N. D. McClelland, J. W., & Dunton, K. H. (2018). Do high Arctic coastal food webs rely on a terrestrial carbon subsidy? *Food Webs*, 15, e00081. doi:10.1016/j.fooweb.2018.e00081

Harrison, W. G, Platt, T., & Irwin, B. (1982). Primary production and nutrient assimilation by natural phytoplankton populations of the eastern Canadian Arctic. *Canadian Journal of Fisheries and Aquatic Science*, 39, 335-345. doi:10.1139/f82-046

Helms, J. R.,Stubbins, A., Ritchie, J. D., Minor, E. C., Kieber, D. J., & Mopper, K. (2008). Absorption spectral slopes and slope ratios as indicators of molecular weight, source, and photobleaching of chromophoric dissolved organic matter. *Limnology and Oceanography,* 53, 955. doi:10.4319/lo.2008.53.3.0955

Hemingway, J. D. (2017b). Fourier transform: Open-source tools for FT-ICR MS data analysis. Retrieved from http://github.com/FluvialSeds/fouriertransform

Hemingway, J. D., Rothman, D. H., Rosengard, S. Z., & Galy, V. V. (2017a). Technical note: An inverse method to relate organic carbon reactivity to isotope composition from serial oxidation, *Biogeosciences*, 14, 5099–5114. https://doi.org/10.5194/bg-14-5099-2017

Hemingway, J. D. (2017c). *rampedpyrox*: open-source tools for thermoanalytical data analysis. http://github.com/FluvialSeds/rampedpyrox

Hinton, M. J., Schiff, S. L., & English, M. C. (1998). Sources and flow paths of dissolved organic carbon during storms in two forested watersheds of the Precambrian Shield. *Biogeochemistry*, 41, 175–197. https://doi.org/10.1023/A:1005903428956

Hinzman, L. D., Bettez, N. D., Bolton, W. R., Chapin, F. S., Dyurgerov, M. B., et al. (2005). Evidence and implications of recent climate change in northern Alaska and other arctic regions. *Climatic Change*, 72, 251–298. https://doi.org/10.1007/s10584-005-5352-2

Holmes, R. M., Coe, M. T., Fiske, G. J., Gurtovaya, T., McClelland, J. W., Shiklomanov, A. I., Spencer, R. G. M., Tank, S. E., & Zhulidov, A. V. (2013). Climate Change Impacts on the Hydrology and Biogeochemistry of Arctic Rivers. Climate Change and Global Warming of Inland Waters: Impacts and Mitigation for Ecosystem and Societies, 3–26.

Holmes, R. M., McClelland, J. W., Peterson, B. J., Tank, S. E., Bulygina, E., Eglinton, T. I., et al. (2012). Seasonal and Annual Fluxes of Nutrients and Organic Matter from Large Rivers to the Arctic Ocean and Surrounding Seas. *Estuaries and Coasts*, 35(2), 369–382. https://doi.org/10.1007/s12237-011-9386-6

Holmes, R. M., McClelland, J. W., Raymond, P. A., Frazer, B. B., Peterson, B. J., & Stieglitz, M. (2008). Lability of DOC transported by Alaskan rivers to the Arctic Ocean. *Geophysical Research Letters*, 35(3), L03402. doi:10.1029/2007GL032837

Hugelius, G., Bockheim, J. G., Camill, P., Elberling, B., Grosse, G., Harden, J. W., et al. (2013). A new data set for estimating organic carbon storage to 3m depth in soils of the northern circumpolar permafrost region. *Earth System Science Data*, 5, 393–402. doi:10.5194/essd-5-393-2013

Hugelius, G., Strauss, J., Zubrzycki, S., Harden, J. W., Schuur, E. A. G., Ping, C.-L., et al. (2014). Estimated stocks of circumpolar permafrost carbon with quantified uncertainty ranges and identified data gaps. *Biogeosciences*, 11, 6573–6593. https://doi.org/10.5194/bg-11-6573-2014

Hussain, N., Church, T. M., & Kim, G. (1999). Use of ^{222}Rn and ^{226}Ra to trace groundwater discharge into the Chesapeake Bay. *Marine Chemistry*, 65, 127–134. https://doi.org/10.1016/S0304-4203(99)00015-8

Inamdar, S. P. & Mitchell, M. J. (2006). Hydrologic and topographic controls on storm-event exports of dissolved organic carbon (DOC) and nitrate across catchment scales. *Water Resources Research*, 42, W03421. doi:10.1029/2005WR004212

Inamdar, S. P. & Mitchell, M. J. (2007). Storm event exports of dissolved organic nitrogen (DON) across multiple catchments in a glaciated forested watershed. *Journal of Geophysical Research,* 112, G02014. doi:10.1029/2006JG000309

Johnston, S. E., Shorina, N., Bulygina, E., Vorobjeva, T., Chupakova, A., Klimov, S. I., Kellerman, A. M., Guillemette, F., Shiklomanov, A., Podgorski, D. C., Spencer, R. G. M. (2018). Flux and Seasonality of Dissolved Organic Matter From the Northern Dvina (Severnaya Dvina) River, Russia. *Journal of Geophysical Research: Biogeosciences.* doi: 10.1002/2017JG004337.

Jones, B. M., Arp, C. D., Jorgenson, M. T., Hinkel, K. M., Schmutz, J. A., & Flint, P. L. (2009). Increase in the rate and uniformity of coastline erosion in Arctic Alaska. *Geophysical Research Letters*, 36, L03503. doi:10.1029/2008GL036205

Jones, J. B., Petrone, K. C., Finlay, J. C., Hinzman, L. D., & Bolton, W. R. (2005). Nitrogen loss from watersheds of interior Alaska underlain with discontinuous permafrost. *Geophysical Research Letters,* 32(2), L02401. doi:10.1029/2004GL021734

Jones, M. N. (1984). Nitrate reduction by shaking with cadmium; alternate to cadmium columns. *Water Resources,* 18(5), 643–646. https://doi.org/10.1016/0043-1354(84)90215-X

Jorgenson, T., Yoshikawa, K., Kanevskiy, M., Shur, Y., Romanovsky, V., Marchenko, S., Grosse, G., Brown, J., & Jones, B. (2008). "Permafrost Characteristics of Alaska," Proceedings of the Ninth International Conference on Permafrost, extended abstracts. June 29– July 3, 2008, Fairbanks, Alaska. Kane, DL & Hinkel, KM (eds). Institute of Northern Engineering, University of Alaska Fairbanks, pp 121-122.

Joyce, S. B. & Anderson, I. C. Nitrogen cycling in coastal sediments. In: Capone DG, Bronk DA, Mulholland MR, Carpenter EJ (eds). Nitrogen in the Marine Environment. 2nd edn. Amsterdam:Academic Press, 2008, 868–915.

Judd, K. E., Crump, B. C., & Kling, G. W. (2006). Variation in dissolved organic matter controls bacterial production and community composition. *Ecology*, 87, 2068–2079. https://doi.org/10.1890/0012-9658(2006)87[2068:VIDOMC]2.0.CO;2

Judd, K. E. & Kling, G. W. (2002). Production and export of dissolved C in arctic tundra mesocosms: The roles of vegetation and water flow. *Biogeochemistry,* 60(3), 213–234. https://doi.org/10.1023/A:1020371412061

Kaleris, V. (2006). Submarine groundwater discharge: Effects of hydrogeology and of near shore surface water bodies. *Journal of Hydrology*, 325(1-4), 96–117. https://doi.org/10.1016/j.jhydrol.2005.10.008

Kane, D. L., Yoshikawa, K. & McNamara, J. P. (2013). Regional groundwater flow in an area mapped as continuous permafrost, NE Alaska (USA). *Hydrogeology Journal*, 21, 41–52. https://doi.org/10.1007/s10040-012-0937-0

Kellerman, A. M., Kothawala, D. N., Dittmar, T., & Tranvik, L. J. (2015). Persistence of dissolved organic matter in lakes related to its molecular characteristics. *Nature Geoscience, 8*(6), 454-457. doi:http://dx.doi.org/10.1038/ngeo2440

Khosh, M. S., McClelland, J. W., Jacobson, A. D., Douglas, T. A., Barker, A. J., & Lehn, G. O. (2017). Seasonality of dissolved nitrogen from spring melt to fall freezeup in Alaskan Arctic tundra and mountain streams. *Journal of Geophysical Research: Biogeosciences*, 122(7), 1718-1737. doi:10.1002/2016JG003377

Kim, G., Lee, K.-K., Park, K.-S., Hwang, D.-W., & Yang, H.-S. (2003). Large submarine groundwater discharge (SGD) from a volcanic island, *Geophysical Research Letters*, 30, 2098. doi:10.1029/2003GL018378

Kling, G. W. (1995). Land-water interactions: the influence of terrestrial diversity on aquatic ecosystems. In: Chapin F.S., Körner C. (eds) Arctic and Alpine Biodiversity: patterns, causes and ecosystem consequences. Ecological Studies (Analysis and Synthesis), 113. Springer, Berlin, Heidelberg

Kling, G. W., Kipphut, G. W., & Miller, M. C. (1991). Arctic lakes and rivers as gas conduits to the atmosphere: implications for tundra carbon budgets. *Science*, 25, 298–301. doi:10.1126/science.251.4991.298

Kluge, T., Ilmberger, J., von Rohden, C., & Aeschbach-Hertig, W. (2007). Tracing and quantifying groundwater inflow into lakes using a simple method for radon222 analysis. *Hydrology and Earth System Science*, 11, 1621–1631. https://doi.org/10.5194/hess-11-1621-2007

Koch, B. P. & Dittmar, T. (2006). From mass to structure: An aromaticity index for high-resolution mass data of natural organic matter. *Rapid Communications in Mass Spectrometry*, 20, 926–932. https://doi.org/10.1002/rcm.2386

Kuzyk, Z. A., Macdonald, R. W., Granskog, M. A., Scharien, R. K., Galley, R. J., Michel, C., Barber, D., & Stern, G. (2008). Sea ice, hydrological, and biological processes in the Churchill River estuary region, Hudson Bay. *Estuarine, Coastal and Shelf Science*, 77, 369–384. https://doi.org/10.1016/j.ecss.2007.09.030

Kwon, E. Y., Kim, G., Primeau, F., Moore, W. S., Cho, H.-M., DeVries, T., Sarmiento, J. L., Charette, M. A., & Cho, Y.-K. (2014). Global estimate of submarine groundwater discharge based on an observationally constrained radium isotope model. *Geophysical Research Letters*, 41, 8438–8444. doi:10.1002/2014GL061574

Lantuit, H. et al., (2011). The arctic coastal dynamics database: a new classification scheme and statistics on arctic permafrost coastlines. *Estuaries and Coasts*, 35, 383-400. doi:10.1007/s12237-010-9362-6

Lecher, A. L. (2017). Groundwater discharge in the Arctic: a review of studies and implications for biogeochemistry. *Hydrology*, 4(3), 41. doi:10.3390/hydrology40300 41

Le Fouest, V., Babin, M., & Tremblay, J. E. (2013). The fate of riverine nutrients on Arctic shelves. *Biogeosciences,* 10(6), 3661–3677. doi:10.5194/bg-10-3661-2013

Lehn, G. O., Jacobson, A. D., Douglas, T. A., McClelland, J. W., Barker, A. J., & Khosh, M. S. (2017). Constraining seasonal active layer dynamics and chemical weathering reactions occurring in North Slope Alaskan watersheds with major ion and isotope ($\delta^{34}S_{SO4}$, $\delta^{13}C_{DIC}$, $^{87}Sr/^{86}Sr$, $\delta^{44/40}Ca$, and $\delta^{44/42}Ca$) measurements. *Geochimica et Cosmochimica Acta*, 217 (Supplement C), 399–420. https://doi.org/10.1016/j.gca. 2017. 07.042

Li, L., Barry, D. A., Stagnitti, F., & Parlange, J.-Y. (1999). Submarine groundwater discharge and associated chemical input to a coastal sea. *Water Resources Research*, 35(11), 3253–3259. doi:10.1029/1999WR900189

Lobbes, J. M., Fitznar, H. P., & Kattner, G. (2000). Biogeochemical characteristics of dissolved and particulate organic matter in Russian rivers entering the Arctic Ocean. *Geochimica et Cosmochimica Acta* 64(17), 2973–2983. https://doi.org/10.1016/ S0016-7037(00)00409-9

Louiseize, N. L., Lafrenière, M. J., & Hastings, M. G. (2014). Stable isotopic evidence of enhanced export of microbially derived NO_3^- following active layer slope disturbance in the Canadian High Arctic. *Biogeochemistry*, 121(3), 565–580. https://doi.org/10.1007/s10533-014-0023-x

Macdonald, R.W. (2000). Arctic Estuaries and Ice: A Positive—Negative Estuarine Couple. In: Lewis E.L., Jones E.P., Lemke P., Prowse T.D., Wadhams P. (eds) The Freshwater Budget of the Arctic Ocean. NATO Science Series (Series 2. Environment Security), vol 70. Springer, Dordrecht

Macdonald, R.W., & Yu, Y. (2006). The Mackenzie Estuary of the Arctic Ocean. Handbook of Environmental Chemistry, 5, 91–120. https://doi.org/10.1007/698 _5_027

Macintyre, S., Wannikhof, R., & Chanton, J. P. (1995). Trace gas exchange across the airwater interface in freshwater and coastal marine environments. In: Matson, P.A., Harriss, R.C. (Eds.), Biogenic Trace Gases: Measuring Emissions From Soil and, Water. pp. 52–57.

Mack, M. C., Schuur, E. A. G., Bret-Harte, M. S., Shaver, G. R., & Chapin, F. S (2004). Ecosystem carbon storage in arctic tundra reduced by long-term nutrient fertilization. *Nature*, 431(7007), 440–443. doi:10.1038/nature02887

MacLean, R., Oswood, M. W., Irons, J. G. & Mcdowell, W. H. (1999). The effect of permafrost on stream biogeochemistry : a case study of two streams in the Alaskan (U. S. A.) taiga. *Biogeochemistry*, 47, 239–267. https://doi.org/10.1007/BF00992909

Mann, P. J., Davydova, A., Zimov, N., Spencer, R. G. M., Davydov, S., Bulygina, E., Zimov, S., & Holmes, R. M. (2012). Controls on the composition and lability of dissolved organic matter in Siberia's Kolyma River basin. *Journal of Geophysical Research*, 117, G01028. https://doi.org/10.1029/2011JG001798

Mann, P. J., Eglinton, T. I., McIntyre, C. P., Zimov, N., Davydova, A., Vonk, J. E., Holmes, R. M., & Spencer, R. G. M. (2015). Utilization of ancient permafrost carbon in headwaters of Arctic fluvial networks. *Nature Communications*, 6, 7856. doi: 10.1038/ncomms8856

Mann, P. J., Sobczak, W. V., Larue, M. M., Bulygina, E., Davydova, A., Vonk, J. E., Schade, J., Davydov, S., Zimov, N., Holmes, R. M., & Spencer, R. G. M. (2014). Evidence for key enzymatic controls on metabolism of Arctic river organic matter. *Global Change Biology*, 20, 1089–1100. https://doi.org/10.1111/gcb.12416

McClelland, J. W., Déry, S. J., Peterson, B. J., Holmes, R. M., & Wood, E. F. (2006). A Pan-Arctic evaluation of changes in river discharge during the latter half of the 20th century. *Geophysical Research Letters*, 33, L06715. doi:10.1029/2006GL025753

McClelland, J. W., Holmes, R. M., Dunton, K. H., & Macdonald, R. W. (2012). The Arctic Ocean Estuary. *Estuaries and Coasts*, 35, 353–368. doi:10.1007/s12237-010-9357-3

McClelland, J. W., Holmes, R. M., Peterson, B. J., Raymond, P. A., Striegl, R. G., Zhulidov, A. V., Zimov, S. A., Zimov, N., Tank, S. E., Spencer, R. G. M., Staples, R., Gurtovaya, T. Y., & Griffin, C. G. (2016). Particulate organic carbon and nitrogen export from major Arctic rivers. *Global Biogeochemical Cycles*, 30(5), 629-643. doi:10.1002/2015GB005351

McClelland, J. W., Tank, S. E., Spencer, R. G. M., & Shiklomanov, A. I. (2015). Coordination and sustainability of river observing activities in the Arctic. *Arctic,* 68(5), 1-10. http://dx.doi.org/10.14430/arctic4448

McClelland, J. W., Townsend-Small, A., Holmes, R. M., Pan, F., Stieglitz, M., Khosh, M., & Peterson, B. J. (2014). River export of nutrients and organic matter from the North Slope of Alaska to the Beaufort Sea. *Water Resources Research*, 50, 1823-1839. https://doi.org/10.1002/2013WR014722

McDonough, L. K., Santos, I. R., Andersen, M. S., O'Carroll, D. O., Rutlidge, H., Meredith, K., Oudone, O., & Baker, A. (2018). Changes in global groundwater organic carbon driven by climate change and urbanization, *EarthArXiv*. doi:10. 31223/osf.io/vmaku.

McGuire, K. J., McDonnell, J. J., Weiler, M., Kendall, C., McGlynn, B. L., Welker, J. M., & Seibert, J. (2005). The role of topography on catchment-scale water residence time. *Water Resources Research,* 41(5), W05002. doi:10.1029/2004WR003657

McNamara, J. P., Kane, D. L., Hinzman, L. D., & Storm, A. (1997). Hydrograph separations in an Arctic watershed using mixing model and graphical techniques in the Upper Kuparuk. *Water Resources Research*, 33(7), 1707–1719. https://doi.org/10.1029/2005JG000055

McNamara, J. P., Kane, D. L., Hobbie, J. E., & Kling, G. W. (2008). Hydrologic and biogeochemical controls on the spatial and temporal patterns of nitrogen and phosphorus in the Kuparuk River, arctic Alaska. *Hydrological Processes,* 22(17), 3294–3309. doi:10.1002/hyp.

McNichol, A. P., Jones, G. A., Hutton, D. L., Gagnon, A. R., & Key, R. M. (1994). The rapid preparation of seawater ΣCO2 for radiocarbon analysis at the National Ocean Sciences AMS Facility. *Radiocarbon* 36, 237–246. https://doi.org/10.1017/S0033822200040522

Mohan, S. D., Connelly, T. L., Harris, C. M., Dunton, K. H., & McClelland, J. W. (2016). Seasonal trophic linkages in Arctic marine invertebrates assessed via fatty acids and compound-specific stable isotopes. *Ecosphere*, 7(8), e01429.10.1002/ecs2.1429

Mooney, R. F. & McClelland, J. W. (2012). Watershed export events and ecosystem responses in the Mission-Aransas National Estuarine Research Reserve, south Texas. *Estuaries and Coasts*, 35, 1468–1485. https://doi.org/10.1007/s12237-012-9537-4

Moore, W. S. (2010). The effect of submarine groundwater discharge on the ocean. *Annual Review of Marine Science*, 2, 59–88. doi:10.1146/annurev-marine-120308-081019

Moore, W.S. & de Oliveira, J. (2008). Determination of residence time and mixing processes of the Ubatuba, Brazil, inner shelf waters using natural Ra isotopes. *Estuarine, Coastal and Shelf Science*, 76(3), 512–521. doi:10.1016/j.ecss.2007.07.042

Neff, J. C., Finlay, J. C., Zimov, S. A., Davydov, S. P., Carrasco, J. J., Schuur, E. A. G., & Davydova, A. I. (2006). Seasonal changes in the age and structure of dissolved organic carbon in Siberian rivers and streams. *Geophysical Research Letters*, 33(23), L23401. doi:10.1029/2006GL028222

Neff, J. C. & Hopper, D. U. (2002). Vegetation and climate controls on potential CO_2, DOC, and DON production in northern latitude soils. *Global Change Biology,* 8(9), 872-856. doi: 10.1046/j.1365-2486.2002.00517.x

Neilson, B. T., Cardenas, M. B., O'Connor, M. T., Rasmussen, M. T., King, T. V., & Kling, G. W. (2018). Groundwater flow and exchange across the land surface explain carbon export patterns in continuous permafrost watersheds. *Geophysical Research Letters*, 45, 7596–7605. https://doi.org/10.1029/2018GL078140

Nelson, N. B., Carlson, C. A., & Steinberg, D. K. (2004). Production of chromophoric dissolved organic matter by Sargasso Sea microbes. *Marine Chemistry*, 89, 273–287. doi:10.1016/j.marchem.2004.02.017

Nguyen, D., Maranger, R., Tremblay, J. É., Gosselin, M. (2012). Respiration and bacterial carbon dynamics in the Amundsen Gulf, western Canadian Arctic. *Journal of Geophysical Research*, 117, C00G16. doi: 10.1029/2011JC007343

O'Donnell, J. A., Aiken, G. R., Butler, K. D., Guillemette, F., Podgorski, D. C., & Spencer, R. G. M. (2016). DOM composition and transformation in boreal forest soils: The effects of temperature and organic-horizon decomposition state. *Journal of Geophysical Research: Biogeoscience*s, 121, 2727–2744. https://doi.org/10.1002/2016JG003431

O'Donnell, J. A., Aiken, G. R., Walvoord, M. A., & Butler, K. D. (2012). Dissolved organic matter composition of winter flow in the Yukon River basin: Implications of permafrost thaw and increased groundwater discharge. *Global Biogeochemical Cycles*, 26, GB0E06. doi:10.1029/2012GB004341

Opsahl, S., Benner, R., & Amon, R. M. W. (1999). Major flux of terrigenous dissolved organic matter through the Arctic Ocean. *Limnology and Oceanography*. 44(8), 2017–2023. http://doi.org/10.4319/lo.1999.44.8.2017

Parkinson, C. L., Cavalieri, D. J., Gloersen, P., Zwally, H. J., & Comiso, J. C. (1999). Arctic sea ice extents, areas and trends, 1978–1996. *Journal of Geophysical Research*, 104(20): 837–856. https://doi.org/10.1029/1999JC900082

Pedersen, S. & Linn, A. Jr. (2005), Kaktovik 2000-2002 subsistence fishery harvest assessment. US Fish Wildlife, Office Subsistence Management, Fishery Information Services Division, Federal Subsistence Fishery Monitoring Program, Final Project Report FIS 01-101, Anchorage AK: 58.

Pellerin, B. A., Wollheim, W. M., Hopkinson, C. S., McDowell, M. H., Williams, M. R., Vorosmarty, C. J., & Daley, M. L. (2004). Role of wetlands and developed land use on dissolved organic nitrogen concentrations and DON/TDN in northeastern US rivers and streams, *Limnology & Oceanography*, 49, 910–918.

Peterson, B., Fry, B., Hullar, M., Saupe, S., & Wright, R. (1994). The distribution and stable carbon isotopic composition of dissolved organic carbon in estuaries. *Estuaries*, 17, 111. https://doi.org/10.2307/1352560

Peterson, B. J., McClelland, J. W., Curry, R., Holmes, R. M., Walsh, J. E., & Agaard, K. (2006). Trajectory shifts in the Arctic and subarctic freshwater cycle. *Science*, 313(5790), 1061-1066. doi: 10.1126/science.1122593

Petrone, K. C., Jones, J. B., Hinzman, L. D., & Boone, R. D. (2006). Seasonal export of carbon, nitrogen, and major solutes from Alaskan catchments with discontinuous permafrost. *Journal of Geophysical Research: Biogeosciences*, 111(G2), G02020. doi:10.1029/2005JG000055

Ping, C.-L., Michaelson, G. J., Guo, L., Jorgenson, M. T., Kanevskiy, M., Shur, Y., Dou, F., & Liang, J. (2011). Soil carbon and material fluxes across the eroding Alaska Beaufort Sea coastline, *Journal of Geophysical Research*, 116, G02004. doi:10.1029/2010JG001588

Plante, A. F., Beaupre, S. R., Roberts, M. L., & Baisden, T. (2013). Distribution of radiocarbon ages in soil organic matter by thermal fractionation. *Radiocarbon*, 55, 1077–1083. doi:10.2458/azu_js_rc.55.16310

Rawlins, M. A., Cai, L., Stuefer, S. L., & Nicolsky, D. (2019). Changing characteristics of runoff and freshwater export from watersheds draining Northern Alaska. *The Cryosphere Discussion,* in review. https://doi.org/10.5194/tc-2019-28

Rawlins, M. A., M. Steele, M. M. Holland, J. C. Adam, J. E. Cherry, J. A. Francis, P. Y. Groisman, L. D. Hinzman, T. G., et al. (2010). Analysis of the Arctic System for Freshwater Cycle Intensification: Observations and Expectations. *Journal of Climate,* 23, 5715–5737. https://doi.org/10.1175/2010JCLI3421.1

Raymond, P. A. & Bauer, J. E. (2000). Bacterial consumption of DOC during transport through a temperate estuary. *Aquatic Microbial Ecology*, 22, 1–12. doi:10.3354/ame022001

Raymond, P. A. & Bauer, J. E. (2001). DOC cycling in a temperate estuary: A mass balance approach using natural ^{14}C and ^{13}C isotopes. *Limnology and Oceanography*, 3. doi: 10.4319/lo.2001.46.3.0655.

Raymond, P. A., McClelland, J. W., Holmes, R. M., Zhulidov, A. V., Mull, K., Peterson, B. J., Striegl, R. G., Aiken, G. R., & Gurtovaya, T. Y. (2007). Flux and age of dissolved organic carbon exported to the Arctic Ocean: A carbon isotopic study of the five largest arctic rivers. *Global Biogeochemical Cycles*, 21(4), GB4011. doi:10.1029/2007GB002934

Retamal, L.,Vincent, W. F., Martineau, C., & Osburn, C. L. (2007). Comparison of the optical properties of dissolved organic matter in two river-influence coastal regions of the Canadian Arctic. *Estuaries, Coastal, and Shelf Science*, 72, 261–272. doi:10.1016/j.ecss.2006.10.022

Romanovsky, V. E. & Osterkamp, T. E. (2000). Effects of unfrozen water on heat and mass transport processes in the active layer and permafrost. *Permafrost Periglacial Processes*, 11, 219–239. doi:10.1002/1099-1530(200007/09)11:3<219::AID-PPP352>3.0.CO;2-7

Romera-Castillo, C., Sarmento, H., Alvarez-Salgado, X. A., Gasol, J. M., & Marraséa, C. (2010). Production of chromophoric dissolved organic matter by marine phytoplankton. *Limnology and Oceanography*, 55, 446–454. doi:10.4319/lo.2010.55.1.0446

Rosenheim, B. E., Day, M. B., Domack, E.W., Schrum, H., Benthien, A., & Hayes, J. M. (2008). Antarctic sediment chronology by programmed temperature pyrolysis:

Methodology and data treatment. *Geochemistry, Geophysics, Geosystems*, 9, Q04 005. https://doi.org/10.1029/2007GC001816

Rosenheim, B. E., Domack, E. W., Santoro, J. A., & Gunter, M. (2013a). Improving Antarctic sediment ^{14}C dating using ramped pyrolysis: An example from the Hugo Island Trough. *Radiocarbon,* 55, 115–126. doi:10.2458/azu_js_rc.v55i1.16234

Rosenheim, B. E. & Galy, V. V. (2012). Direct measurement of riverine particulate organic carbon age structure. *Geophysical Research Letters,* 39, L19703. https://doi.org/10.1029/2012GL052883

Rosenheim, B. E., Roe, K. M., Roberts, B. J., Kolker, A. S., Allison, M. A., & Johannesson, K. H. (2013b). River discharge influences on particulate organic carbon age structure in the Mississippi/Atchafalaya River System. *Global Biogeochemical Cycles*, 27, 154–166. https://doi.org/10.1002/gbc.20018

Santi-Temkiv, T., Finster, K., Dittmar, T., Hansen, B. M., Thyrhaugt, R., Nielsen, N. W., & Karlson, U. G. (2013). Hailstones: A window into the microbial and chemical inventory of a storm cloud. *PLoS One*. https://doi.org/10.1371/journal.pone.0053550

Sawyer, A. H., David, C. H., & Famiglietti, J. S. (2016). Continental patterns of submarine groundwater discharge reveal coastal vulnerabilities. *Science*, 353(6300), 705–707. doi: 10.1126/science.aag1058

Schädel C., Bader, M. K. F., Schuur, E. A. G., Biasi, C., Bracho, R., Čapek, P., et al. (2016). Potential carbon emissions dominated by carbon dioxide from thawed permafrost soils. *Nature Climate Change*, 6, 950–953. doi: 10.1038/nclimate3054

Schell, D. M., Daniel, P. M., & Ziemann, P. J. (1984). Chapter 5 primary production, nutrient dynamics, and trophic energetic. Environmental Characterization and Biological use of Lagoons in the Eastern Beaufort Sea: 369–432

Schiff, S. L., Devito, K. J., Elgood, R. J., McCrindle, P. M., Spoelstra, J., & Dillon, P. (2002). Two adjacent forested catchments: Dramatically different NO_3^- exports. *Water Resources Research*, 38(12), 1292. doi:10.1029/2000WR000170

Schreiner, K. M., Bianchi, T. S., & Rosenheim, B. E. (2014). Evidence for permafrost thaw and transport from an Alaskan North Slope watershed. *Geophysical Research Letters*, 41, 3117– 3126. doi:10.1002/2014GL059514

Schuur, E. A. G., Abbott, B. W., Bowden, W. B., et al. (2013). Expert assessment of vulnerability of permafrost carbon to climate change. *Climate Change*, 119(2), 359–374. doi:10.1007/s10584-013-0730-7

Schuur, E. A. G., McGuire, A. D., Schädel, C., Grosse, G., Harden, J. W., Hayes, D. J., et al. (2015). Climate change and the permafrost carbon feedback. *Nature*, 520, 171–179. doi:10.1038/ nature14338

Shaver, G. R., et al. (2014). Terrestrial Ecosystems at Toolik Lake, Alaska, in *Alaska's Changing Arctic: Ecological Consequences for Tundra, Streams, and Lakes*, edited by J. E. Hobbie and G. W. Kling, pp. 90–142, Oxford University Press, New York.

Shiklomanov, A. I. (1998). World water resources: A new appraisal and assessment for the 21st Century. NESCO International Hydrological Programme Publications (p. 37), France, Paris.

Sleighter, R. L., Cory, R. M., Kaplan, L. A., Abdulla, H. A. N., & Hatcher, P. G. (2014). A coupled geochemical and biogeochemical approach to characterize the bioreactivity of dissolved organic matter from a headwater stream. *Journal of Geophysical Research: Biogeosciences*, 119, 1520– 1537. doi:10.1002/2013JG002600

Sleighter, R. L. & Hatcher, P. G. (2007). The application of electrospray ionization coupled to ultrahigh resolution mass spectrometry for the molecular characterization of natural organic matter. *Journal of Mass Spectrometry*, 42, 559–574. doi:10.1002/jms.1221

Sleighter, R. L. & Hatcher, P. G. (2008). Molecular characterization of dissolved organic matter (DOM) along a river to ocean transect of the lower Chesapeake Bay by ultrahigh resolution electrospray ionization Fourier transform ion cyclotron resonance mass spectrometry. *Marine Chemistry*, 110 (3-4), 140–152. https://doi.org/10.1016/j.marchem.2008.04.008

Sleighter, R. L., Liu, Z., Xue, J., & Hatcher, P. G. (2010). Multivariate Statistical Approaches for the Characterization of Dissolved Organic Matter Analyzed by Ultrahigh Resolution Mass Spectrometry, *Environmental Science & Technology*, 44 (19), 7576–7582. doi:10.1021/es1002204

Smith, L. C., Pavelsky, T. M., MacDonald, G. M., Shiklomanov, A. I., & Lammers, R. B. (2007). Rising minimum daily flows in northern Eurasian rivers: A growing influence of groundwater in the high-latitude hydrologic cycle. *Journal of Geophysical Research*, 112, G04S47. doi:10.1029/2006JG000327

Sobczak, W. V. & Findlay, S. (2010). Variation in Bioavailability of Dissolved Organic Carbon among Stream Hyporheic Flowpaths. *Ecological Society of America*, 83, 3194–3209. https://doi.org/10.1890/0012-9658(2002)083[3194:VIBODO]2.0.CO;2

Spencer, R. G. M., Aiken, G. R., Butler, K. D., Dornblaser, M. M., Striegl, R. G., & Hernes, P. J. (2009). Utilizing chromophoric dissolved organic matter measurements to derive export and reactivity of dissolved organic carbon exported to the Arctic Ocean: A case study of the Yukon River, Alaska. *Geophysical Research Letters*, 36, L06401. doi:10.1029/2008GL036831.

Spencer, R. G. M., Aiken, G. R., Wickland, K. P., Striegl, R. G., & Hernes, P. J. (2008). Seasonal and spatial variability in dissolved organic matter quantity and composition from the Yukon River basin, Alaska. *Global Biogeochemical Cycles*, 22(4), GB4002. doi:10.1029/2008GB003231

Spencer, R. G. M., Guo, W., Raymond, P. A., Dittmar, T., Hood, E., Fellman, J., & Stubbins, A. (2014). Source and biolability of ancient dissolved organic matter in glacier and lake ecosystems on the Tibetan Plateau. *Geochimica et Cosmochimica Acta*, 142, 64–74. https://doi.org/10.1016/j.gca.2014.08.006

Spencer, R. G. M., Mann, P. J., Dittmar, T., Eglinton, T. I., McIntyre, C., Holmes, R. M., Zimov, N., & Stubbins, A. (2015). Detecting the signature of permafrost thaw in Arctic rivers. *Geophysical Research Letters,* 42, 2830–2835. doi:10.1002/2015 GL063498

St. Jacques, J. M. & Sauchyn, D. J. (2009). Increasing winter baseflow and mean annual streamflow from possible permafrost thawing in the Northwest Territories, Canada. *Geophysical Research Letters,* 36, L01401. doi:10.1029/2008GL035822

Striegl, R. G., Aiken, G. R., Dornblaser, M. M., Raymond, P. A., & Wickland, K. P. (2005). A decrease in discharge-normalized DOC export by the Yukon River during summer through autumn. *Geophysical Research Letters*, 32, L21413. doi:10.1029/ 2005GL024413

Stroeve, J., Serreze, M., Drobot, S., Gearheard, S., Holland, M., Maslanik, J., Meier, W., & Scambos, T. (2008). Arctic sea ice extent plummets in 2007. Eos, Transactions, American Geophysical Union, 89. doi:10.1029/2008EO020001

Stubbins, A., Hood, E., Raymond, P. a., Aiken, G. R., Sleighter, R. L., Hernes, P. J., & Spencer, R. G. M. (2012). Anthropogenic aerosols as a source of ancient dissolved organic matter in glaciers. *Nature Geoscience*, *5*(3), 198–201. https://doi.org/10. 1038/ ngeo1403

Stuiver, M. & Polach, H. A. (1997). Discussion Reporting of ^{14}C data. *Radiocarbon,* 19 (3), 355–363. https://doi.org/10.1017/S0033822200003672

Subt, C., Fangman, K. A. Wellner, J. S., & Rosenheim, B. E. (2016). Sediment chronology in Antarctic deglacial sediments: Reconciling organic carbon ^{14}C ages to carbonate ^{14}C ages using Ramped PyrOx. *The Holocene*, 26, 265–273. https:// doi.org/10.1177/0959683615608688

Taniguchi, M., Ishitobi, T., & Shimada, J. (2006). Dynamics of submarine groundwater discharge and freshwater-seawater interface. *Journal of Geophysical Research: Oceans*, 111, C01008. doi:10.1029/2005JC002924.

Taniguchi, M. & Iwakawa, H. (2004). Submarine groundwater discharge in Osaka Bay, Japan. *Limnology*, 5, 25–32. https://doi.org/10.1007/s10201-003-0112-3

Tank, S. E., Manizza, M., Holmes, R. M., McClelland, J. W., & Peterson, B. J. (2012). The Processing and Impact of Dissolved Riverine Nitrogen in the Arctic Ocean. *Estuaries and Coasts*, 35(2), 401–415. https://doi.org/10.1007/s12237-011-9417-3

Tanski, G., Couture, N., Lantuit, H., Eulenburg, A., & Fritz, M. (2016). Eroding permafrost coasts release low amounts of dissolved organic carbon (DOC) from

ground ice into the nearshore zone of the Arctic Ocean. *Global Biogeochemical Cycles*, 30, 1054–1068. doi:10.1002/2015GB005337

Tarnocai, C., Canadell, J. G., Schuur, E. A. G., Kuhry, P., Mazhitova, G., & Zimov, S. A. (2009). Soil organic carbon pools in the northern circumpolar permafrost region. *Global Biogeochemical Cycles*, 23, GB2023. doi:10.1029/2008GB003327

Textor, S. R., Guillemette, F., Zito, P. A., & Spencer, R. G. M. (2018). An assessment of dissolved organic carbon biodegradability and priming in blackwater systems. *Journal of Geophysical Research: Biogeosciences*, 123, 2998–3015. https://doi.org/10.1029/2018JG004470

Townsend-Small, A., McClelland, J. W., Holmes, R. M., & Peterson, B. J. (2011). Seasonal and hydrologic drivers of dissolved organic matter and nutrients in the upper Kuparuk River, Alaskan Arctic. *Biogeochemistry,* 103(1-3), 109–124. doi: 10.1007/s10533-010-9451-4

von Biela, V. R., Zimmerman, C. E. & Moulton, L. L. (2011). Long-term increases in young-of-the-year growth of Arctic cisco *Coregonus autumnalis* and environmental influences. *Journal of Fish Biology*, 78: 39–56. doi:10.1111/j.1095-8649.2010.02832.x

Vonk, J. E., Mann, P. J., Davydov, S., Davydov, A., Spencer, R. G. M., Schade, J., Sobczak, W. V., Zimov, N., Zimov, S., Bulygina, E., Eglinton, T., I., Holmes, R. M. (2013b). High biolability of ancient permafrost carbon upon thaw. *Geophysical Research Letters*, 40, 2689–2693. doi:10.1002/grl.50348.gm

Vonk, J. E., Mann, P. J., Dowdy, K. L., Davydova, A., Davydov, S. P., Zimov, N., Spencer, R. G. M., Bulygina, E. B., Eglinton, T., Holmes, R. M. (2013a). Dissolved organic carbon loss from Yedoma permafrost amplified by ice wedge thaw. *Environmental Research Letters*, 8(3), 035023. doi:10.1088/1748-9326/8/3/035023

Vonk, J. E., Tank, S. E., Mann, P. J., Spencer, R. G. M., Treat, C. C., Striegl, R. G., Abbott, B. W., & Wickland, K. P. (2015). Biodegradability of dissolved organic carbon in permafrost soils and aquatic systems: a meta-analysis, *Biogeosciences*, 12, 6915–6930. https://doi.org/10.5194/bg-12-6915-2015

Wales, N. A., Gomez-Velez, J. D., Newman, B. D., Wilson, C. J., Dafflon, B., Kneafsey, T. J., & Wullschleger, S. D. (2019). Understanding the Relative Importance of Vertical and Horizontal Flow in Ice-Wedge Polygons, Hydrology and Earth System Sciences Discussion, in review. https://doi.org/10.5194/hess-2019-25

Walvoord, M. A. & Striegl, R. G. (2007). Increased groundwater to stream discharge from permafrost thawing in the Yukon River basin: potential impacts on lateral export of carbon and nitrogen. *Geophysical Research Letters*, 34(12), L12402. doi:10.1029/2007GL030216

Walvoord, M. A., Voss, C. I., & Wellman, T. P. (2012). Influence of permafrost distribution on groundwater flow in the context of climate-driven permafrost thaw: Example from Yukon Flats Basin, Alaska, United States. *Water Resources Research,* 48, W07524. doi:10.1029/2011WR011595

Ward, C. P. & Cory, R. M. (2015). Chemical composition of dissolved organic matter draining permafrost soils. *Geochimica et Cosmochimica Acta*, 167, 63–79. http://doi.org/ 10.1016/j.gca.2015.07.001

Wickland, K. P., Aiken, G. R., Butler, K., Dornblaser, M. M., Spencer, R. G. M., & Striegl, R. G. (2012). Biodegradability of dissolved organic carbon in the Yukon River and its tributaries: seasonality and importance of inorganic nitrogen. *Global Biogeochemical Cycles*, 26, GB0E03. doi:10.1029/2012GB004342

Wickland, K. P., Neff, J. C., & Aiken, G. R. (2007). Dissolved organic carbon in Alaskan Boreal forest, sources, chemical characteristics, and biodegradability. *Ecosystems*, 10, 1323–1340. https://doi.org/10.1007/s10021-007-9101-4

Williams, E. K., Rosenheim, B. E., McNichol, A. P., & Masiello, C. A. (2014). Charring and non-additive chemical reactions during ramped pyrolysis: Applications to the characterization of sedimentary and soil organic material, *Organic Geochemistry*, 77, 106-114. https://doi.org/10.1016/j.orggeochem.2014.10.006

Winn, N., Williamson, C. E., Abbitt, R., Rose, K., Renwick, W., Henry, M., & Saros, J. (2009). Modeling dissolved organic carbon in subalpine and alpine lakes with GIS and remote sensing. *Landscape Ecology*, 24, 807–816.

Xenopoulos, M. A., Lodge, D. M., Frentress, J., Kreps, T. A, Bridgham, S. D, Grossman, E., Jackson, C. J (2003). Regional comparisons of watershed determinants of dissolved organic carbon in temperate lakes from the Upper Great Lakes region and selected regions globally. *Limnology & Oceanography*, 48, 2321–2334. https:// doi.org/ 10.4319/lo.2003.48.6.2321

Xu, X., Trumbore, S. E., Zheng, S., Southon, J. R., McDuffee, K. E., Luttgen, M., & Liu, J. C. (2007). Modifying a sealed tube zinc reduction method for preparation of AMS graphite targets: Reducing background and attaining high precision. *Nuclear Instruments and Methods in Physics Research Section B: Beam Interactions with Materials and Atoms*, 259(1), 320–329. https://doi.org/10.1016/j.nimb.2007.01.175

Yang, D., Kane, D., Hinzman, L., Zhang, X., Zhang, T. & Ye, H. (2002). Siberian Lena River hydrologic regime and recent change. *Journal of Geophysical Research*, 107, 4694. doi:10.1029/ 2002JD002542

Zektser, I. S. & Loaiciga, H. A. (1993). Groundwater fluxes in the global hydrologic cycle: past, present and future. *Journal of Hydrology*, 144, 405–427. https://doi.org/ 10.1016/0022-1694(93)90182-9

Zhang, X., Bianchi, T. S., Cui, X., Rosenheim, B. E., Ping, C.-L., Hanna, A. J. M., Kanevskiy, M., Schreiner, K. M., & Allison, M. A. (2017). Permafrost organic

carbon mobilization from the watershed to the Colville River delta: Evidence from ^{14}C ramped pyrolysis and lignin biomarkers. *Geophysical Research Letters*, 44, 11,491–11,500. https://doi.org/10.1002/2017GL075543

Zhang, X., Harvey, K. D., Hogg, W. D. & Yuzyk, T. R. (2000). Trends in Canadian streamflow. *Water Resources Research*, 37, 987–998. https://doi.org/10.1029/2000 WR900357

Zigah, P. K., Minor, E. C., McNichol, A. P., Xu, L. & Werne, J. P. (2017). Constraining the sources and cycling of dissolved organic carbon in a large oligotrophic lake using radiocarbon analyses. *Geochimica Et Cosmochimica Acta*, 208, 102–118. https:// doi.org/10.1016/j.gca.2017.03.021